

Title	ポリビニルアルコールコンポジットハイドロゲルの作製とその解析
Author(s)	趙, 義博
Citation	
Issue Date	2022-03
Type	Thesis or Dissertation
Text version	ETD
URL	http://hdl.handle.net/10119/17778
Rights	
Description	Supervisor:松村 和明, 先端科学技術研究科, 博士

Doctor's Thesis

Preparation and characterization of composited poly(vinyl alcohol) hydrogel

Zhao Yibo

Supervisor: Kazuaki Matsumura

Graduate School of Advanced Science and Technology
Japan Advanced Institute of Science and Technology
(Materials science)

March 2022

Contents

<i>Chapter 1 General Introduction</i>	1
1.1 Introduction	2
1.1.1 Hydrogel	2
1.1.2 Articular cartilage	4
1.1.3 Biomaterials for cartilage	6
1.1.4 PVA and PVA-H	7
1.1.5 Modification of PVA-H	8
1.1.6 Preparations of PVA-H	10
1.2 Research objectives.....	12
1.3 Thesis composition	13
References:.....	14
<i>Chapter 2 Preparation and characterization of GO composited PVA-H by low temperature crystallization method</i>	18
2.1 Introduction	19
2.2 Materials and methods	20
2.2.1 Preparation of GO	20

2.2.2	Preparation of PVA hydrogels	21
2.2.3	Preparation of PVA-GO hydrogels	21
2.3	Experiments	23
2.3.1	XPS spectrum measurement of GO	23
2.3.2	SEM measurements of PVA-H/PVA-GO-H	23
2.3.3	Water content measurement of hydrogels.....	23
2.3.4	Contact angle measurements	23
2.3.5	Tensile test.....	23
2.3.6	Cell culture.....	24
2.4	Results and discussion	25
2.4.1	XPS spectrum of GOs	25
2.4.2	SEM images of PVA-H/PVA-GO-H	26
2.4.3	Control of water content	26
2.4.4	Hydrophilicity evaluation	27
2.4.5	Mechanical properties	28
2.4.6	Cell attachment and proliferation.....	30

2.5	Conclusions	35
	References	37
<i>Chapter 3 Preparation and characterization of GO composited PVA-H by hot pressing method.....</i>		
		39
3.1	Introduction	40
3.2	Materials and methods	41
3.2.1	Preparation of GO	41
3.2.2	Preparation of pure PVA-H	42
3.2.3	Preparation of GO composited PVA-H	43
3.2.4	XPS spectrum measurement of GO	47
3.2.5	Elution of PVA.....	47
3.2.6	Morphology of PVA-GO hydrogels	48
3.2.7	Control of water content	49
3.2.8	Tensile test.....	49
3.2.9	DMA measurement	50
3.2.10	Contact angle measurement.....	50

3.2.11	Protein absorption test.....	51
3.2.12	Cell culture.....	51
3.3	Results and discussion.....	53
3.3.1	XPS spectrum measurement of GO	53
3.3.2	Elution ratio of hydrogels	54
3.3.3	SEM images of PVA-GO hydrogels.....	55
3.3.4	TEM observation of PVA-GO hydrogels.....	56
3.3.5	Control of water content of PVA-GO hydrogels.....	57
3.3.6	Tensile test of hydrated hydrogels.....	59
3.3.7	DMA.....	64
3.3.8	Contact angel measurement.....	65
3.3.9	Protein absorption test.....	66
3.3.10	Cell culture.....	67
3.4	Conclusion.....	70
	References.....	71

Chapter 4 Preparation and characterization of monovalent metal salt composited

<i>PVA-H by hot pressing method</i>	72
4.1 Introduction	73
4.2 Materials and methods	74
4.2.1 Preparation of pure PVA-H	74
4.2.2 Preparation of salt composited PVA-H.....	75
4.2.3 Determination of PVA content by mass measurement	78
4.2.4 FTIR spectra	78
4.2.5 Swelling ratio of hydrated hydrogels.....	78
4.2.6 EDS analysis.....	79
4.2.7 Tensile test.....	79
4.2.8 DSC.....	79
4.2.9 DMA.....	80
4.2.10 Protein absorption test.....	80
4.2.11 Cell culture.....	80
4.3 Results and discussion	81

4.3.1	Determination of PVA content by mass measurement	81
4.3.2	FTIR.....	84
4.3.3	Swelling ratio of hydrated hydrogels	87
4.3.4	EDS analysis	87
4.3.5	Tensile test.....	90
4.3.6	DSC.....	97
4.3.7	DMA.....	99
4.3.9	Cell culture.....	102
4.4	Conclusion.....	104
	References	105
	<i>Chapter 5 Preparation and characterization of divalent metal salt composited PVA-H by hot pressing method</i>	<i>107</i>
5.1	Introduction	108
5.2	Materials and methods	109
5.2.1	Preparation of pure PVA-H	109
5.2.2	Preparation of salt composited PVA-H.....	109

5.2.3	Determination of PVA content by mass measurement	110
5.2.4	FTIR spectra	111
5.2.5	Swelling ratio of hydrated hydrogels	111
5.2.6	EDS analysis	111
5.2.7	Tensile test	112
5.2.8	DSC	112
5.2.9	DMA	112
5.2.10	Protein absorption test	112
5.2.11	Cell culture	113
5.3	Results and discussion	114
5.3.1	Determination of PVA content by mass measurement	114
5.3.2	FTIR	115
5.3.3	Swelling ratio of hydrated hydrogels	119
5.3.4	EDS analysis	120
5.3.5	Tensile test	122
5.3.6	DSC	126

5.3.7	DMA.....	127
5.3.8	Protein absorption test.....	128
5.3.9	Cell culture.....	129
5.4	Conclusion.....	131
	References.....	132
	<i>Chapter 6 General conclusion</i>	133

Chapter 1
General Introduction

1.1 Introduction

1.1.1 Hydrogel

Hydrogel is defined as a polymer having a three-dimensional network structure that is insoluble in any solvent and its swelling body. Owing to the three-dimensional network, hydrogels exhibit the properties of elastic solids with deformability and softness [1]. Hydrogels can be divided into groups based on their structure (Fig. 1.1) [2]:

Based on the types of the cross-link junctions, hydrogels can be classified as physical and chemical hydrogel [3]. The cross-link chains of physical hydrogels are held together by ionic, hydrogen bonding or dipolar interactions. Physical hydrogels are response to a change in environmental conditions such as pH, temperature or ionic concentration. Chemical hydrogels are consisted of cross-link formed by covalent bonding that introduces mechanical integrity and degradation resistance.

Based on the methods of preparation, hydrogels can be divided into homopolymer, copolymer, and interpenetrating network hydrogels. Homopolymer hydrogels contain only one type of monomer in their structure [4] while copolymer hydrogels are comprised of two or more different

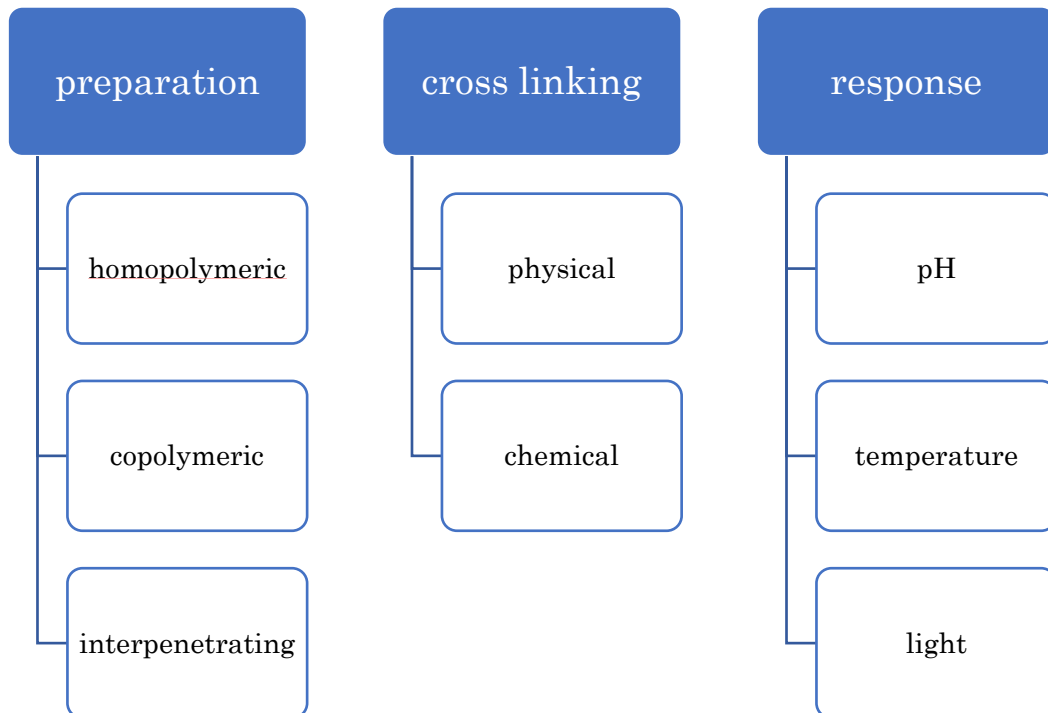


Fig. 1.1 Classification of hydrogels

monomer species, of which at least one hydrophilic component is arranged in random, block or alternating configurations along the chain of the polymer network [5]. Interpenetrating polymeric hydrogels are made of two independent cross-linked synthetic or natural polymer component, contained in a network form [6].

Based on the response to environment (pH, temperature, light and so on), hydrogels can be widely applied in various fields such as pH-sensitive hydrogels in drug delivery system [7] and light-responsive hydrogels for photosensor [8]

Compared to conventional biomaterials such as ceramics and metals, hydrogels possess an unique capability to swell water owing to its three-dimensional network structure, which is similar to biological tissue [9]. Furthermore, hydrogels present a wide range of moisture content, thereby exhibit a wide range of Young's moduli (Fig. 1.2) [10]. These unique properties allow hydrogel to widely used in the fields of tissue engineering [11-13], drug delivery system [7, 14-16] and artificial skin [17,18] muscle [19] or cartilage [20-22].

Previous studies showed that the frictional coefficient of hydrogel decreases in the presence of branched polymer chains [23], demonstrating its suitability for use as an artificial articular cartilage material. In this research, I

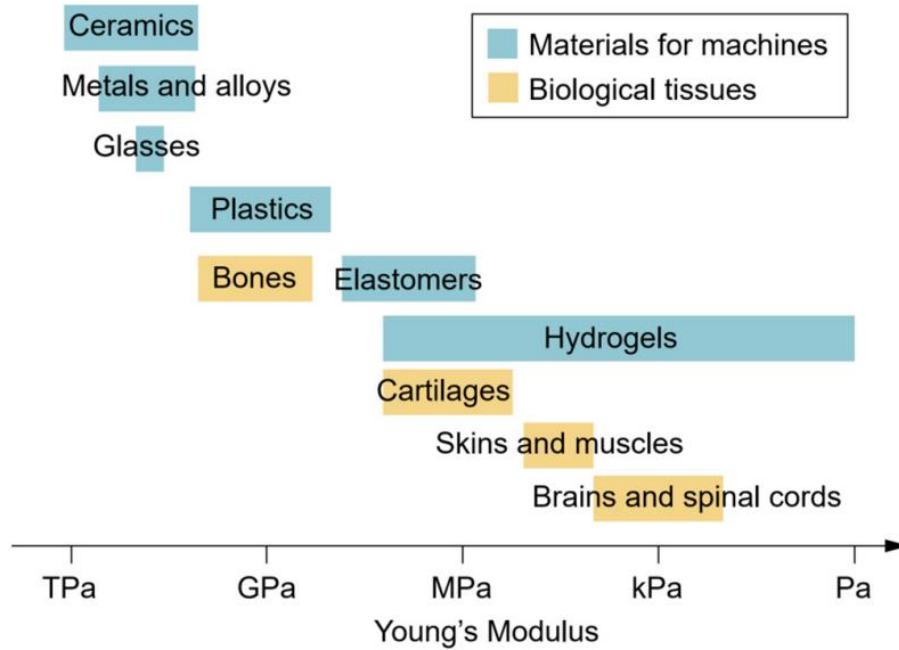


Fig. 1.2 Young's moduli of biological tissues and common materials for machines

concentrated on the application of hydrogels for artificial articular cartilage.

1.1.2 Articular cartilage

Joint is the connecting part of bones and is a very essential organ for the movement of living organisms. Different from other combinations, joint moves smoothly without being filled with tissue, and plays an important role in responding to the large load generated by exercise. Among the joints, what supports the largest load and performs strenuous exercise is the hip joint (Fig. 1.3) In some cases, it is reported that the load is about 5 to 7 times the body weight [24]. The structure of the hip joint is shown in Fig 1.4. The head of round femoral at the top of the femur fits into the acetabulum of the pelvis, forming the joint. The layer with a thickness of about 2 to 4 mm covering the femoral head is called articular cartilage, which absorbs the impact on the hip joint and also plays an important role in preventing friction between bones. Without that cartilage, the bones rub against each other when bending, and the bones are easy to wear out [25].

In current, however, it is estimated that about 10% of the population of over 60-year-old worldwide has clinical symptoms caused by osteoarthritis [26], which is a type of joint disease that results from breakdown of articular cartilage. Once damaged, cartilage tissue is considered to have low possibilities of self-repair because requisite nutrients for repairing are hardly



Fig.1.3 Hip joint

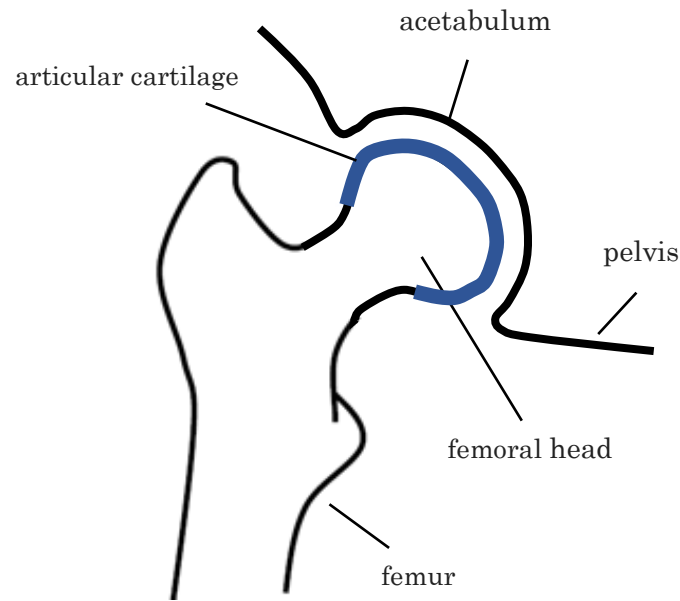


Fig. 1.4 Structure of hip joint

supplied. Therefore, if articular cartilage is damage by an accident or disease, a replacement surgery must be carried out.

For articular cartilage disease, total hip arthroplasty (THA) is a highly reliable treatment method to reconstruct the normal function of hip joint and is widely practiced in the world.

However, by THA, the entire hip joint must be resected and replaced by artificial hip joint, which is a burden to the healthy section. In addition, walking abilities of patients after THA have become poor compared to healthy people even after a long period of postoperative time due to the decrease in hip extension angle during walking [27]. Recently, on the other hand, a new treatment method – resurfacing hip arthroplasty (RHA) has been developed by which only affected cartilage needs to be replaced with artificial cartilage (Fig. 1.5) [28]. The greatest advantage of RHA is that almost all the femur of patients can be preserved, which makes it easier to operate for future revisions.

As a result, the development of artificial cartilage replacement materials has become a popular topic nowadays. However, artificial cartilage materials for resurfacing in RHA have very demanding requirements: they need to have similar mechanical properties as that of human cartilage and shows features such as low wear, nontoxicity, and biocompatibility. conventional hydrogels usually possess limited mechanical strength and are easily damaged

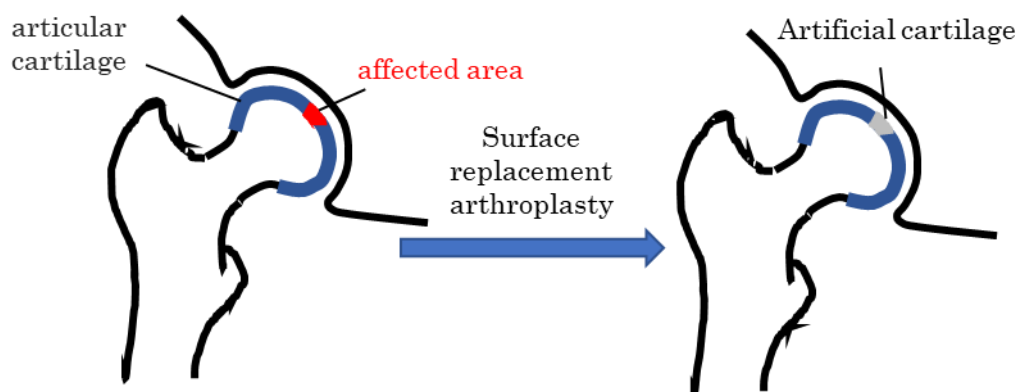


Fig.1.5 Resurfacing hip arthroplasty (RHA)

permanently. Therefore, hydrogels with improved physical and chemical properties were recently developed by innovative chemistry and composition design [29].

1.1.3 Biomaterials for cartilage

Nowadays, there are a large amount of research on artificial cartilage reported. Rampichová, et al [30] prepared a hydrogel by a mixture of fibrin and hyaluronic acid (HA) with high molecular weight as a suitable scaffold for chondrocyte seeding and pig knee cartilage regeneration. The viability of chondrocytes cells in the hydrogel scaffold was over 93% after 14 days of cultivation. Moreover, the regenerated cartilage was found to have good biomechanical and histological properties only 6 months after implantation. Buyanov, A. L., et al [31] synthesized a composite hydrogel based on cellulose and poly(acrylamide) and tested mechanical characteristics mainly for rabbit knee meniscus and found the average-strength of hydrogel was very close to articular cartilage in all mechanical characteristics (compression modulus, viscoelastic behavior, etc.) Wang, Ke, et al [32] succeeded in synthesizing a double-network (DN) hydrogel by bacterial cellulose (BC) and silk fibroin (SF). Through fundamental physical characterizations, the hydrogel was found to have high mechanical strength and biocompatibility and be able to be used as a cartilage repair material in clinical application. Arakaki, Kazunobu, et al [33] prepared a DN hydrogel by poly-(2-Acrylamido-2-methylpropane sulfonic acid)/poly-(N,N'-dimethyl acrylamide) (PAMPS/PDMAAm) and evaluated the *in vivo* influence on counterface cartilage in rabbit knee joints and its *ex vivo* friction properties on normal cartilage. No pathological damage was observed and the gel was found to have very low friction coefficient on normal cartilage.

Among all the artificial cartilage materials, there is a very common and widely used polymer - polyvinyl alcohol (PVA), which has high strength, good biocompatibility and is easy to prepare [34]. In this research, I will concentrate on the application of PVA on artificial cartilage.

1.1.4 PVA and PVA-H

Polyvinyl alcohol (PVA) is a water-soluble synthetic polymer. The structure of PVA was shown in Fig. 1.6. Since vinyl alcohol is thermodynamically unstable, PVA cannot be prepared from the monomer vinyl alcohol, but can only be prepared by hydrolysis of polyvinyl acetate (PVAc, Fig 1.7). The conversion of polyvinyl esters is usually carried out by catalyze-based transesterification with ethanol:

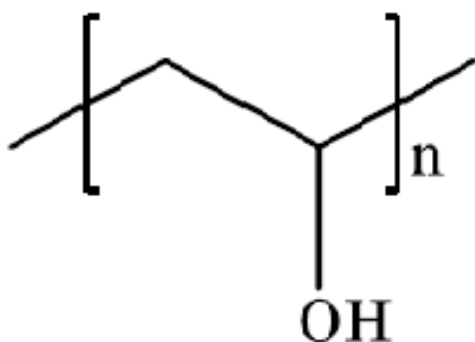
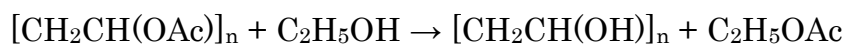


Fig. 1.6 Structural formula of PVA

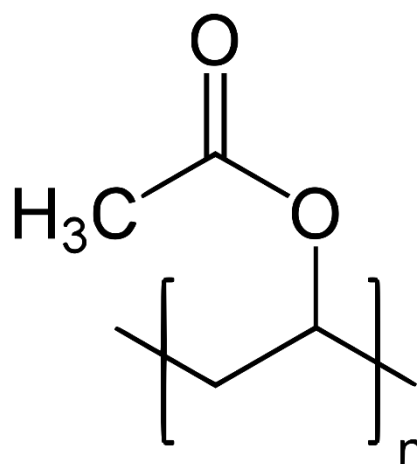


Fig. 1.7 Structural formula of PVAc

PVA can be physically crosslinked via microcrystals form by hydrogen bonding (Fig. 1.8) and physically crosslinked PVA hydrogel (PVA-H) is considered to be a good artificial cartilage material due to its similar friction behavior as that of cartilage and its porous structure, which closely resembles cartilage.

However, PVA-H is known to be a bioinert material and is therefore extremely difficult to adhere and affix to the surface of a living joint [35]. In addition, pure PVA-H possess poor mechanical strength and lubricity which are not capable of replacing articular cartilage [36].

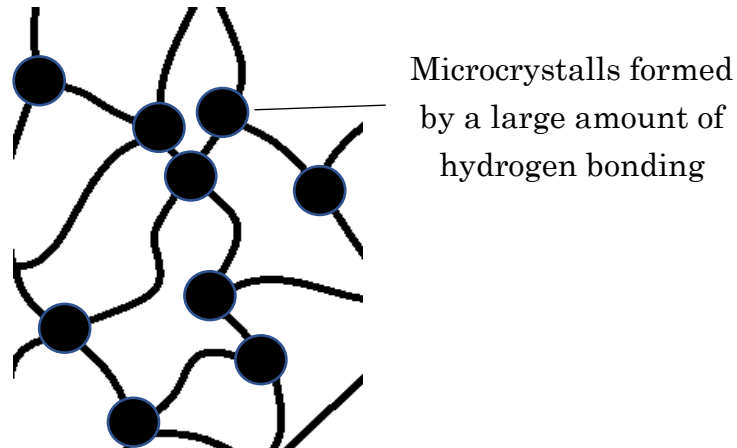


Fig.1.8 Structure of physically crosslinked PVA-H

1.1.5 Modification of PVA-H

Because of the poor mechanical strength and cell adhesion of PVA-H, extensive research has been undertaken in improving the mechanical strength and cell compatibility of PVA-H.

By adjusting the preparation method or condition, the wear and friction coefficient can be controlled [37,38]. Ushio, et al [39] created a composite osteo-chondral device (COD) by intruding PVA into titanium fiber mesh (Fig. 1.9) and found the COD showed good bonding with the vertebral bodies for an extended period of 30 months.

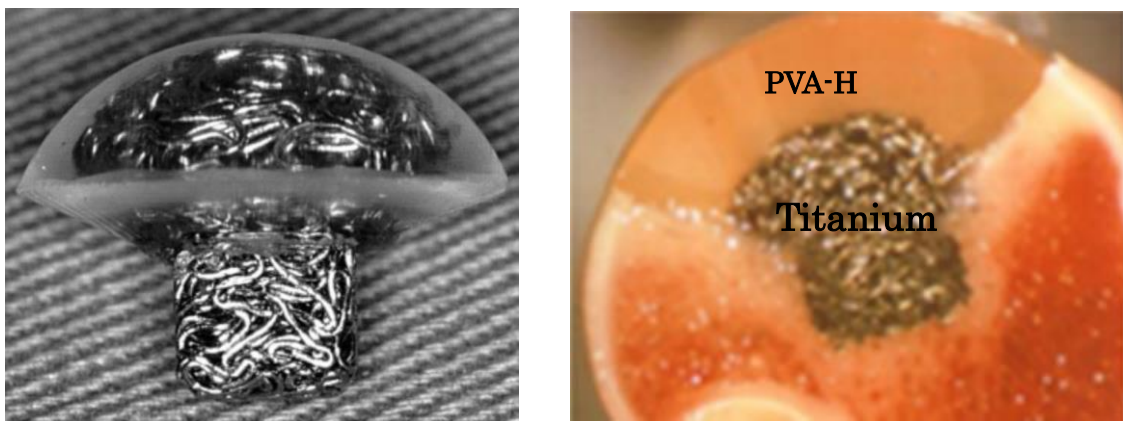


Fig. 1.9 PVA-H was bound to a canine femoral head via Titanium.

In addition, research on composite PVA-H has been considerably reported recently. Zhang, et al [40] prepared PVA/PEG double-network composite hydrogels and found an increase on hardness and insignificant wear rate on the surface. Kanca et al [41] investigated in-vitro tribological performance of the articular cartilage on PVA/PVP composite hydrogel and found the composite hydrogels showed low friction coefficient values which were close to the cartilage-on-cartilage articulation. Some [42-45] blended PVA with chitosan and gelatin and achieved higher tensile strength and better cell proliferation on PVA composite gels. For instance, Liu, et al [42] blended PVA chitosan, gelatin, or starch, and formed hydrogels by subjecting the solutions to freeze-thaw cycles followed by coagulation bath immersion. They found these three composite PVA-H showed a certain increase in both protein adsorption (Table 1.1) and cell attachment (Fig. 1.10).

Table 1.1 Protein adsorption onto the hydrogels with different additives

	PVA	PVA/Chitosan	PVA/Gelatin	PVA/Starch
Average(μg)	31.8 \pm 24.2	191.0 \pm 10.6	338.5 \pm 55.2	188.7 \pm 17.5

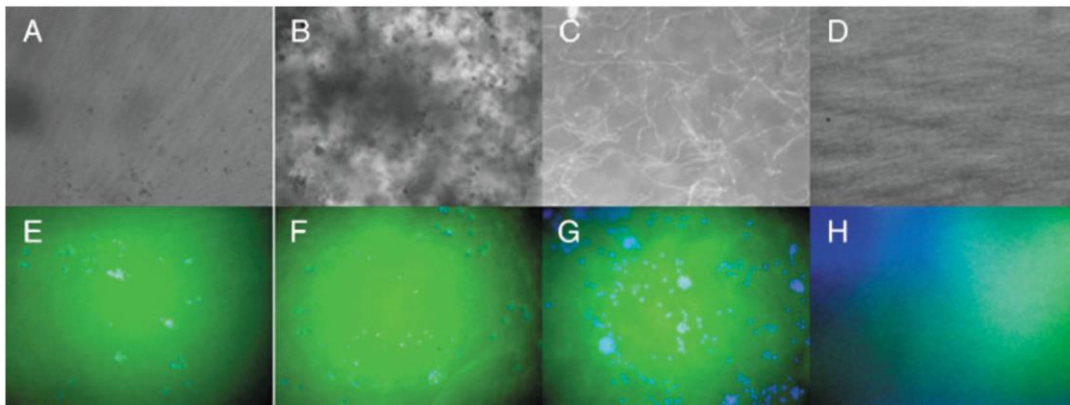


Fig. 1.10 Surface morphology and endothelial cell attachment on to the PVA-based hydrogels. (A,E) PVA/chitosan, (B, F) PVA/starch (C, G) PVA gelatin, and (D, H) PVA (Mag \times 10)

1.1.6 Preparations of PVA-H

Yasuo Sone [46] first noticed the gelation phenomenon of PVA aqueous solution in the 1950s in the 20th century, opening a new path for hydrogels. Nowadays, preparation methods of physical cross-linking PVA-H are mainly summarized into three: cast-drying method (CD) [47], freeze-thawing method (FT) [48], and low temperature crystallization method (LTC) [49].

By FT, the microcrystalline region and amorphous coexist. No matter how much the production conditions are changed, the network structure is non-uniform (Fig.1.11), and white turbidities present (Fig.1.12). In addition, the operation of repeated freezing and thawing is complicated and takes a considerable amount of time.

In general, CD is used to prepare hydrogels with high strength and transparency. However, it is unlikely to obtain composited hydrogels with good dispersion of composite because of the precipitation of the composite.

LTC is a method that microcrystals are formed at low temperature and composite as cross-linking points. The gels produced by LTC are transparent with high strength. However, when water is used as the solvent, the solution freezes below the freezing point and phase separation occurs, resulting in a low-strength and non-uniform gel. Therefore, dimethyl sulfoxide (DMSO) (Fig. 1.13) is used as a cryoprotectant. DMSO is considered to be harmful for our bodies and the addition of DMSO, therefore, is not beneficial for biocompatible materials.

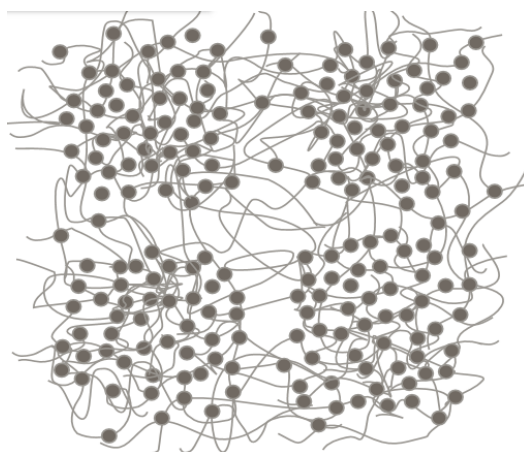


Fig. 1.11 Network structure of FT gels



Fig 1.12 Exterior of FT gels

In our previous research [50], PVA-Hs were successfully prepared using a novel method called hot pressing method. By this method, PVA-H with high transparency (Fig.1.14) and high strength can be easily obtained without using any organic solvent.

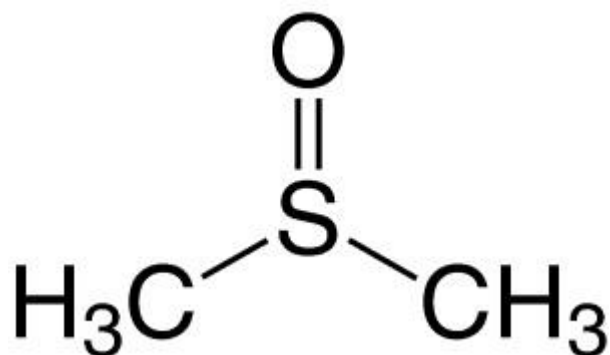


Fig.1.13 Structural formula of DMSO

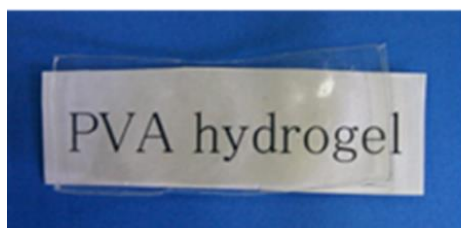


Fig. 1.14 PVA-H prepared by hot pressing method

1.2 Research objectives

In this research, I would use the novel hot pressing method to prepare PVA-H with high biocompatibility. In addition, we tried to prepare PVA composite hydrogel to get high mechanical strength and better cell adhesion. Graphene oxide (GO) (Fig. 1.15) and salt (Fig. 1.16) were used as composite materials to prepare PVA composite hydrogels. The mechanical and thermal properties of each gel were measured. Moreover, toxicity and biocompatibilities of each gel were also evaluated, aiming to develop a biomaterial for artificial cartilage with high strength and biocompatibility.

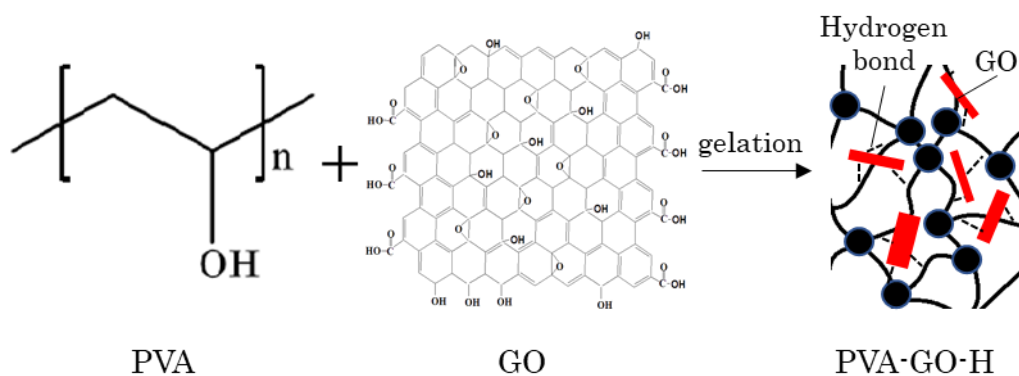


Fig.1.15 PVA-GO composite hydrogel

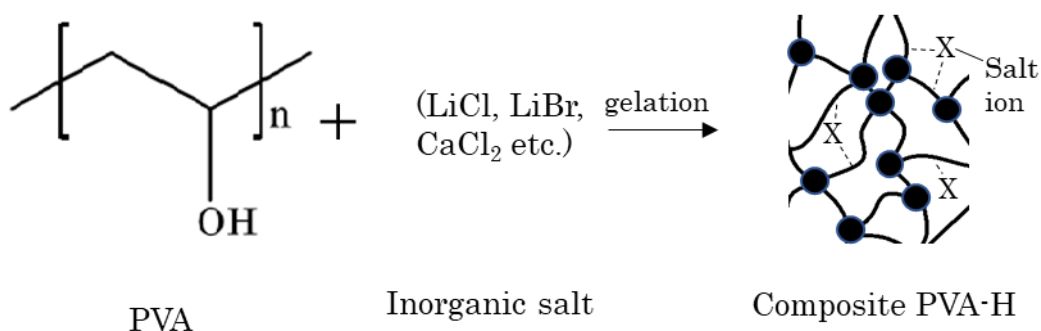


Fig.1.16 Salt-PVA composite hydrogel

1.3 Thesis composition

In chapter 2, the normal LTC was used to prepare graphene oxide (GO) composited PVA-H. The effects of adding GO were discussed.

In chapter 3, the novel hot pressing method was used to prepare GO composited PVA-H for better biocompatibility.

In chapters 4 and 5, monovalent salt and divalent salt were used as composite materials, respectively, to prepare salt composited PVA-H by hot pressing method. The effects of adding salt were discussed separately.

References:

1. Hong W, Zhao X, Zhou J, et al. A theory of coupled diffusion and large deformation in polymeric gels[J]. *Journal of the Mechanics and Physics of Solids*, 2008, 56(5): 1779-1793.
2. Bahram M, Mohseni N, Moghtader M. An introduction to hydrogels and some recent applications[M]//Emerging concepts in analysis and applications of hydrogels. IntechOpen, 2016.
3. Hacker M C, Krieghoff J, Mikos A G. Synthetic polymers[M]//Principles of regenerative medicine. Academic press, 2019: 559-590.
4. Iizawa T, Taketa H, Maruta M, et al. Synthesis of porous poly (N - isopropylacrylamide) gel beads by sedimentation polymerization and their morphology[J]. *Journal of applied polymer science*, 2007, 104(2): 842-850.
5. Yang L, Chu J S, Fix J A. Colon-specific drug delivery: new approaches and in vitro/in vivo evaluation[J]. *International journal of pharmaceutics*, 2002, 235(1-2): 1-15.
6. Dragan E S. Design and applications of interpenetrating polymer network hydrogels. A review[J]. *Chemical Engineering Journal*, 2014, 243: 572-590.
7. Lv X, Zhang W, Liu Y, et al. Hygroscopicity modulation of hydrogels based on carboxymethyl chitosan/Alginate polyelectrolyte complexes and its application as pH-sensitive delivery system[J]. *Carbohydrate polymers*, 2018, 198: 86-93.
8. An R, Zhang B, Han L, et al. Strain-sensitivity conductive MWCNTs composite hydrogel for wearable device and near-infrared photosensor[J]. *Journal of Materials Science*, 2019, 54(11): 8515-8530.
9. Allan, S.H. Hydrogels for biomedical applications. *Adv. Drug Deliv. Rev.*, 2012, 64, 18-23.
10. Liu X, Liu J, Lin S, et al. Hydrogel machines[J]. *Materials Today*, 2020, 36: 102-124.
11. Wang H, Heilshorn S C. Adaptable hydrogel networks with reversible linkages for tissue engineering[J]. *Advanced Materials*, 2015, 27(25): 3717-3736.
12. Spicer C D. Hydrogel scaffolds for tissue engineering: the importance of polymer choice[J]. *Polymer Chemistry*, 2020, 11(2): 184-219.
13. Nezhad-Mokhtari P, Ghorbani M, Roshangar L, et al. A review on the construction of hydrogel scaffolds by various chemically techniques for tissue engineering[J]. *European Polymer Journal*, 2019, 117: 64-76.
14. Gholamali I, Asnaashariisfahani M, Alipour E. Silver nanoparticles incorporated in pH-sensitive nanocomposite hydrogels based on carboxymethyl chitosan-poly (vinyl alcohol) for use in a drug delivery system[J]. *Regenerative Engineering and*

- Translational Medicine, 2020, 6(2): 138-153.
15. Agric J. Development of pH Sensitive Alginate/Gum Tragacanth Based Hydrogels for Oral Insulin Delivery, Food Chem. 2018, 66, 44, 11784–11796
 16. Sun Z, Song C, Wang C, et al. Hydrogel-based controlled drug delivery for cancer treatment: a review[J]. Molecular pharmaceutics, 2019, 17(2): 373-391.
 17. Zhang K, Wang Y, Wei Q, et al. Design and fabrication of sodium alginate/carboxymethyl cellulose sodium blend hydrogel for artificial skin[J]. Gels, 2021, 7(3): 115.
 18. Low Z W K, Li Z, Owh C, et al. Recent innovations in artificial skin[J]. Biomaterials science, 2020, 8(3): 776-797.
 19. Park N, Kim J. Hydrogel - Based Artificial Muscles: Overview and Recent Progress[J]. Advanced Intelligent Systems, 2020, 2(4): 1900135.
 20. Wang K, Ma Q, Zhang Y M, et al. Preparation of bacterial cellulose/silk fibroin double-network hydrogel with high mechanical strength and biocompatibility for artificial cartilage[J]. Cellulose, 2020, 27(4): 1845-1852.
 21. Lee J M, Sultan M, Kim S H, et al. Artificial auricular cartilage using silk fibroin and polyvinyl alcohol hydrogel[J]. International journal of molecular sciences, 2017, 18(8): 1707.
 22. Yarimitsu S, Sasaki S, Murakami T, et al. Evaluation of lubrication properties of hydrogel artificial cartilage materials for joint prosthesis[J]. Biosurface and Biotribology, 2016, 2(1): 40-47.
 23. Gong, J.P.; Kurokawa, T.; Narita, T.; Kagata, G.; Osada, Y.; Nishimura, G.; and Kinjo, M. Synthesis of Hydrogels with Extremely Low Surface Friction. J. Am. Chem. Soc., 2001, 123, 5582–5583.
 24. 筏義人, 生体材料学, 産業図書, 1994.
 25. 笹田 直, 塚本 行男, 馬淵 清資, バイオトライボロジー : 関節の摩擦と潤滑, 1988
 26. Tiku M L, Sabaawy H E. Cartilage regeneration for treatment of osteoarthritis: a paradigm for nonsurgical intervention[J]. Therapeutic advances in musculoskeletal disease, 2015, 7(3): 76-87.
 27. 南角 学, 術後早期における人工股関節置換術患者の歩行分析, 理学療法科学, 2005, 20(2): 121-125,
 28. Wagner H. Surface replacement arthroplasty of the hip[J]. Clinical orthopaedics and related research, 1978 (134): 102-130.
 29. Zhang Y S, Khademhosseini A. Advances in engineering hydrogels[J]. Science, 2017, 356(6337).
 30. Rampichová, Michala, et al. "Fibrin/hyaluronic acid composite hydrogels as

- appropriate scaffolds for in vivo artificial cartilage implantation." *ASAIO journal* 56.6 (2010): 563-568.
31. Buyanov, A. L., et al. "High-strength biocompatible hydrogels based on poly (acrylamide) and cellulose: synthesis, mechanical properties and perspectives for use as artificial cartilage." *Polymer Science Series A* 55.5 (2013): 302-312.
 32. Wang, Ke, et al. "Preparation of bacterial cellulose/silk fibroin double-network hydrogel with high mechanical strength and biocompatibility for artificial cartilage." *Cellulose* 27.4 (2020): 1845-1852.
 33. Arakaki, Kazunobu, et al. "Artificial cartilage made from a novel double - network hydrogel: In vivo effects on the normal cartilage and ex vivo evaluation of the friction property." *Journal of Biomedical Materials Research Part A: An Official Journal of The Society for Biomaterials, The Japanese Society for Biomaterials, and The Australian Society for Biomaterials and the Korean Society for Biomaterials* 93.3 (2010): 1160-1168.
 34. Baker, Maribel I., et al. "A review of polyvinyl alcohol and its uses in cartilage and orthopedic applications." *Journal of Biomedical Materials Research Part B: Applied Biomaterials* 100.5 (2012): 1451-1457.
 35. Yamaoka, T.; Tabata, Y.; and Ikada, Y. Comparison of body distribution of poly(vinyl alcohol) with other water-soluble polymers after intra-venous administration. *J. Pharm. Pharmacol.*, 1995, 47, 479–486.
 36. Chen Y, Song J, Wang S, et al. PVA - Based Hydrogels: Promising Candidates for Articular Cartilage Repair[J]. *Macromolecular Bioscience*, 2021, 21(10): 2100147.
 37. 佐々木沙織, 鎗光清道, 村上輝夫, 等. ポリビニルアルコールキャストドライゲルの乾燥条件が摩擦特性に及ぼす影響[J]. *高分子論文集*, 2015, 72(12): 760-764.
 38. Yarimitsu S, Sasaki S, Murakami T, et al. Evaluation of lubrication properties of hydrogel artificial cartilage materials for joint prosthesis[J]. *Biosurface and Biotribology*, 2016, 2(1): 40-47.
 39. Ushio K, Oka M, Hyon S H, et al. Attachment of artificial cartilage to underlying bone[J]. *Journal of Biomedical Materials Research Part B: Applied Biomaterials: An Official Journal of The Society for Biomaterials, The Japanese Society for Biomaterials, and The Australian Society for Biomaterials and the Korean Society for Biomaterials*, 2004, 68(1): 59-68.
 40. Zhang Z, Ye Z, Hu F, et al. Double - network polyvinyl alcohol composite hydrogel with self - healing and low friction[J]. *Journal of Applied Polymer Science*, 2021, 139(4): 51563.
 41. Kanca Y, Milner P, Dini D, et al. Tribological properties of PVA/PVP blend hydrogels

- against articular cartilage[J]. *Journal of the mechanical behavior of biomedical materials*, 2018, 78: 36-45.
42. Liu, Y., Vrana, N.E., Cahill, P.A., and McGuinness, G.B. Physically crosslinked composite hydrogels of PVA with natural macromolecules: Structure, mechanical properties, and endothelial cell compatibility. *J. Biomed Mater. Res. B. Appl. Biomater.*, 2009, 90B, 492-502.
 43. Koyano, T.; Minoura, N.; Nagura, M.; and Kobayashi, K. Attachment and growth of cultured fibroblast cells on PVA/chitosan - blended hydrogels. *J Biomed. Mater. Res.*, 1998, 39, 486-490.
 44. Thangprasert A, Tansakul C, Thuaksubun N, et al. Mimicked hybrid hydrogel based on gelatin/PVA for tissue engineering in subchondral bone interface for osteoarthritis surgery[J]. *Materials & Design*, 2019, 183: 108113.
 45. Fan L, Yang H, Yang J, et al. Preparation and characterization of chitosan/gelatin/PVA hydrogel for wound dressings[J]. *Carbohydrate polymers*, 2016, 146: 427-434.
 46. 曾根康夫. ポリビニルアルコール濃厚溶液およびゲルに関する研究[D]. 京都大学, 1959.
 47. Komatsu, M., Inoue, T., and Miyasaka, K. Light-scattering studies on the sol-gel transition in aqueous solutions of poly(vinyl alcohol). *Polym. Prepr. Jpn.*, 1986, 24, 303-311.
 48. Peppas, N.A. Turbidimetric studies of aqueous poly(vinyl alcohol) solutions. *Makromol. Chem.*, 1975, 176, 3433-3440.
 49. Hyon, S-H.; Cha, W-I.; and Ikada, Y. Preparation of transparent poly(vinyl alcohol) hydrogel. *Polym. Bull.*, 1989, 22, 119-122.
 50. Sakaguchi, T., Nagano, S., Hara, M., Hyon, S.H., Patel, M., Matsumura, K., Facile preparation of transparent poly (vinyl alcohol) hydrogels with uniform microcrystalline structure by hot-pressing without using organic solvents. *Polymer J.*, 2017, 49, 535-542.

Chapter 2
Preparation and
characterization of GO
composited PVA-H by
low temperature
crystallization method

2.1 Introduction

As mentioned in chapter 1, physically crosslinked polyvinyl alcohol hydrogel (PVA-H) is considered to be a good artificial cartilage material due to its similar friction behavior as that of cartilage and its porous structure, which closely resembles cartilage. However, PVA-H is known to be a bioinert material and is therefore extremely difficult to adhere and affix to the surface of a living joint [1]. In addition, graphene oxide (GO) is single-layer graphene with oxygen functionalities and is known as an excellent nanofiller. GO not only exhibits the physical properties of graphene but also shows dispersability in water and other organic solvents due to the presence of oxygen functionalities. This important property enables mixing of GO with PVA on a molecular level. Some studies [2-6] on PVA/GO composite materials reported good dispersion of GO in a PVA matrix.

Moreover, some studies on GO composite PVA hydrogels or films applied for artificial cartilage were already reported. Shi, Y et al [7]. investigated the friction properties of GO composited PVA-H and found that PVA/GO hydrogel with GO content of 0.1 wt% presented the better compressive properties and creep resistance, which was similar to those observed in natural articular cartilage. J. R. Chen et al. [8] found that GO composited PVA hydrogels with 3 mg/ml GO content showed higher compression modulus (5.3-fold) and high breaking elongation (2.5-fold) compared with pure PVA hydrogels and GO/PVA hydrogels showed similar cytotoxicity levels to those of pure PVA hydrogels.

In this study, GO was used as a composite material to prepare a PVA/GO composite hydrogel (PVA-GO-H). As mentioned in chapter 1, several methods are used to prepare PVA-H, such as the cast-drying method (CD) [9], the freeze-thawing method (FT) [10], and low-temperature crystallization (LTC) [11]. In general, CD is used to prepare hydrogels with high strength and transparency. However, it is unlikely to obtain PVA-GO-H with good dispersion by the CD method because of the precipitation of GO in solution. Consequently, we used the LTC method to prepare PVA-GO-H. PVA-H and PVA-GO-H with different GO concentrations prepared using different oxidation times for GO were prepared and then their contact angles, mechanical properties, and biocompatibilities were investigated. As a result of this study, high-water-content hydrogels suitable as artificial cartilage materials with excellent mechanical properties and biocompatibilities could be anticipated.

2.2 Materials and methods

2.2.1 Preparation of GO

GO used in this research was prepared by Dr. Koji Matsuura of Okayama University using graphene as a raw material by the Hummers method [3,12]. The procedure is shown below:

1. 6 g graphite powder, 50 mL H_2SO_4 , and 10 g $\text{K}_2\text{S}_2\text{O}_8$ were mixed at 80 °C
2. P_4O_{10} was slowly added into the mixture and stirred for 3 h. The mixture was filtered and the filtrated powders were dried overnight
3. 150 mL of H_2SO_4 was added to the dried solid at 4 °C
4. 6.5 g of NaNO_3 and 20 g of KMnO_4 were slowly added into the suspension
5. The ice bath was removed and the temperature of the suspension was kept at 35 °C for 0.5 or 30 h. The time was regarded as oxidation time of GO
6. 305 mL of distilled water was added. The suspension rested for 0.5 h and then diluted with DW to a total volume of 620 mL
7. 33 mL of H_2O_2 was added to remove residual KMnO_4 and MnO_2 , and the resulting suspension was stirred for 0.5 h.
8. The suspension was diluted with 500 mL of distilled water. Then the supernatant was removed.
9. The pH of the GO suspension increased on distilled water dilution using a crossflow system with a hollow fiber and centrifugation (8000 rpm, 5 min) for several times.

Finally, paste of GO was obtained and the concentration was controlled at 3 wt %. We denoted GO samples subjected to the oxidation process (procedure 5) for 0.5 and 30 h as GO(0.5 h) and GO(30 h), respectively.

2.2.2 Preparation of PVA hydrogels

In this study, PVA of 1700 degree of polymerization (DP) and 99.0% degree of saponification (DS) was used. The procedure is shown below:

1. 90 g of a dimethyl sulfoxide (DMSO)/H₂O solution (DMSO/H₂O = 80:20 w/w) was prepared and stirred until reaction heat dissipated
2. 10 g of PVA powder (DP: 1700, DS: 99.0%) was dissolved in the dispersion and the mixture was stirred at 95 °C for 3 h.
3. After that, the dispersion was sealed in autoclave and maintained at 120 °C for 30 min and then naturally cooled to room temperature to get a well-dispersed solution.
4. The solution was then poured between two brass plates with a 3-mm-thick spacer and cooled to -20 °C for 24 h.
5. After gelation, the obtained gels were immersed in ethanol at room temperature for 3 days, wherein the ethanol was exchanged twice a day to remove the DMSO.
6. Then, the obtained hydrogels without DMSO were kept at room temperature for one day and subsequently dried under vacuum for 3 days to remove water and organic solvents remaining in the gels.
7. An annealing treatment under vacuum was carried out at different temperatures to control the water content of gels.
8. Finally, dried gels were immersed in distilled water for 3 days to rehydrate.

2.2.3 Preparation of PVA-GO hydrogels

GO with two different oxidation time (0.5h and 30h) obtained in 2.2.1 was used. GO composited PVA hydrogels were prepared by the following procedure:

1. 90 g of a dimethyl sulfoxide (DMSO)/H₂O solution (DMSO/H₂O = 80:20 w/w) was prepared and stirred until reaction heat dissipated.

2. GO(0.5h) or GO(30h) was dispersed in solution to obtain GO/DMSO/H₂O dispersions of different GO concentrations.
3. 10 g of PVA powder (DP: 1700, DS: 99.0%) was dissolved in the dispersion and the mixture was stirred at 95 °C for 3 h.
4. After that, the dispersion was sealed in autoclave and maintained at 120 °C for 30 min and then naturally cooled to room temperature to get a well-dispersed solution.
5. The solution was then poured between two brass plates with a 3-mm-thick spacer and cooled to -20 °C for 24 h.
6. After gelation, the obtained gels were immersed in ethanol at room temperature for 3 days, wherein the ethanol was exchanged twice a day to remove the DMSO.
7. Then, the obtained hydrogels without DMSO were kept at room temperature for one day and subsequently dried under vacuum for 3 days to remove water and organic solvents remaining in the gels.
8. An annealing treatment under vacuum was carried out at different temperatures to control the water content of gels.
9. Finally, dried gels were immersed in distilled water for 3 days to rehydrate.

2.3 Experiments

2.3.1 XPS spectrum measurement of GO

The elemental ratio of GO(0.5 h) and GO(30 h) was determined using X-ray photoelectron spectrometry (AXIS-ULTRA DLD). The area ratios of each peak were obtained by XPSPEAK software and peak fitting was performed using a linear combination function of the Gaussian and Lorentz functions.

2.3.2 SEM measurements of PVA-H/PVA-GO-H

In order to get the information about the surface topography of gels, scanning electron microscope (SEM) S-5200, was used to obtain the SEM images of PVA-H and PVA-GO-H of 0.05% and 0.40% GO concentrations.

2.3.3 Water content measurement of hydrogels

Water content of the hydrogels was calculated by the following formula (1);

$$WC = \frac{W_{wet} - W_{dry}}{W_{wet}} \times 100\% \quad (1)$$

where W_{wet} is the weight of rehydrated gel and W_{dry} is the weight of dried gel after annealing treatment. Each hydrogel was tested for three times to take the average.

2.3.4 Contact angle measurements

Hydrophilicity was evaluated using an automatic contact angle meter DM-301, and an image analysis software FAMAS. First, the obtained gels were placed on the DM-301. Then, a 2 μ L droplet of water was dropped onto the gel. Contact angle of the dropped droplets was measured by the contact angle meter.

2.3.5 Tensile test

A universal testing machine (Autograph, Shimadzu Co., Ltd., Kyoto, Japan) was used to determine the tensile mechanical properties of the hydrogels. The samples were cut to JIS dumbbell 7 type specimens(gauge

length: 25 mm, width: 2 mm). In order to eliminate the effect of deflection of the gels, an initial load of 0.01 N was applied. The test was performed at the speed of 5 mm/min and was repeated at least three times to ensure reproducibility.

2.3.6 Cell culture

The hydrogels were expected to be artificial cartilage materials, therefore, in order to confirm the adhesion of gel to bone, osteoblast cells MC3T3, which arranged on the surface of bone tissue were seeded on gels to evaluate cell attachment and proliferation. The gels were cut into circles of 10 mm in diameter and were immersed in 70% ethanol for 2 days to sterilize and then immersed in Dulbecco's modified eagle medium (DMEM) to rehydrate. The rehydrated gels were placed in the well of a culture plate (24-well multiplate, Iwaki, Japan). Then, 1 mL of a suspension of osteoblast (2×10^4 cells per mL) in DMEM containing 10% fetal bovine serum (FBS) was added to the well. The cells were then cultured at 37 °C in 5% CO₂ for a given period of time. After culturing, the cells were fluorescently stained by Calcein-AM (Dojindo, Kumamoto, Japan), and the fluorescence of cells attached to the gels was observed with a fluorescence microscope (Biozero, Keyence, Osaka, Japan). To infer the number of surviving cells on gels objectively, the gels were immersed in trypsin at 37 °C to separate the cells from the gels, and the number of living cells were counted by trypan-blue staining. In addition, to evaluate the initial cell adhesiveness of gels, a 10 µL concentrate of 10%FBS–DMEM containing 2×10^4 osteoblast cells were added onto the surface of gels and cultured at 37 °C in 5% CO₂ for 2 h and then observation of the fluorescence and cell counting were carried out.

2.4 Results and discussion

2.4.1 XPS spectrum of GOs

The obtained elemental ratio of GO is shown in Table 2.1. The ratio of C and O was roughly C:O = 7:3, suggesting GO was successfully obtained, and a slight change in the ratio was observed with a change in the oxidation time.

Oxidation time [h]	0.5	30
C:O	71:28	69:29

Table 2.1. Atomic ratio of carbon and oxygen in GO as determined by XPS.

For quantification of the degree of oxidation, C1s peak fitting profiles are shown in Figure 2.1 and the ratio of five peak fitting areas to the area of the C–C peak is shown in Table 2.2. From this result, no obvious change was seen in the ratio of functional groups due to different oxidation time of GO except hydroxyl (OH). 0.5 h oxidized GO has two times larger amount of hydroxyl groups than that of 30 h oxidized GO. This may be due to the hydroxyl groups being oxidized to carboxyl groups (O–C=O) or carbonyl groups (C=O) with increasing oxidation time. The proportions of both carbonyl groups and carboxyl groups slightly increased with the oxidation time, as shown in Table 2.2, GO(0.5 h) contained more hydroxyl groups and is thus likely to have better mechanical properties as it is expected to exhibit stronger interactions with PVA owing to hydrogen bonds.

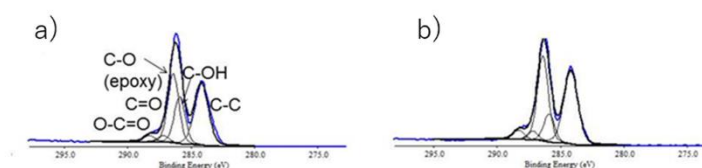


Fig. 2.1. C1s peak fitting profile of (a) GO(0.5 h) and (b) GO(30 h).

Table 2.2. Ratio of various functional groups to C-C peak of GO as determined by XPS.

Functional Group	GO(0.5 h)	GO(30 h)
C-C	1.00	1.00
C-OH	0.60	0.30
C-O (epoxy)	0.87	0.90
C=O	0.087	0.094
O-C=O	0.082	0.099

2.4.2 SEM images of PVA-H/PVA-GO-H

SEM images of PVA-H and PVA-GO-H of 0.05% and 0.4% GO concentration are shown in Figure 2.2. As shown in Figure 2.2, no visible pore structures were seen in the top layers of gels. In addition, the surface of gels of high GO concentration (d,e) were observed to be rugged, indicating the addition of GO can increase roughness of gel surfaces. GO flakes were disorderly distributed on the surface and some part formed few crosslinking points some part formed more thus caused these rough structures on surface.

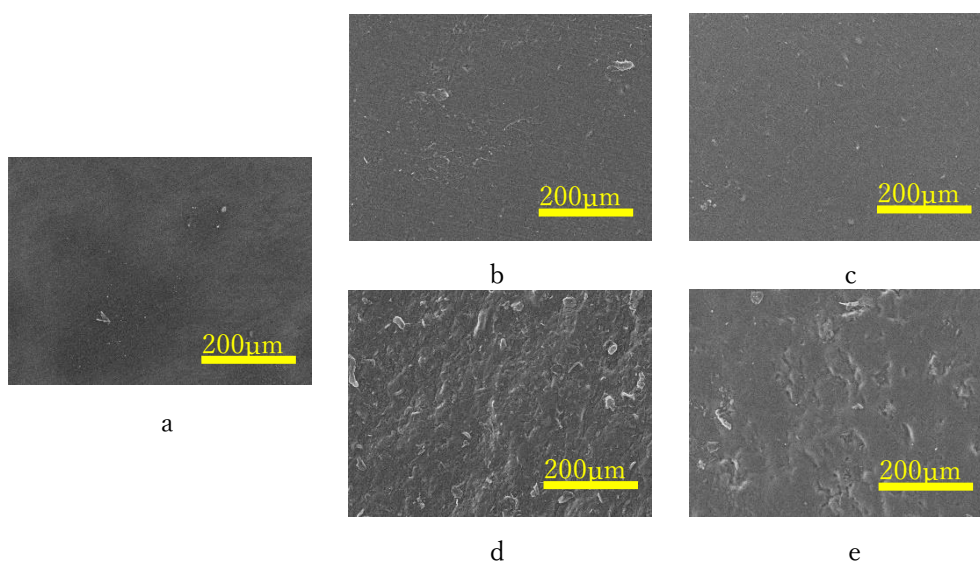


Fig. 2.2. SEM images of (a) PVA-H and PVA-GO-H. Oxidation time and concentration of GO: (b) 0.5h 0.05%, (c) 30h 0.05%, (d) 0.5h 0.4%, (e) 30h 0.4%

2.4.3 Control of water content

Water contents of each sample under a variety of heating conditions are shown in Figure 2.3, where samples subjected to 160 °C for 4 h and 180 °C for 2 h are denoted as 160-4 and 180-2. The gels subjected to treatment at 160 °C showed a much lower water content compared to the untreated samples. Gels under the 180 °C treatment showed an even lower water content. Crystallization degrees of gels can be increased by the annealing treatment under vacuum [13]. Gels with high degrees of crystallization are believed to have access to less water and thus exhibit low water content. In addition, the WC values of the gels subjected to annealing treatment were larger than that of the untreated gels. This can be explained by the surface of the cut gel was not being flat. The uneven surface was caused during the drying process of gels; thus, it is necessary to fix the gels to avert curling while drying.

It is worth mentioning that the untreated gels exhibited a water content of around 70%, which is close to that of human cartilage. Since the crystallization degree has a great influence on the mechanical properties, the mechanical strength of gels can be controlled by different annealing temperatures and it is expected that we can prepare gels with high strength by such annealing treatments.

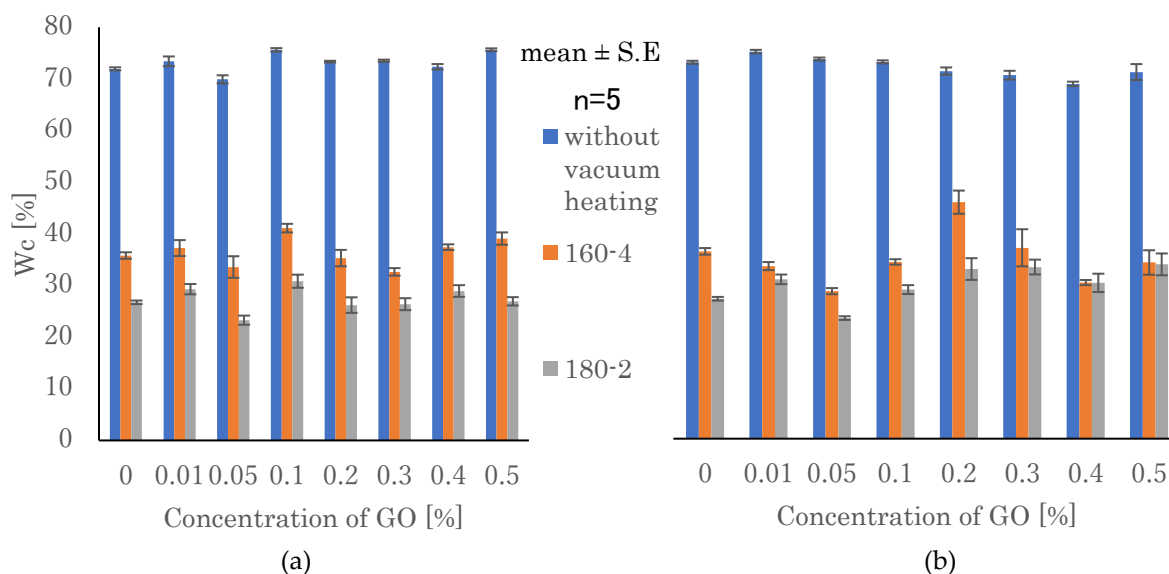


Fig. 2.3. Water content of PVA-GO-H with (a) GO(0.5 h) and (b) GO(30 h).

2.4.4 Hydrophilicity evaluation

Results of contact angle tests of hydrogels are shown in Figure 2.4. the hydrophobicity was found to have no significant change at low GO concentration. With GO concentration increasing, it was found that the surface of PVA-GO-H exhibited hydrophobicity compared to that of PVA-H.

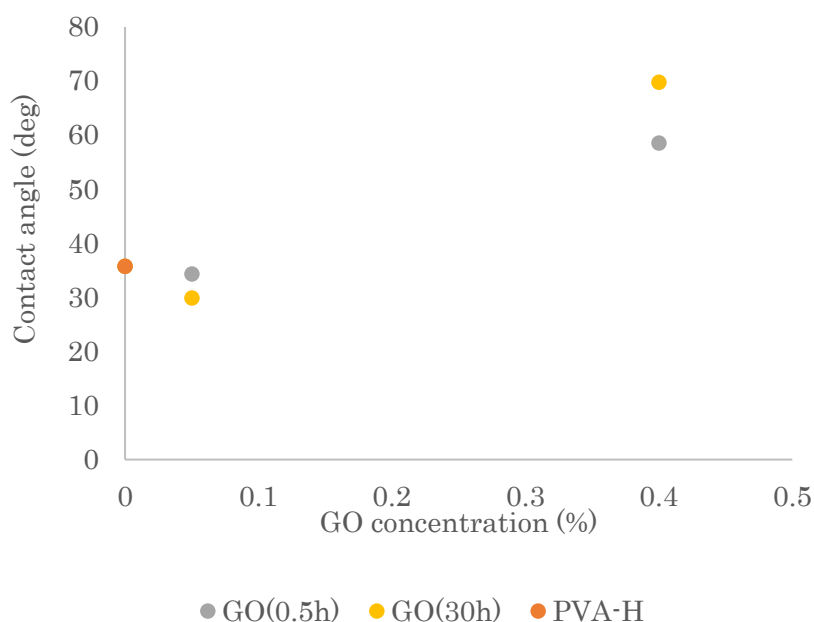


Fig. 2.4. Contact angle of PVA-GO-H.

It seemed that the hydrophilic part of PVA and GO formed hydrogen bonds and the hydrophobic part of GO was exposed on the surface. Moreover, no significant difference was observed for different oxidation times of GO. It is known that differences of surface properties including hydrophilicity affect cell attachment and proliferation, leading to different behavior of seeded cells on gels.

2.4.5 Mechanical properties

Hydrogels with different water content (WC) values were obtained as mentioned in 2.4.3. It is necessary to evaluate the Young's modulus of gels at an identical WC. However, even if a hydrogel is produced under the same condition, an error may occur in determining the value of the WC, which affects the measurement result.

In order to eliminate the influence of WC, a tensile test was carried out by using samples immediately after gelation (before immersion in ethanol). The result is shown in Figure 2.5. PVA-GO-H was found to have a higher Young's modulus than PVA-H and a significant improvement in the Young's modulus was observed with increasing GO concentration. For comprehensive analysis of the mechanical strength of gels, the Young's modulus of gels at different WC were measured and the result is shown in Figure 2.6. To compare the Young's modulus trend of each sample, approximate curves are

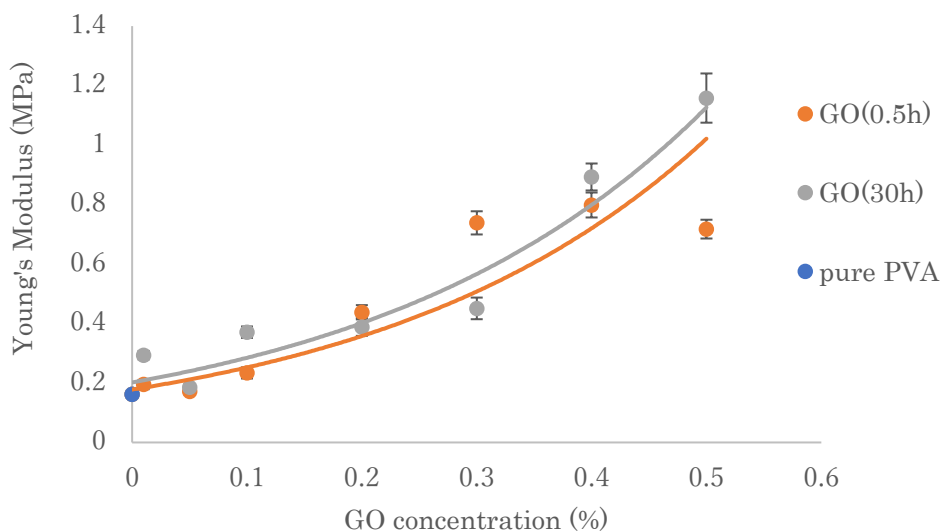


Fig 2.5. Young's modulus of PVA-GO-H

shown. Gels with low water content were observed to have high Young's modulus values and it was intuitively observed that the addition of GO can improve the Young's modulus of gels. However, according to Figure 2.6, the oxidation time of GO seemed to have no significant influence on the measured Young's modulus.

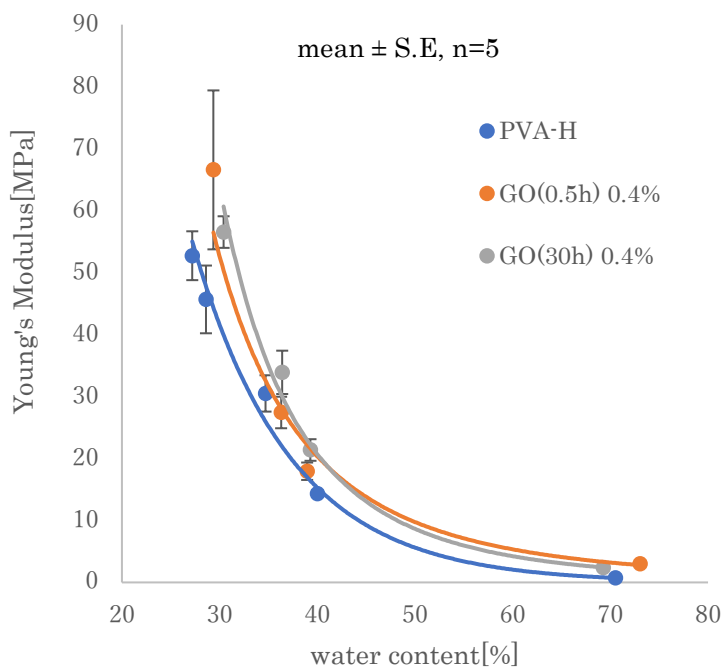


Fig. 2.6. Young's modulus of PVA-GO-H at different WC values.

Figure 2.7 shows the measured Young's modulus at different WC. Although high WC lead to low Young's modulus, the difference in the Young's modulus between PVA-H and PVA-GO-H was clear even at all WC areas. From this result, it can be suggested that hydrogels with both high moisture content and high strength can be produced by adding GO.

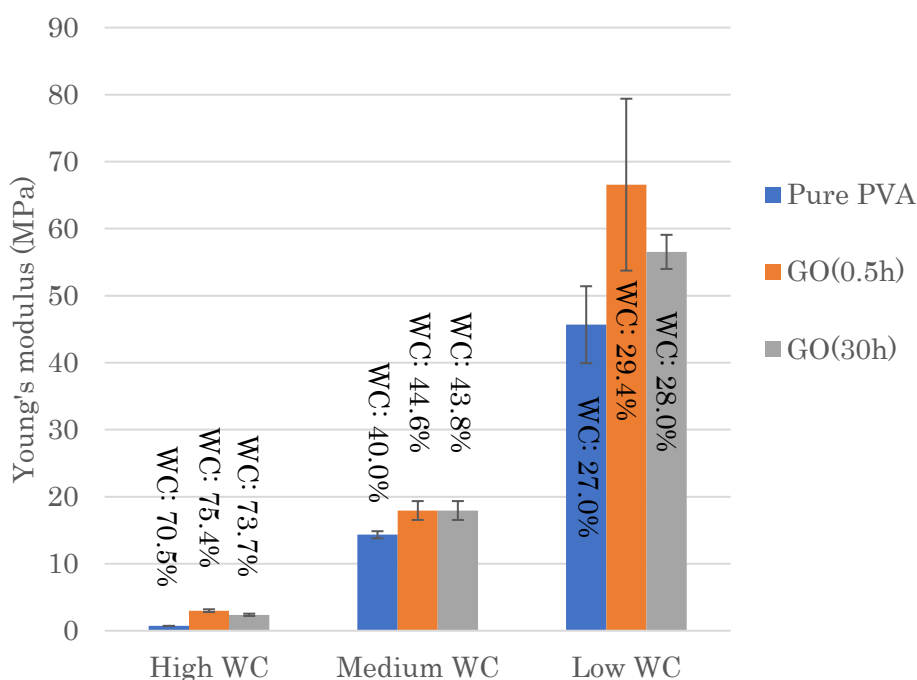


Figure 2.7. Comparison of Young's modulus of each sample at different WC.

2.4.6 Cell attachment and proliferation

The results of fluorescence observation and cell counting are shown in Figure 2.8 – 2.13. The initial cell attachment can be evaluated by the results of fluorescence observation and cell counting of 2-h-cultured cells. A 10 μ L concentrate of osteoblast cells was injected onto the surface of gel so as not to flow it down the gel, excluding external factors such as precipitation or uneven dispersion of cells. As shown in Figure 2.8, many more cells adhered to PVA-GO-H than to PVA-H after 2 hours of inoculation. The gels were washed twice by PBS(-) before counting so the numbers of cells shown in Figure 2.9 are believed to reflect cell adhesion state. Numbers of adhered cells increased with increasing GO concentration, revealing that GO can improve cell attachment and that the GO surface is a good environment for cell proliferation.

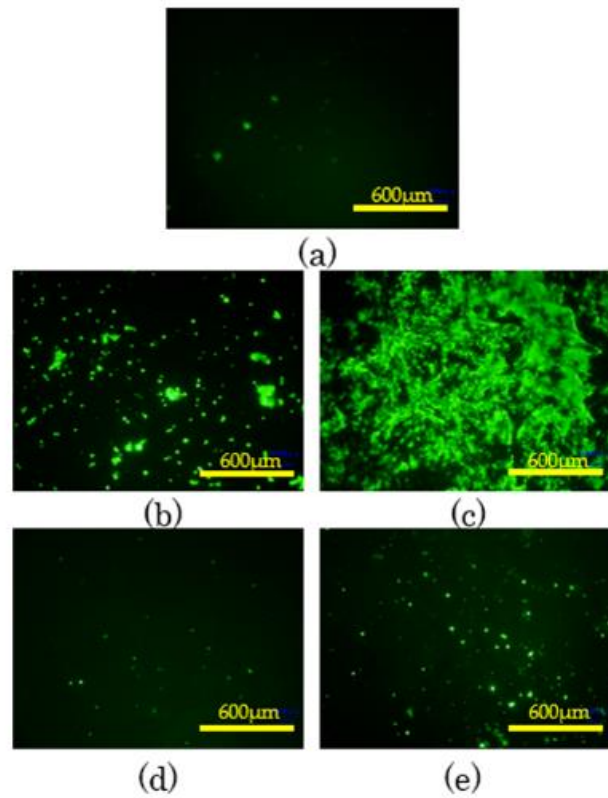


Fig. 2.8. Fluorescence of cells cultured for 2 hours: (a) PVA-H, (b) 0.05% GO(0.5 h), (c) 0.40% GO(0.5 h), (d) 0.05% GO(30 h), and (e) 0.40% GO(30 h).

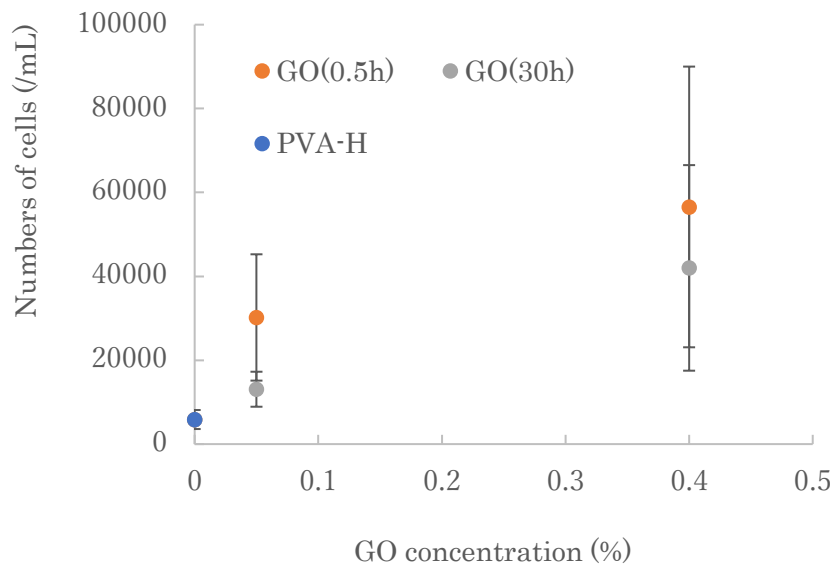


Fig.2.9. Number of cells attached to gels after 2 hours of culturing.

Similar results appeared after 3 days' culturing, as shown in Figure 2.10 and 2.11. The variation in the number of attached cells between samples prepared under the same conditions was very large, which may due to the difference in surface texture and incomplete detachment of cells when counting the number of adherent cells. It was confirmed that GO can improve cell attachment in initial culture, whereas the oxidation time of GO seemed to have no significant influence on cell compatibility, based on the results of cell count (Figure 2.9 and 2.11).

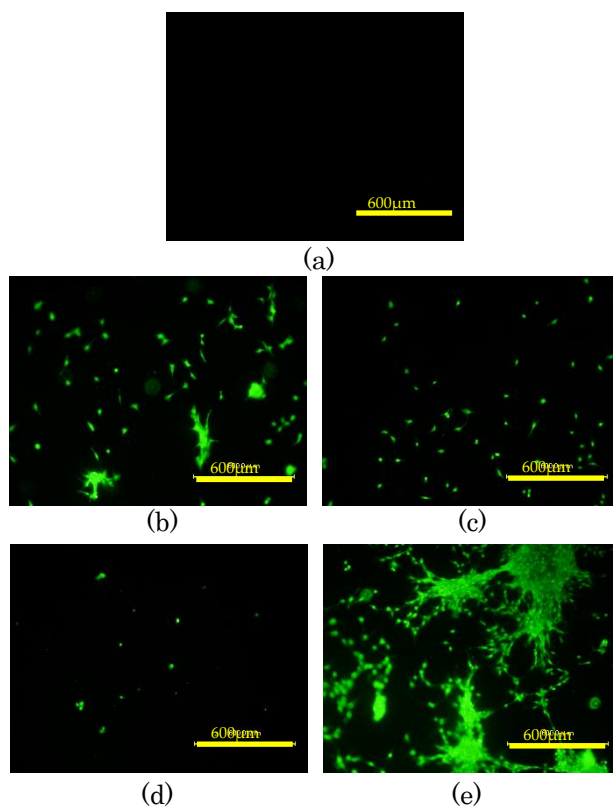


Figure 2.10. Fluorescence cells cultured for 3 days: (a) PVA-H, (b) 0.05% GO(0.5 h), (c) 0.40% GO(0.5 h), (d) 0.05% GO(30 h), and (e) 0.40% GO(30 h).

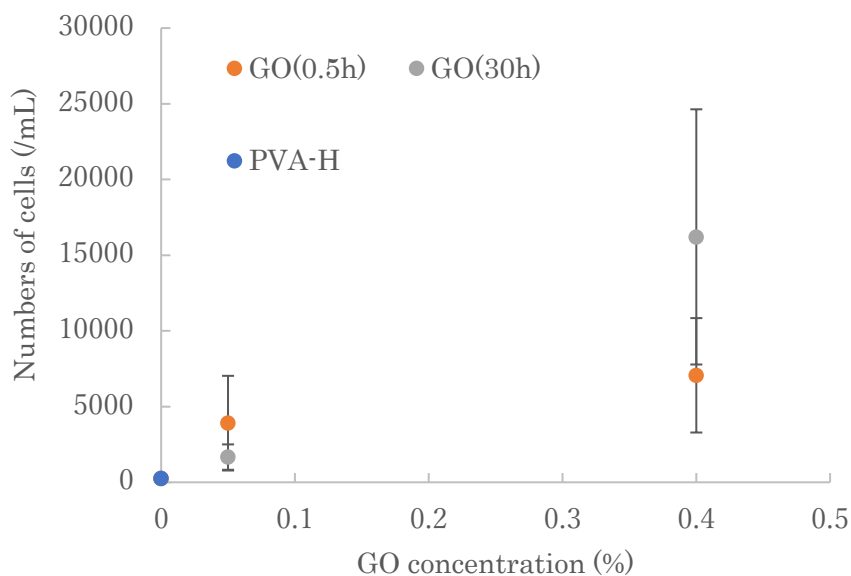


Figure 2.11. Number of cells attached to gels after 3 days of culturing.

Figure 2.12 and 2.13 show fluorescence observation and cell counting of a prolonged culture (12 days). It should be noted that these two group of experiments (3 days and 12 days) were not using the same samples because the gels should be abandoned after Calcein staining. The difference between numbers of cells for 3 days and 12 days of culturing may be due to the variations of samples and experimental operations. Although PVA-GO-H surfaces showed better cell adherence, cells did not show an exponential growth in prolonged culturing except the 0.4% 0.5 h sample; however, the numbers of cells adhered on PVA-GO-H were still more than that of PVA-H, indicating that GO surface is a good environment for cell proliferation. 0.4% 0.5 h PVA-GO-H may be an excellent material, but further research is required to elucidate the mechanism.

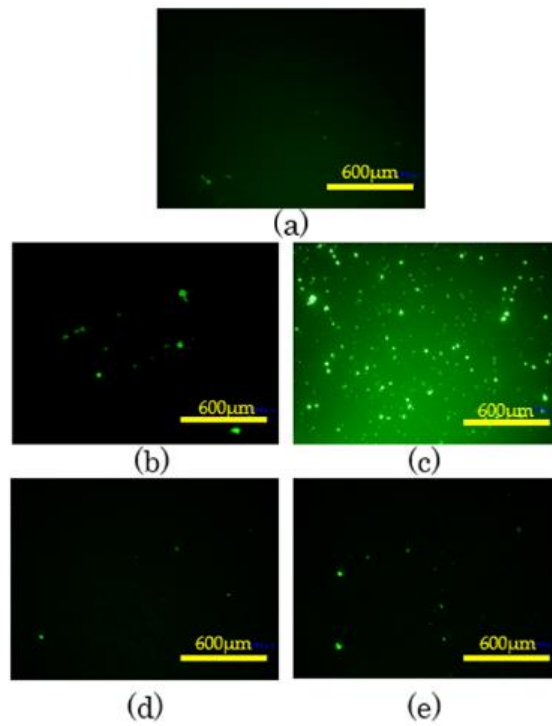


Fig. 2.12. Fluorescence of cells cultured for 12 days: (a) PVA-H, (b) 0.05% GO(0.5 h), (c) 0.40% GO(0.5 h), (d) 0.05% GO(30 h), and (e) 0.40% GO(30 h).

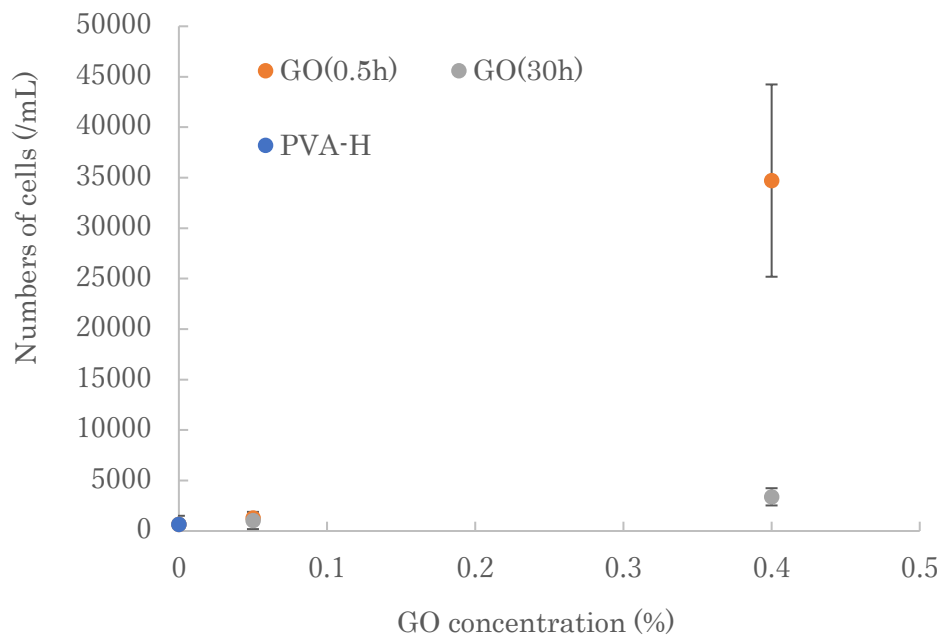


Fig. 2.13. Number of cells attached to gels after 12 days culturing.

2.5 Conclusions

Physically crosslinked PVA-GO-H has been successfully prepared by low-temperature crystallization. The interaction between PVA and GO can be described to be as shown in Figure 2.14 (a), wherein hydrogen atoms of hydroxyl and carboxyl groups of GO interact with oxygen atoms of hydroxyl groups in PVA while hydrogen atoms of hydroxyl groups in PVA interact with oxygen atoms of hydroxyl, carboxyl, epoxy, and carbonyl groups in GO [14]. When mechanical load is applied to such a structure, GO is oriented in the tensile direction, as shown in Figure 2.14 (b). Owing to this, the Young's modulus increases when GO is added. The effect of vacuum heating on the water content can be explained by the increasing density of microcrystals restricting the ability of swelling [15-17].

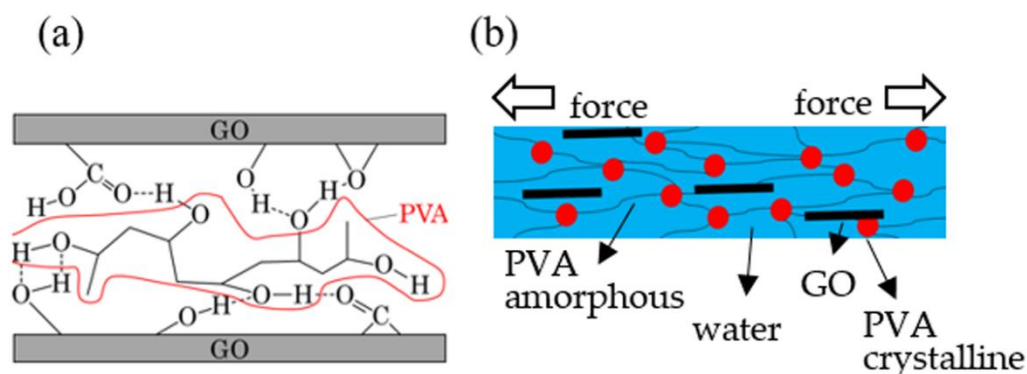


Fig. 2.14. Schematic illustration of the mechanism of GO and PVA interactions. (a) interactions between functional groups of PVA-H and GO, (b) deformation model of PVA-GO-H during application of force.

From the tensile tests, GO was found to have a reinforcing effect on the Young's modulus. Unexpectedly, however, it was difficult to prepare PVA-GO-H with a GO concentration of over 0.4 % due to its high viscosity. The influence of the oxidation time of GO on the Young's modulus is still being estimated. By hydrophilicity evaluation, PVA-GO-H was found to exhibit hydrophobicity compared with PVA-H. With the addition of GO, cell attachment of gels improved obviously and it seems that rough structure observed in Section 2.4.2 is beneficial to cell adherence [6]. However, cells did not proliferate as expected on PVA-GO-H after long time culturing. This can be explained as follow: osteoblasts cells are easy to adhere to where GO aggregates during initial culturing. However, due to the heterogeneous dispersion of GO, cells grow only in the areas where GO exposed and are difficult to proliferate to the entire gel. Some residual ethanol on the hydrogel might cause toxicity response thus affected cell proliferation. In conclusion, although we need further investigations about the mechanisms of

biocompatibility of GO and the detailed experiments for biomechanics, this nanocomposite approach might open new path for the high strength and high biocompatible hydrogel materials for the potential to artificial articular cartilages.

References

1. Yamaoka, T.; Tabata, Y.; and Ikada, Y. Comparison of body distribution of poly(vinyl alcohol) with other water-soluble polymers after intra-venous administration. *J. Pharm. Pharmacol.*, 1995, 47, 479–486.
2. Qi, Y.Y.; Tai, Z.X.; Sun, D.F.; Chen, J.T.; Ma, H.B.; Yan, X.B.; Liu, B.; and Xue, Q.J. Fabrication and Characterization of Poly(vinyl alcohol)/Graphene Oxide Nanofibrous Biocomposite Scaffolds. *J. Appl. Polym. Sci.*, 2013, 127, 1885-1894.
3. Liang, J.J.; Huang, Y.; Zhang, L.; Wang, Y.; Ma, Y.F.; Guo, T.Y.; and Chen, Y.S. Molecular-Level Dispersion of Graphene into Poly(vinyl alcohol) and Effective Reinforcement of their Nanocomposites. *Adv. Funct. Mater.*, 2009, 19, 2297-2302.
4. Sharma, S.K.; Prakash, J.; and Rujari, P.K. Effects of the molecular level dispersion of graphene oxide on the free volume characteristics of poly(vinyl alcohol) and its impact on the thermal and mechanical properties of their nanocomposites. *Phys. Chem. Chem. Phys.*, 2015, 17, 29201-29209.
5. Zhang, L.; Wang, Z.P.; Xu, C.; Li, Y.; Gao, J.P.; Wang, W.; and Liu, Y. High strength graphene oxide/polyvinyl alcohol composite hydrogels. *J. Mater. Chem.*, 2011, 21, 10399-10406.
6. Shi, X.T.; Chang, H.X.; Chen, S.; Lai, C.; Khademhosseini, A.; and Wu, H.K. Regulating Cellular Behavior on Few-Layer Reduced Graphene Oxide Films with Well-Controlled Reduction States. *Adv. Funct. Mater.*, 2012, 22, 751-759.
7. Shi, Y., Xiong, D., Li, J. et al. Tribological Rehydration and Its Role on Frictional Behavior of PVA/GO Hydrogels for Cartilage Replacement Under Migrating and Stationary Contact Conditions. *Tribol Lett* 69, 7 (2021)
8. Chen, J.R., Shi, X.T., Ren, L., Wang, Y. J., Graphene oxide/PVA inorganic/organic interpenetrating hydrogels with excellent mechanical properties and biocompatibility, *Carbon*, Volume 111, 2017, Pages 18-27,
9. Komatsu, M.; Inoue, T.; and Miyasaka, K. Light-scattering studies on the sol-gel transition in aqueous solutions of poly(vinyl alcohol). *Polym. Prepr. Jpn.*, 1986, 24, 303-311.
10. Peppas, N.A. Turbidimetric studies of aqueous poly(vinyl alcohol) solutions. *Makromol. Chem.*, 1975, 176, 3433-3440.
11. Hyon, S-H.; Cha, W-I.; and Ikada, Y. Preparation of transparent poly(vinyl alcohol) hydrogel. *Polym. Bull.*, 1989, 22, 119-122.
12. Qi, Y.Y.; Tai, Z.X.; Sun, D.F.; Chen, J.T.; Ma, H.B.; Yan, X.B.; Liu, B.; and Xue, Q.J. Fabrication and Characterization of Poly(vinyl alcohol)/Graphene Oxide Nanofibrous Biocomposite Scaffolds. *J. Appl. Polym. Sci.*, 2013, 127, 1885-1894.
13. Cha, W.I.; Hyon, S.H.; Ikada, Y. Microstructure of poly(vinyl alcohol) hydrogels investigated with differential scanning calorimetry. *Die Makromol. Chem.*, 1993, 194, 2433-2441.

14. Zhang, L.; Wang, Z.P.; Xu, C.; Li, Y.; Gao, J.P.; Wang, W.; and Liu, Y. High strength graphene oxide/polyvinyl alcohol composite hydrogels. *J. Mater. Chem.*, 2011, 21, 10399-10406.
15. Cha, W.I.; Hyon, S.H.; Ikada, Y. Microstructure of poly(vinyl alcohol) hydrogels investigated with differential scanning calorimetry. *Die Makromol. Chem.*, 1993, 194, 2433-2441.
16. Sakaguchi, T.; Nagano, S.; Hara, M.; Hyon, S.H.; Patel, M.; Matsumura, K. Facile preparation of transparent poly (vinyl alcohol) hydrogels with uniform microcrystalline structure by hot-pressing without using organic solvents. *Polymer J.*, 2017, 49, 535-542.
17. Otsuka, E.; Komiya, S; Sasaki, S.; Xing, J.W.; Bando, T.; Hirashima, Y.; Sugiyama, M.; Suzuki, A. Effects of preparation temperature on swelling and mechanical properties of PVA cast gels. *Soft Matter*, 2012, 8, 812-8136.

Chapter 3
Preparation and
characterization of GO
composited PVA-H by hot
pressing method

3.1 Introduction

In chapter 2, GO composited PVA-H was successfully prepared by low temperature crystallization method (LTC) and it was found that the addition of GO could enhance Young's modulus and improve cell attachment of pure PVA-H. However, in LTC method, dimethyl sulfoxide (DMSO) was used as cryoprotectant, which is supposed to be harmful for our bodies.

Actually, there was a huge amount of studies on composited PVA hydrogels up until now. However almost all of them used either freeze-thawing method or low temperature crystallization method. As mentioned in chapter 1, both of them had their disadvantages. In this study, a novel hot pressing method would be used to prepare GO composited PVA hydrogels. By this method, no organic solvent was used and PVA concentration can be achieved at 50wt% [1].

In the case of previous study [1], PVA of 1700 degree of polymerization (DP) was used and the concentration of PVA was set up to 50 wt %. However, we have already tried this condition to make GO composited PVA-H. the gel was non - uniformed and some small circle of stains could be clearly seen on the surface. It was thought that PVA with lower molecular weight is difficult to wrap GO as a polymer due to its short chain length. Therefore, in this study, we tried to use PVA of high DP (5000) to make PVA-GO-H. High DP of PVA can not only combine with GO molecular better, but also have strong crystallinity due to its strong intramolecular interaction, and hydrogels of higher strength could be obtained.

Same as chapter 2, GO was obtained by Hummers method [2,3], in which graphite was oxidized by KMnO_4 . Different oxidation degree would cause difference in quantity of oxygen functional groups of GO, which may have some effect on the performance of hydrogels. As a result, two kinds of GO with different oxidation time were synthesized by the Hummers method.

3.2 Materials and methods

3.2.1 Preparation of GO

GO used in this research was created by Dr. Koji Matsuura of Okayama University using graphene as a raw material by the Hummers method [2,3]. The procedure is shown below:

10. 6 g graphite powder, 50 mL H_2SO_4 , and 10 g $\text{K}_2\text{S}_2\text{O}_8$ were mixed at 80 °C
11. P_4O_{10} was slowly added into the mixture and stirred for 3 h. The mixture was filtered and the filtrated powders were dried overnight
12. 150 mL of H_2SO_4 was added to the dried solid at 4 °C
13. 6.5 g of NaNO_3 and 20 g of KMnO_4 were slowly added into the suspension
14. The ice bath was removed and the temperature of the suspension was kept at 35 °C for 0.5 or 30 h. The time was regarded as oxidation time of GO
15. 305 mL of distilled water was added. The suspension rested for 0.5 h and then diluted with DW to a total volume of 620 mL
16. 33 mL of H_2O_2 was added to remove residual KMnO_4 and MnO_2 , and the resulting suspension was stirred for 0.5 h.
17. The suspension was diluted with 500 mL of distilled water. Then the supernatant was removed.
18. The pH of the GO suspension increased on distilled water dilution using a crossflow system with a hollow fiber and centrifugation (8000 rpm, 5 min) for several times.

Finally, paste of GO was obtained and the concentration was controlled at 3 wt %. We denoted GO samples subjected to the oxidation process (procedure 5) for 0.5 and 30 h as GO(0.5 h) and GO(30 h), respectively.

3.2.2 Preparation of pure PVA-H

In the case of previous study [1], PVA of 1700 degree of polymerization (DP) was used and the concentration of PVA was set up to 50 wt %. However, in this research PVA of 5000 DP and 99.0% degree of saponification (DS) would be used. The concentration of 50 wt % was no longer applicable. Therefore, we firstly tried different concentration of PVA to find out the optimal concentration. The procedure is shown below:

9. PVA powder (DP: 5000, DS: 99.0%) was mixed with distilled water at different mass ratio in a polyethylene bottle and mixed well.
10. After 10 min swelling, the mixture was well dispersed in a metal frame mold sandwiched by two silicon sheets (Fig.3.1)
11. The mold was then placed in hot pressing machine (Fig.3.2) at 95°C temperature and 2-20MPa pressure for a total 30 min (2 MPa for 5 min, 10 MPa for 10 min, and 20 MPa for 15 min)
12. After heating and pressing, hydrogels enclosed by silicon sheets were taken out and were allowed to gelate in zipper bags for two days
13. The obtained hydrogels were exposed to air and kept at room temperature for 3 days
14. Then the hydrogels were further dried under vacuum for 3 days to remove water remaining in the gels
15. An annealing treatment under vacuum was carried out at different temperatures to control the water content of hydrogels
16. The obtained dried gels were immersed in distilled water for 3 days to rehydrate.

The gels obtained in steps 6 and 7 were call “dried gels” while the gels obtained in step 8 were called “hydrated gels”.

By trying different concentrations of PVA, is was found water was not swollen well and overflow during compress at PVA concentration of 35%. In addition, by comparing the exteriors of gels at PVA concentration of 40%, 45%



Fig.3.1 Before compression



Fig.3.2 hot press machine

and 50%, gel with 45% PVA concentration was observed to be most clean and transparent. Therefore, PVA concentration was set up to 45 wt %

3.2.3 Preparation of GO composited PVA-H

In the previous section, the optimal PVA concentration was found to be 45 wt %. We would fix the PVA concentration at 45% and change GO concentration. In addition, optimal condition of temperature and pressure might change due to the addition of GO. Therefore, we tried several conditions to make sure which is the most appropriate for GO composited PVA-H. The procedure is shown below:

1. GO paste was dissolved in distilled water and ultrasonic wave was done to obtain uniform solution
2. PVA powder (DP: 5000, DS: 99.0%) was added into GO suspension in a polyethylene bottle and mixed well.
3. After 10 min swelling, the mixture was well dispersed in a metal frame mold sandwiched by two silicon sheets
4. Then the mold was placed in hot pressing machine at several conditions (85-120°C, 2-30MPa 25-35 min)
5. After heating and pressing, hydrogels enclosed by silicon sheets were taken out and were allowed to gelate in zipper bags for two days

6. The obtained hydrogels were exposed to air and kept at room temperature for 3 days
7. Then the hydrogels were further dried under vacuum for 3 days to remove water remaining in the gels
8. An annealing treatment under vacuum was carried out at different temperatures to control the water content of hydrogels
9. The obtained dried gels were immersed in distilled water for 3 days to rehydrate.

Same as the previous section, gels obtained in steps 7 and 8 were call “dried gels” and the gels obtained in step 9 were called “hydrated gels”.

Due to high viscosity of GO, the usage of GO was very little: 0.05 wt % - 1.0 wt % of GO paste obtained before. For ease of description, the concentration of GO paste was recorded as GO concentration. The actual concentration needed to multiply it by 3%, which was the GO concentration of GO paste.

The exteriors of dried PVA-GO hydrogels (0.1% GO) obtained by different conditions were shown in Fig. 3.3, and related conditions were shown in Table 3.1. When the temperature was too high, large defects would appear on the surface of the gels (c, d) due to massive evaporation of water during the experiment. on the other hand,

when the temperature was too low (b) or the reaction time was insufficient (f), the dissolution of PVA was insufficient and the surface of the gels were uneven. In addition, when the pressure was too high, the entire surface of the gel became non-uniform. Moreover, when the reaction time was increased, no significant appearance was observed. Therefore, we selected the condition a in Table 3.1 (95 °C, 30min, 2-20MPa) to prepare all PVA-GO hydrogels.

The exteriors of dried PVA-GO hydrogels of different GO concentrations were shown in Fig. 3.4. Although it was unavoidable to form some slightly uneven portion on the surface of the gels, the whole gels were transparent and uniform. It was also observed that when GO concentration was increased, the gels became black and tended to become opaque.

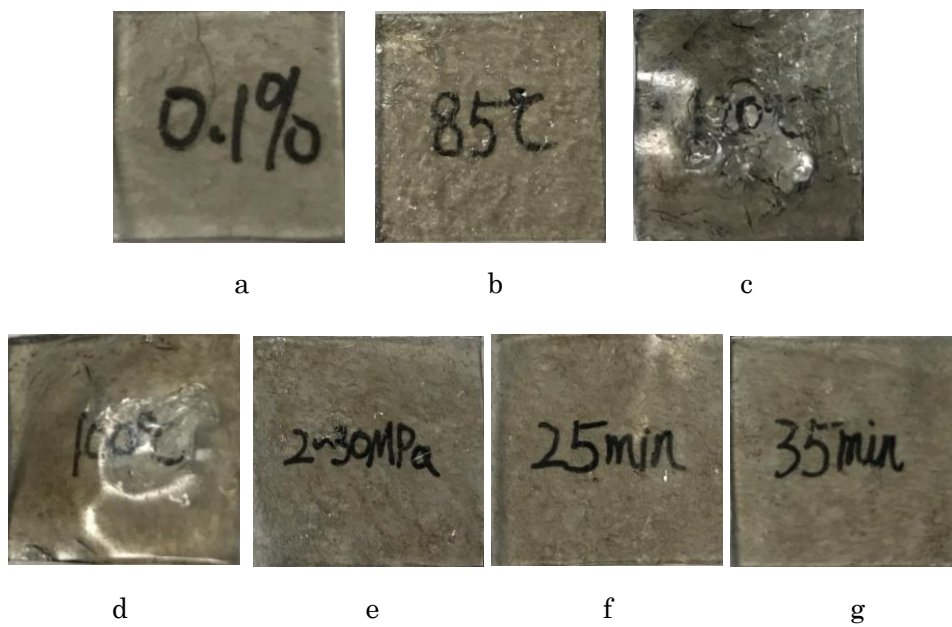


Fig.3.3 Photos of dried gels with different preparation conditions

Table 3.1 preparation condition of each sample

	Temperature(°C)	Time(min)	Press (MPa)
a	95	30 (5+10+15)	2-20 (2, 10, 20)
b	85	30 (5+10+15)	2-20 (2, 10, 20)
c	120	30 (5+10+15)	2-20 (2, 10, 20)
d	100	30 (5+10+15)	2-20 (2, 10, 20)
e	95	30 (5+10+15)	2-30 (2, 15, 30)
f	95	25 (5+8+12)	2-20 (2, 10, 20)
g	95	35 (5+12+18)	2-20 (2, 10, 20)

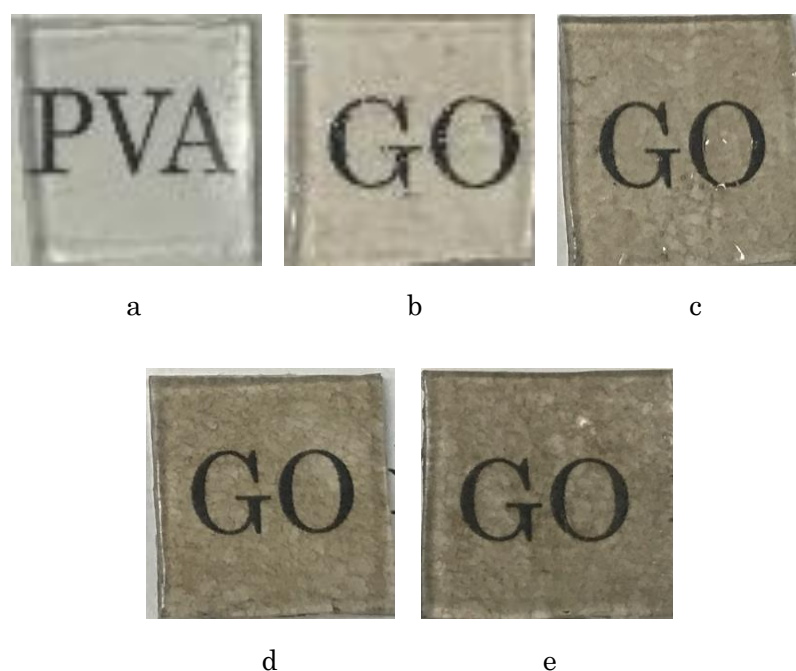


Fig. 3.4 Photos of PVA-GO-H
GO concentration: b: 0.05%; c: 0.10%; d: 0.15%; d: 0.20%

3.2.4 XPS spectrum measurement of GO

The elemental ratio of two kinds of GO of different oxidation time was determined using X-ray photoelectron spectrometry (XPS). The area ratios of each peak were obtained by XPS PEAK software and peak fitting was performed using a linear combination function of the Gaussian and Lorentz functions.

3.2.5 Elution of PVA

In hot pressing method, the condition of high temperature and compression creates possibility for the mixture of PVA and H₂O to form microcrystals. These microcrystals need to furtherly grow to form network structures and finally form a gel. There are many ways to evaluate whether the gel is completely formed such as test tube tilt method [4], ball dropping method [5], viscosity - light transmittance method [6] and so on. However, these methods are not applicable to this study due to the characteristics of hot pressing method. Considering the properties of gel that gels can swell in a solvent but are insoluble in the solvent, we determined the progress of gelation by

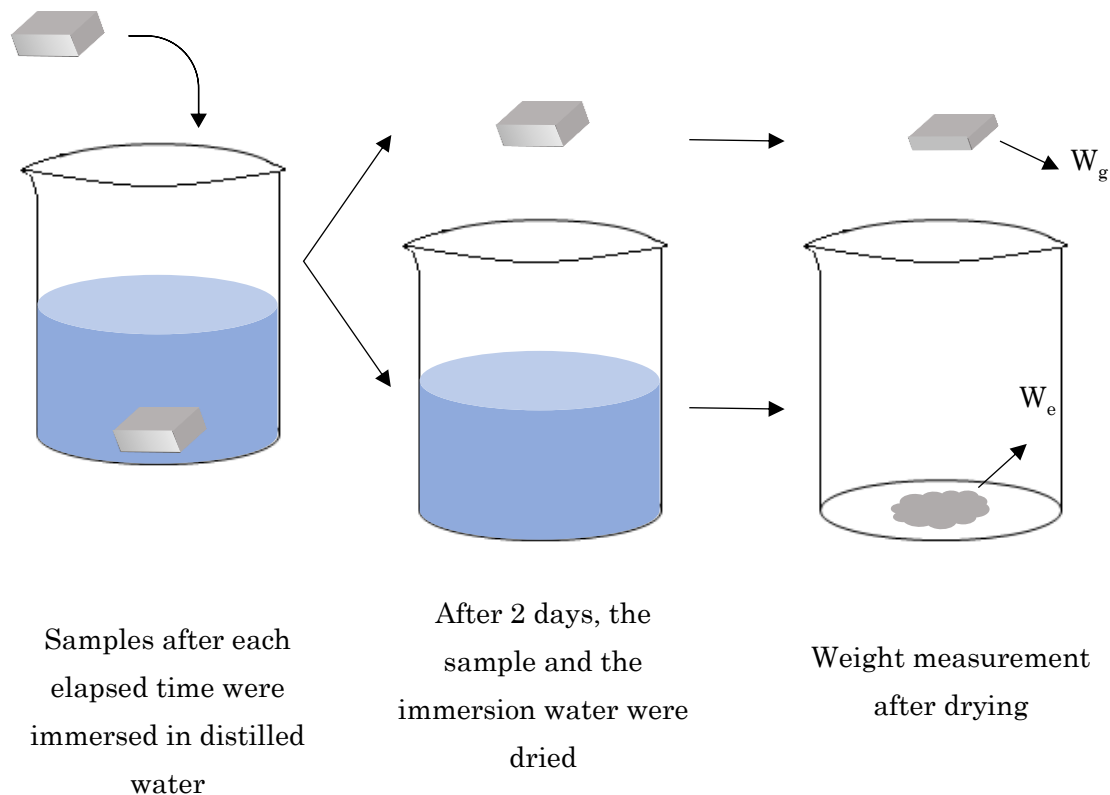


Fig.3.5 Measurement of dissolution rate of gels.

measuring the elution ratio of samples.

The solubility of the gel at each elapsed time was measured immediately after heating and pressing (Fig 3.5). After each predetermined time, the sample was immersed in pure water and then was taken out dried. When the immersion water was completely dried, the weight was measured as W_e , and the weight of the left gel were measured as W_g . The elution ratio ω of sample was calculated by the following formula:

$$\omega = \frac{W_e}{W_g + W_e} \times 100\%$$

3.2.6 Morphology of PVA-GO hydrogels

Morphology of the surface of hydrogels was analyzed by Scanning Electron Microscope (SEM) using TM3030plus. The dispersion of GO was analyzed by Transmission Electron Microscope (TEM) using H-7100.

3.2.7 Control of water content

By annealing treatment, microcrystals of the gel grew, and became difficult to cleave while swelling, which caused decrease in the water content. By measuring the weight of samples before and after hydrating, water content (WC) could be calculated by the following formula:

$$WC = \frac{W_{wet} - W_{dry}}{W_{wet}} \times 100\%$$

where W_{dry} was the weight of dried gel after annealing and W_{wet} was the weight of hydrated gel.

3.2.8 Tensile test

The tensile mechanical properties of the hydrogels were determined by tensile test underwater (Fig 3.6). The samples were cut to JIS dumbbell 7 type specimens (Fig 3.7). An initial load of 0.01 N was applied to eliminate the effect of deflection of the gels. The test was performed at the speed of 5 mm/min and was repeated 5 times to ensure reproducibility.

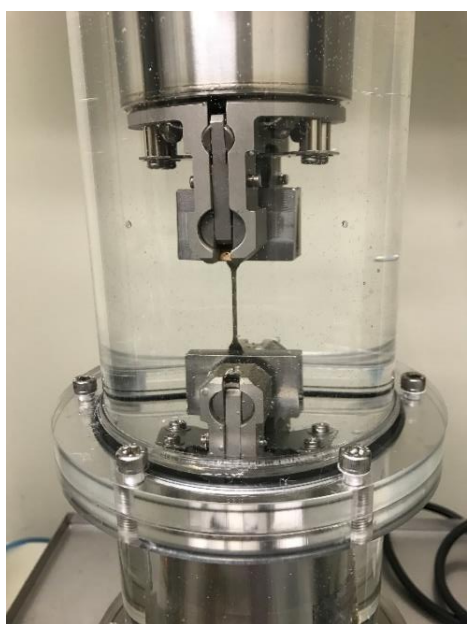


Fig.3.6 Tensile test underwater

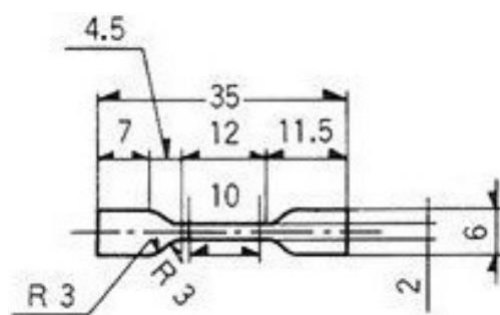


Fig.3.7 JIS dumbbell 7 type

3.2.9 DMA measurement

Dynamic mechanical analysis of dried gels was carried out by using Rheosol-G5000 (Fig 3.8) The samples were cut to 5 mm × 30 mm rectangles. Dynamic viscoelasticity of gels on temperature dispersion was measured from 25 – 100 °C at a heating rate of 3 °C/min and the frequency was 1 Hz.

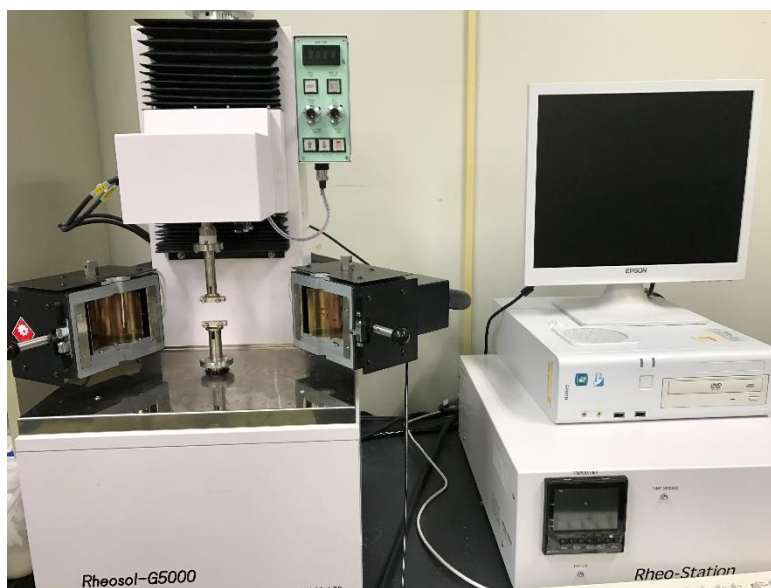


Fig.3.8 Rheosol-G5000

3.2.10 Contact angle measurement

Hydrophilicity was evaluated using an automatic contact angle meter DM-301 (Fig. 3.9). The hydrated gels were first placed on the DM-301. Then, a

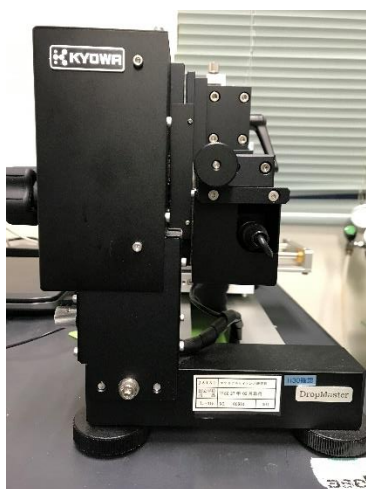


Fig.3.9 DM-301

2 μ L droplet of water was dropped onto the gel. Contact angle of the dropped droplets was measured by the contact angle meter.

3.2.11 Protein absorption test

Protein absorption of each hydrated hydrogel was measured by the following procedure:

1. Samples were cut into cylinders with a diameter of 3 mm
2. Three samples from identical gels were added into 1 ml of low glucose-Dulbecco's modified Eagle's medium (DMEM) containing 10% fetal bovine serum (FBS) and incubated at 37°C for 1 h
3. After the medium removed, samples were washed by 2 mL PBS five times to remove the unadhered protein
4. The samples were put into 1 mL of 5% SDS, and then vortexed and sonicated several times to recover the absorbed proteins
5. The supernatants were collected for the measurement of protein concentrations

Protein concentrations were determined by a bicinchoninic acid (BCA) assay [7], using an albumin BSA standard curve according to the manufacturer's instructions (Thermo Fisher Scientific). The absorbance of BCA solutions was measured at 562 nm using a microplate reader. Three identical samples were tested one time for average and each sample were tested three times.

3.2.12 Cell culture

Biocompatibility of gels was evaluated by cell culture. First the gels were immersed in 70% ethanol for 2 days to sterilize and then immersed in Dulbecco's modified eagle medium (DMEM) for 1 day to rehydrate. After that Osteoblast cells MC3T3 were seeded on gels to evaluate cell attachment and proliferation. The rehydrated gels were placed in the well of a culture plate (24-well multiplate, Iwaki, Japan). Then, 1 mL of a suspension of osteoblast (2×10^4 cells per mL) in DMEM containing 10% fetal bovine serum (FBS) was

added to the well. The cells were then cultured at 37 °C in 5% CO₂ for a given period of time. After culturing, the cells were fluorescently stained by Calcein-AM (Dojindo, Kumamoto, Japan), and the fluorescence of cells attached to the gels was observed with a fluorescence microscope (Biozero, Keyence, Osaka, Japan). To infer the number of surviving cells on gels objectively, the gels were immersed in trypsin at 37 °C to separate the cells from the gels, and the number of living cells were counted by trypan-blue staining.

3.3 Results and discussion

3.3.1 XPS spectrum measurement of GO

Table 3.2 Atomic ratio of carbon and oxygen in GO as determined by XPS

Oxidation time(h)	0.5	30
C:O	71:28	69:29

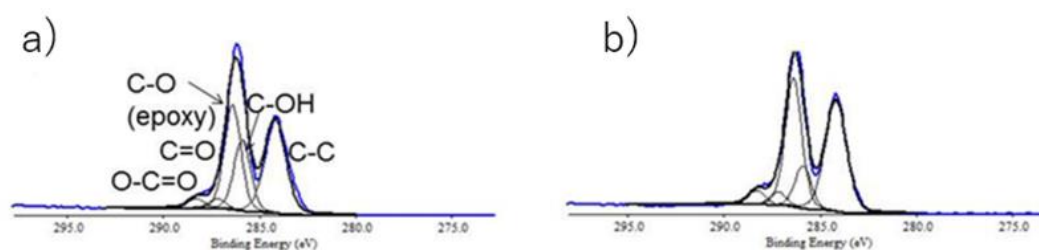


Fig. 3.10 C1s peak fitting profile of (a) GO(0.5 h) and (b) GO(30 h)

Table 3.2 showed the obtained elemental ratio of GO. The ratio of C and O was near to 7:3, suggesting GO was successfully obtained. a slight change in the ratio was observed with a change in the oxidation time. For quantification of the degree of oxidation, peak separation was performed on the XPS spectrum of the obtained C1s (Fig. 3.10), and the area ratio of each peak was examined (Table 3.3). From the result, no obvious change was seen in the ratio of functional groups due to different oxidation time of GO except hydroxyl (-OH). 0.5 h oxidized GO has two times larger amount of hydroxyl groups than that of 30 h oxidized GO. This may be due to the hydroxyl groups being oxidized to carboxyl groups (O-C=O) or carbonyl groups (C=O) with increasing oxidation time. The proportions of both carbonyl groups and carboxyl groups slightly increased with the oxidation time, as shown in Table 3.3. GO (0.5 h) contained more hydroxyl groups and is thus likely to have better mechanical properties as it is expected to exhibit stronger interactions with PVA owing to hydrogen bonds.

Table 3.3 Ratio of various functional groups to C-C peak of GO as determined by XPS

Functional Group	GO(0.5 h)	GO(30 h)
C-C	1	1
C-OH	0.6	0.3
C-O (epoxy)	0.87	0.9
C=O	0.087	0.094
O-C=O	0.082	0.099

3.3.2 Elution ratio of hydrogels

By the measurement of the dissolution rate of samples at different storage times after heating and compression (Fig. 3.11), it was found that the samples had a initial dissolution rate of about 33%, suggesting that the gelation was not yet completed immediately after heating and compression. Then, after a storage time of 44 h, the samples were almost insoluble in water, indicating that hydrogels were successfully prepared and required 2 days for gelation.

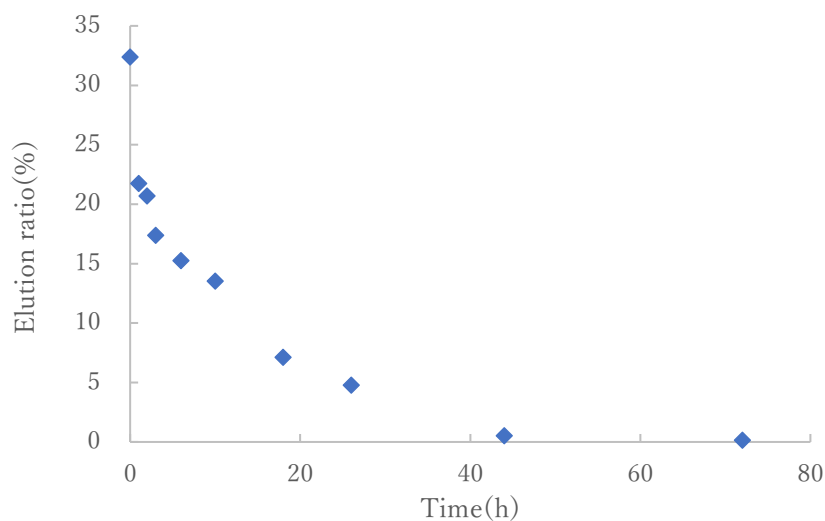


Fig.3.11 Elution ratio of HP gel at different storage times

3.3.3 SEM images of PVA-GO hydrogels

Scanning Electron Microscope (SEM) images of pure PVA hydrogels and PVA-GO hydrogels were shown in Fig.3.12. It was observed that the surface of PVA hydrogel (a) was smooth overall, yet some undissolved PVA still existed. For GO composited hydrogels, no visible porous structure was seen. GO was found to irregularly distribute on the surface like a layer (c, d), and both PVA and GO aggregations were observed on the surface (b). These showed flake GO molecules would not present in the formation of microcrystals but combined with PVA molecules layer by layer.

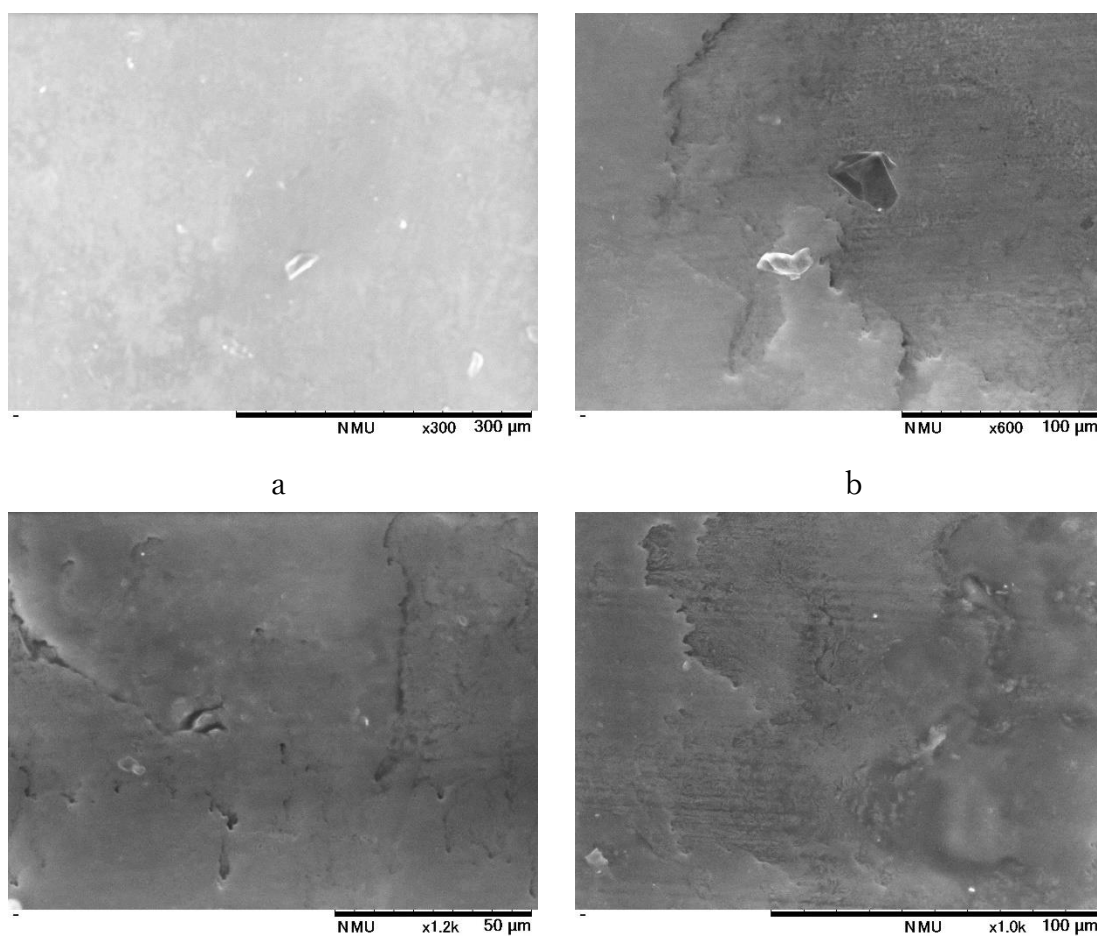


Fig.3.12 SEM images of PVA-GO hydrogel
a: pure PVA, b, c: 0.5h GO 1.0%, d: 30h GO 1.0%

3.3.4 TEM observation of PVA-GO hydrogels

Transmission Electron Microscope (TEM) images of PVA-GO hydrogels were shown in Fig. 3.13. Since pure PVA-H was transparent and GO presented a very deep black with the concentration arising, the black part in the images can be regarded as the concentration of GO. It was observed that the dark parts distributed non-uniformly as a whole, indicating that GO may

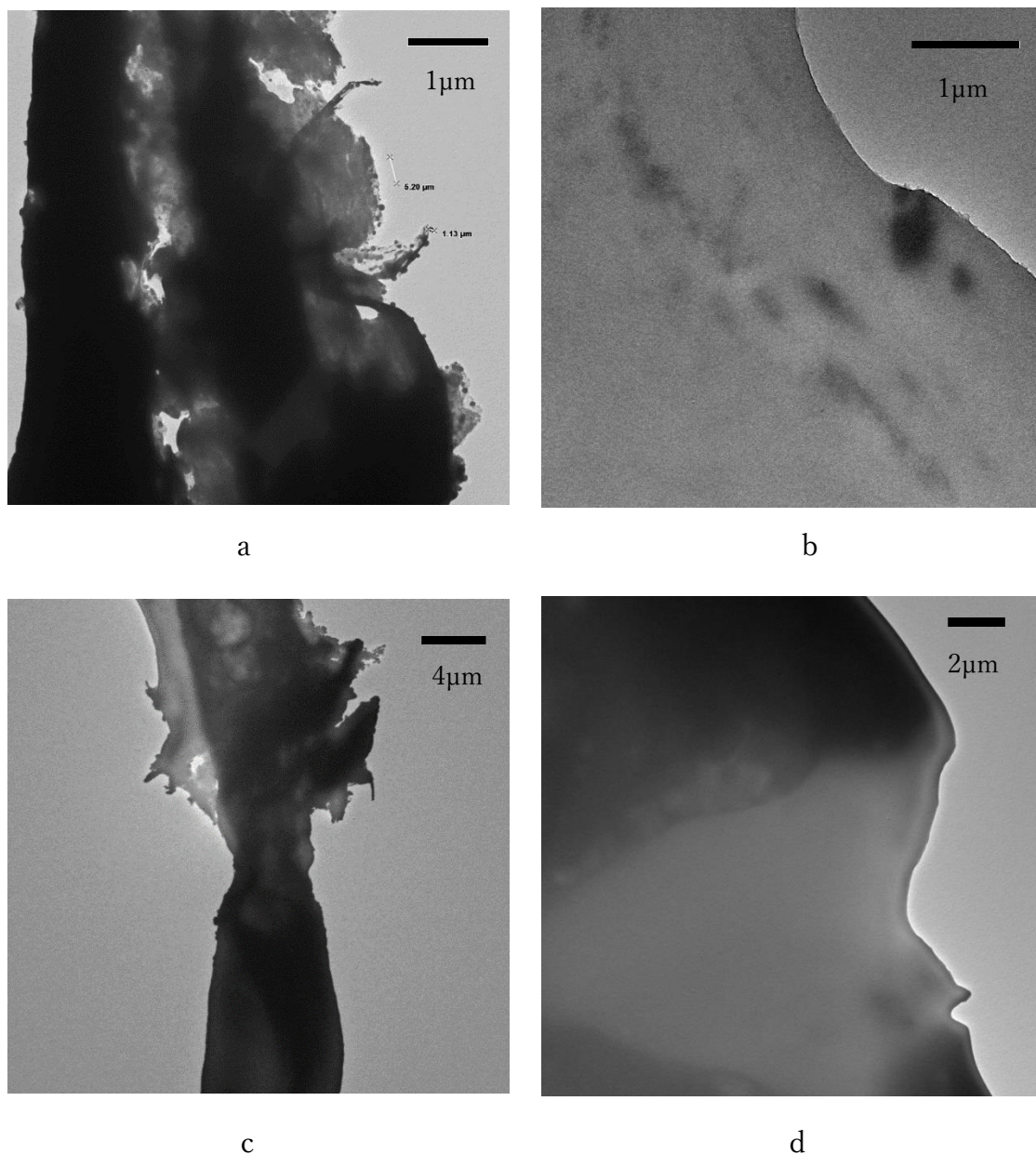


Fig. 3.13 TEM images of PVA-GO-H
GO concentration: a, b: 0.05%, c, d: 0.10%

not disperse well in the gel. This may be caused by high viscosity and molecular weight of GO. Although we dissolved it in water by ultrasound, high viscosity of GO made it concentrated again and difficult to disperse in PVA molecular when mixed with PVA powder. Inhomogeneous dispersion of GO may have some effect on mechanical properties of gels.

3.3.5 Control of water content of PVA-GO hydrogels

Water content (WC) of hydrated gels of different annealing conditions were shown in Fig. 3.14. It could be observed that by changing heating temperature, WC could be controlled from about 35% to 65%. By annealing treatment, microcrystals of the gels grew, and became difficult to cleave when swelling. On the other hand, because the distance between microcrystals became shorter, there was less space for holding on the water, causing a decrease on water content. It was also found that GO composited hydrogels showed a slight increase in WC compared to pure PVA hydrogels. Since it was heated on vacuum, the oxygen functional groups of GO were retained. The increase on WC may be due to the oxygen functional groups of GO

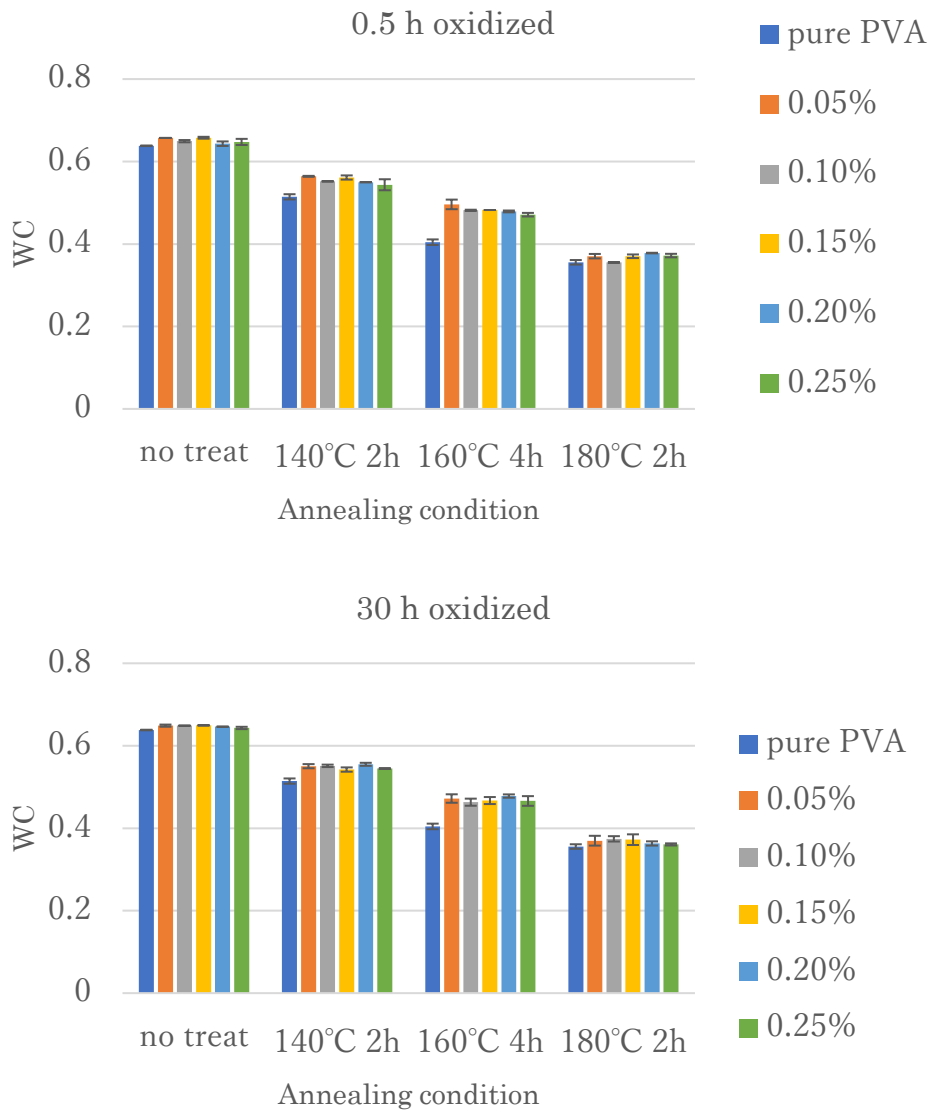


Fig.3.14 WC of hydrogels by each annealing condition

3.3.6 Tensile test of hydrated hydrogels

It is known from the previous section that although samples were heated at same temperature, difference in WC will still exist. Since water content (WC) has great influence on mechanical properties of hydrogels, it is meaningless to compare samples with different WC. Therefore, under each annealing condition we prepared multiple samples to ensure that each hydrogel with similar WC can be obtained. Young's modulus of each hydrogel with different GO content at similar WC were shown in Fig.3.15. GO composited hydrogels with both two oxidation time of GOs showed the same tendency that Young's modulus of GO composited hydrogels were higher than that of pure PVA hydrogels at similar WC. In addition, The increase in Young's modulus seemed to reach the highest near 0.15% concentration of GO and then trend to decrease with the increasement of GO concentration. Since GO and PVA molecules were combined through hydrogen bonds, the intermolecular force became stronger. As a result, the hydrogel received a stronger force when stretching, resulting in the increase of Young's modulus. However, over a certain concentration, the excessive GO may cause defect intermolecular, resulting in the decrease on Young's modulus. Moreover, the breaking strengths were measured to evaluate the mechanical strength of each hydrogel.

The results of breaking strength of two different heating conditions were shown in Fig. 3.16. From the result, it was found that the breaking strength had a significant decrease with the addition of GO. This may be due to the inhomogeneous dispersion of GO, which was observed from TEM images before. The possible network structures of PVA-GO hydrogels were shown in Fig. 3.17. Ideally, single layer of GO molecules would be evenly dispersed in the gel and combine with PVA molecules through hydrogen bonds. In fact, however, GO was easy to aggregate itself and caused the heterogeneous dispersion. When applying force to such a structure shown in Fig.3.17. right, initial cracks appeared on the parts of GO aggregation with very small force. The gels easily broke and showed very low breaking strength.

In addition, the effect of oxidation time of GO on Young's modulus was also investigated. The results were shown in Fig. 3.18. For a more intuitive comparison, we compared sample with different GO concentration at both high and low WC. Hydrogels with low water content were observed to have

high Young's modulus values and it was intuitively observed that the addition of GO(0.5h) can improve the Young's modulus better than GO(30h), indicating that 0.5h oxidated GO had more stable combinations with PVA molecules. Considering the results of XPS of GO, 0.5h oxidized GO was found to have two times larger amount of hydroxyl groups than that of 30h oxidized GO. Hydroxyl groups of GO seemed to have better combinations with PVA molecules than other functional groups such as carboxyl groups and carbonyl

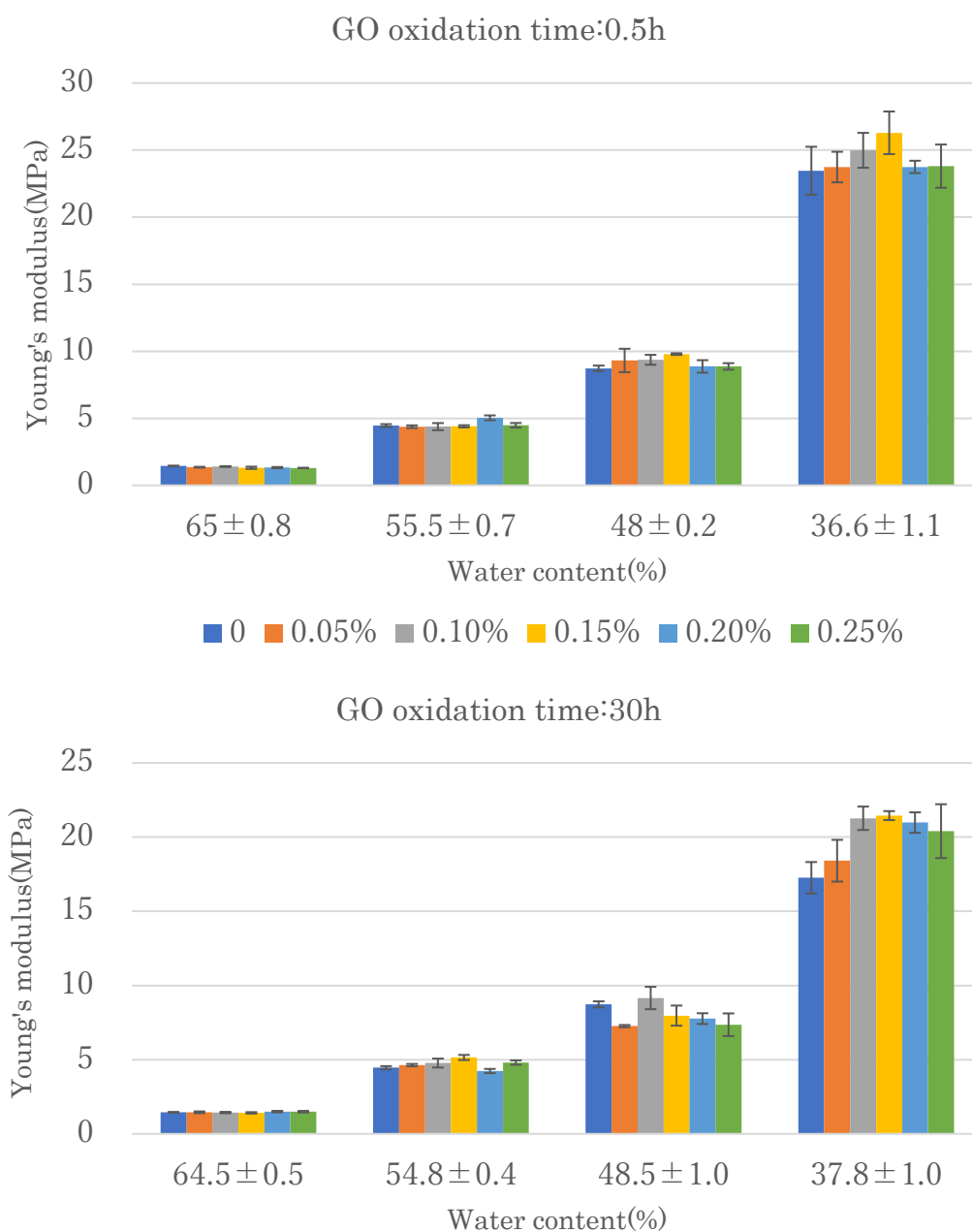


Fig.3.15 Young's modulus at similar WC

groups.

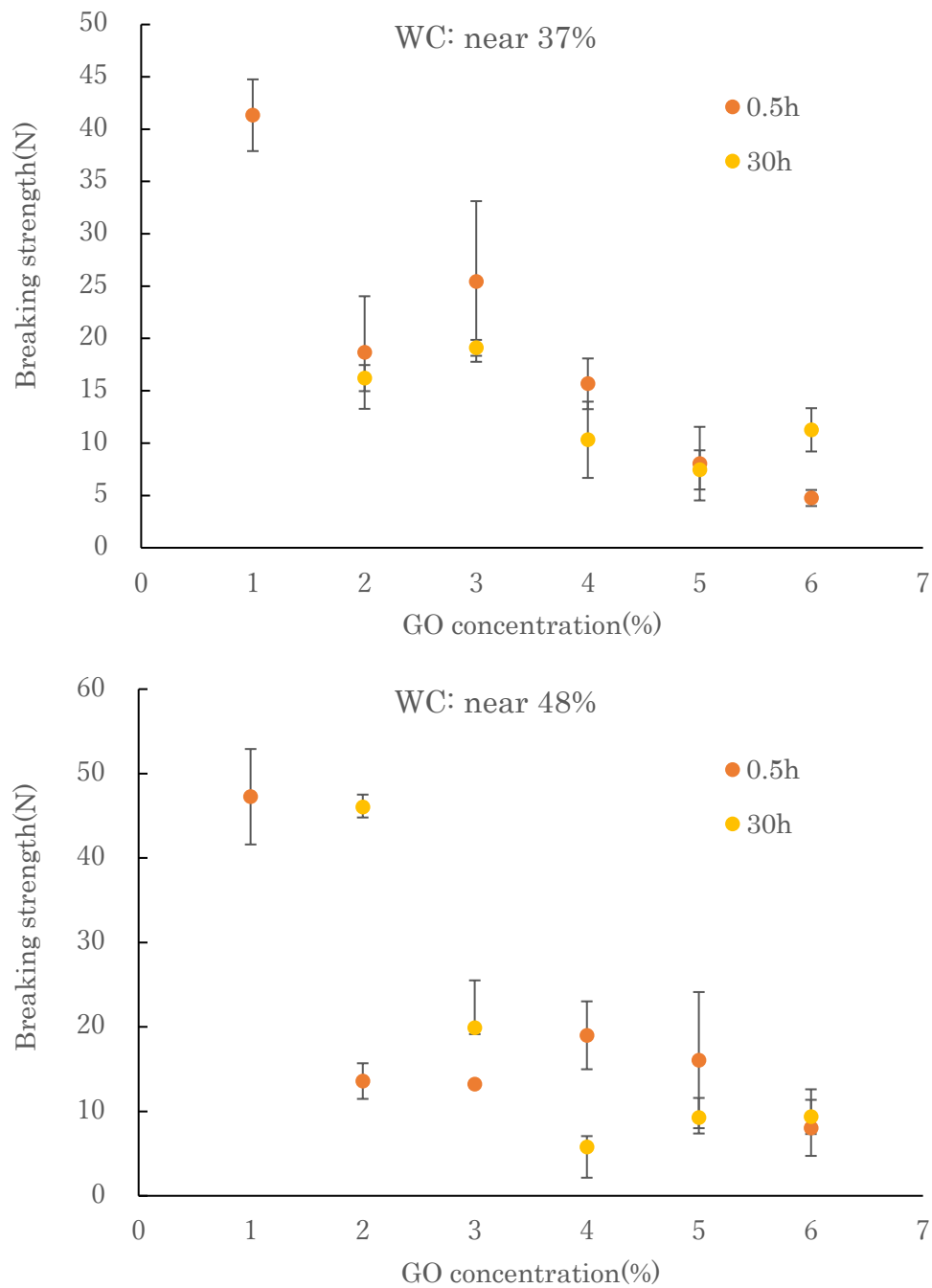


Fig. 3.16 Breaking strength of each hydrogel

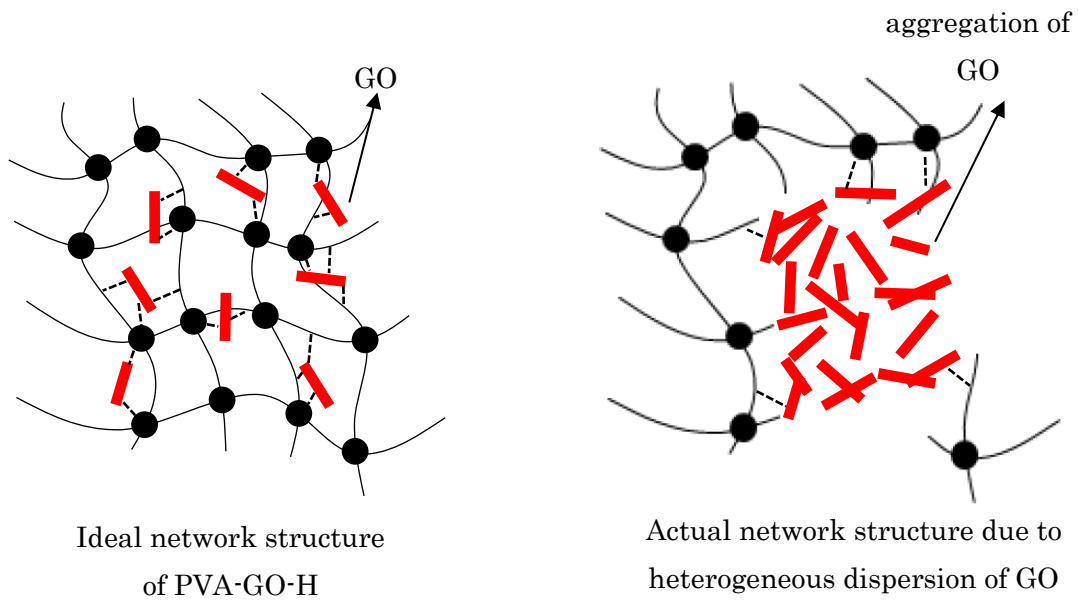


Fig. 3.17 Possible network structure of GO composited PVA hydrogel

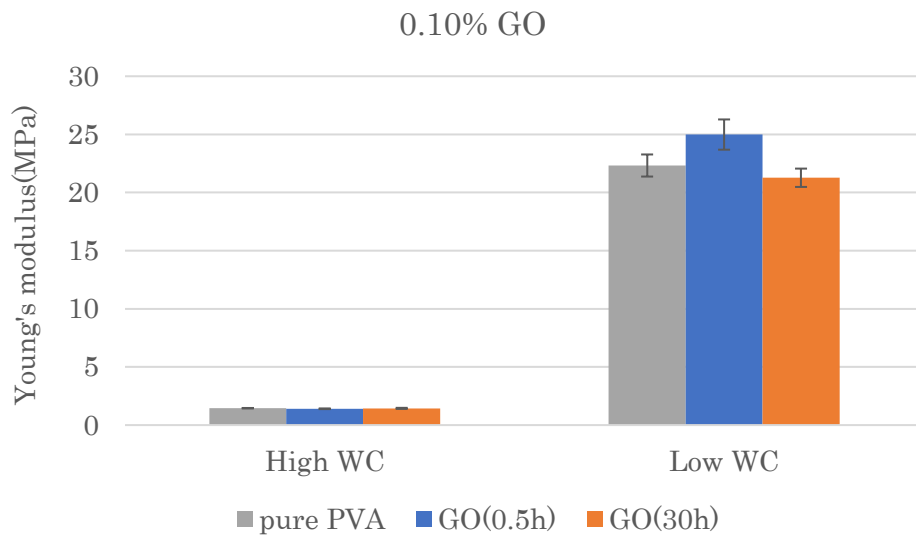


Fig. 3.18 Young's modulus of gels of different GO oxidation time at a high and low WC

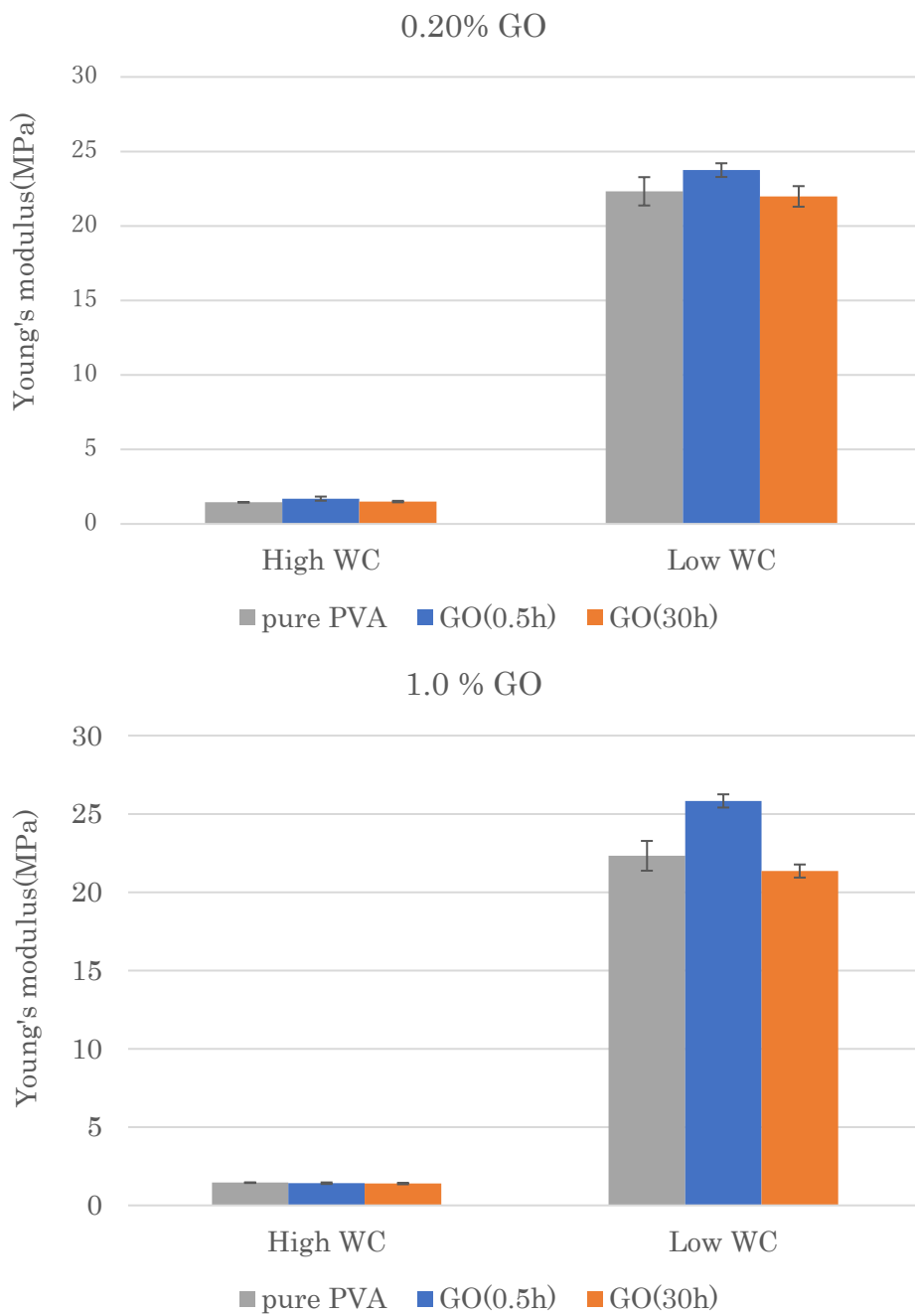


Fig. 3.18 Young's modulus of gels of different GO oxidation time at a high and low WC

3.3.7 DMA

Dynamic viscoelasticity of gels on temperature dispersion was measured from 25 to 100 °C. Loss tangent ($\tan\delta$) of hydrogels with 0.5 h oxidated GO composited with different GO concentration at a temperature range of 25 to 70 °C, for example, was shown in Fig. 3.19. Within this temperature range, each curve clearly showed a peak, which was treated as glass transition temperature T_g . The obtained T_g of each sample were shown in Fig. 3.20. From the result, T_g were significantly reduced by adding GO, especially 0.5 h oxidated GO. There were many factors for the decrease of T_g such as the flexibility of molecular chain, decrease on molecular weight, addition of plasticizer, and so on. It was inferred that the decrease in T_g was due to the increase in molecular flexibility in this study. Flake GO molecules were combined with PVA chains through hydrogen bonds in amorphous parts and played a role as a plasticizer in some way.

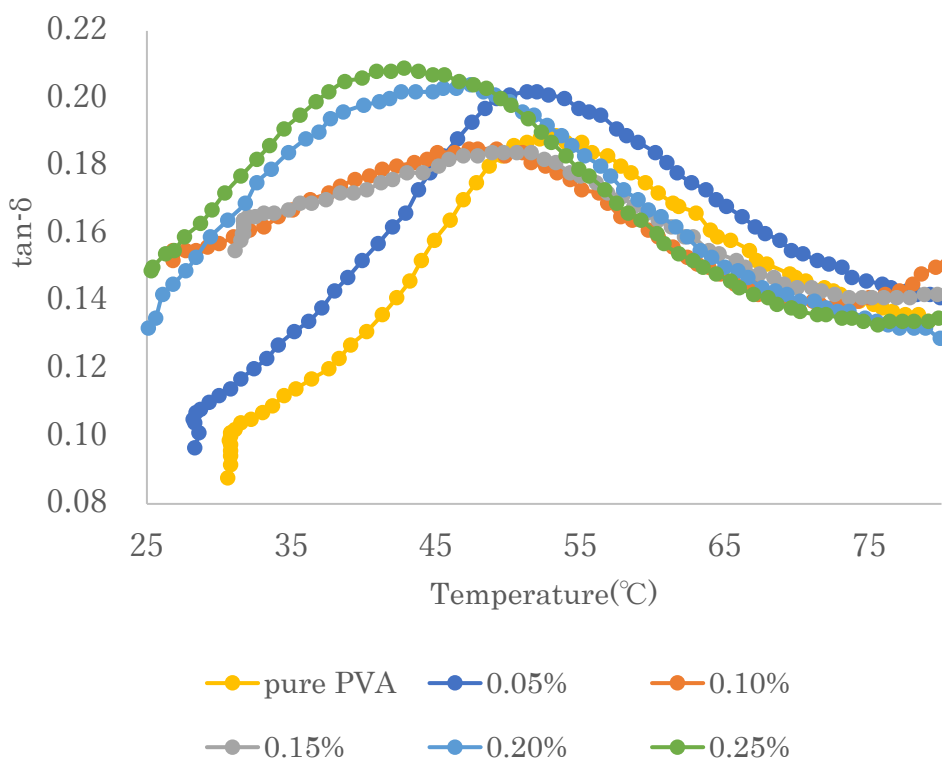


Fig. 3.19 $\tan\delta$ on temperature dispersion of each sample

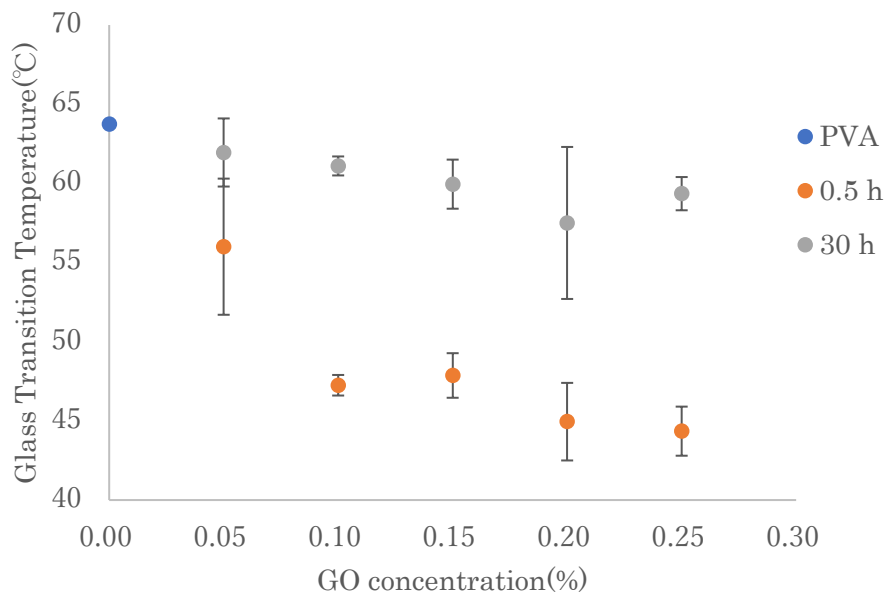


Fig. 3.20 T_g of each gels at various GO concentrations

3.3.8 Contact angel measurement

Results of contact angles of hydrogels were shown in Fig. 3.21. It was found that the surface of GO composited hydrogels exhibited hydrophobicity with increasing GO concentration compared to that of pure PVA hydrogel. It seemed that the hydrophilic part of PVA and GO formed hydrogen bonds and the hydrophobic part of GO was exposed on the surface. Moreover, a slight increase on contact angle was observed in the samples of 30 h oxidated GO, compared to that of 0.5 h oxidated GO. significant difference was observed for different oxidation times of GO. This may be due to the difference in the number of oxygen functional groups GO.

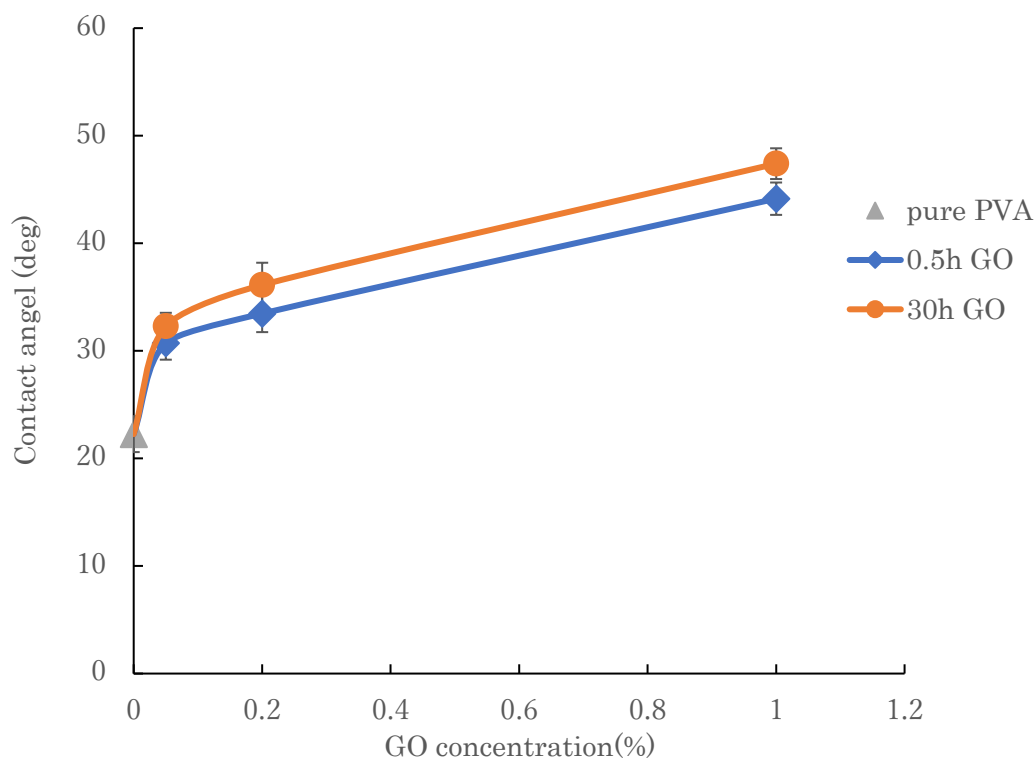


Fig. 3.21 Contact angles of samples with different GO concentrations

3.3.9 Protein absorption test

Concentrations of protein absorbed on unit surface area of each sample were shown in Fig. 3.22. From the result, it was found the gels absorbed more protein as GO concentration increased, indicating that GO attached to the surface can improve the absorption of protein of PVA hydrogels. Besides, oxidation of GO seemed to have no effect on protein absorption. GO composited gels were expected to have better cell attachment due to the surface properties including hydrophilicity and protein absorption.

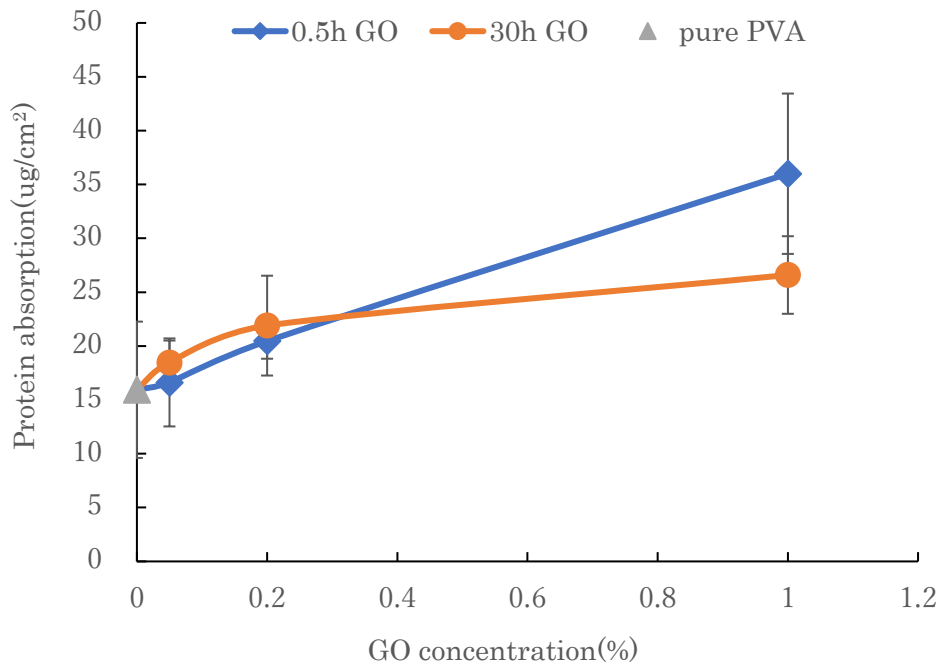


Fig. 3.22 Protein absorption of samples with different GO

3.3.10 Cell culture

Fig. 3.23 showed the fluorescence observation of PVA hydrogels and two kinds of GO composited hydrogels after 3 days culturing. It can be clearly seen that more cells adhered to the GO composited samples than to the pure PVA sample. In addition, it was found that high GO concentration led to more cell adherent. The result of cell counting were shown in Fig. 3.24, which basically consistent with the results of fluorescence observation. It was inferred that the high error occurred in 1.0% GO concentration in cell counting was due to the fact that the cells aggregated only in the part where GO exposed. However, the effect of GO oxidation time on cell adherence was not clear from these results

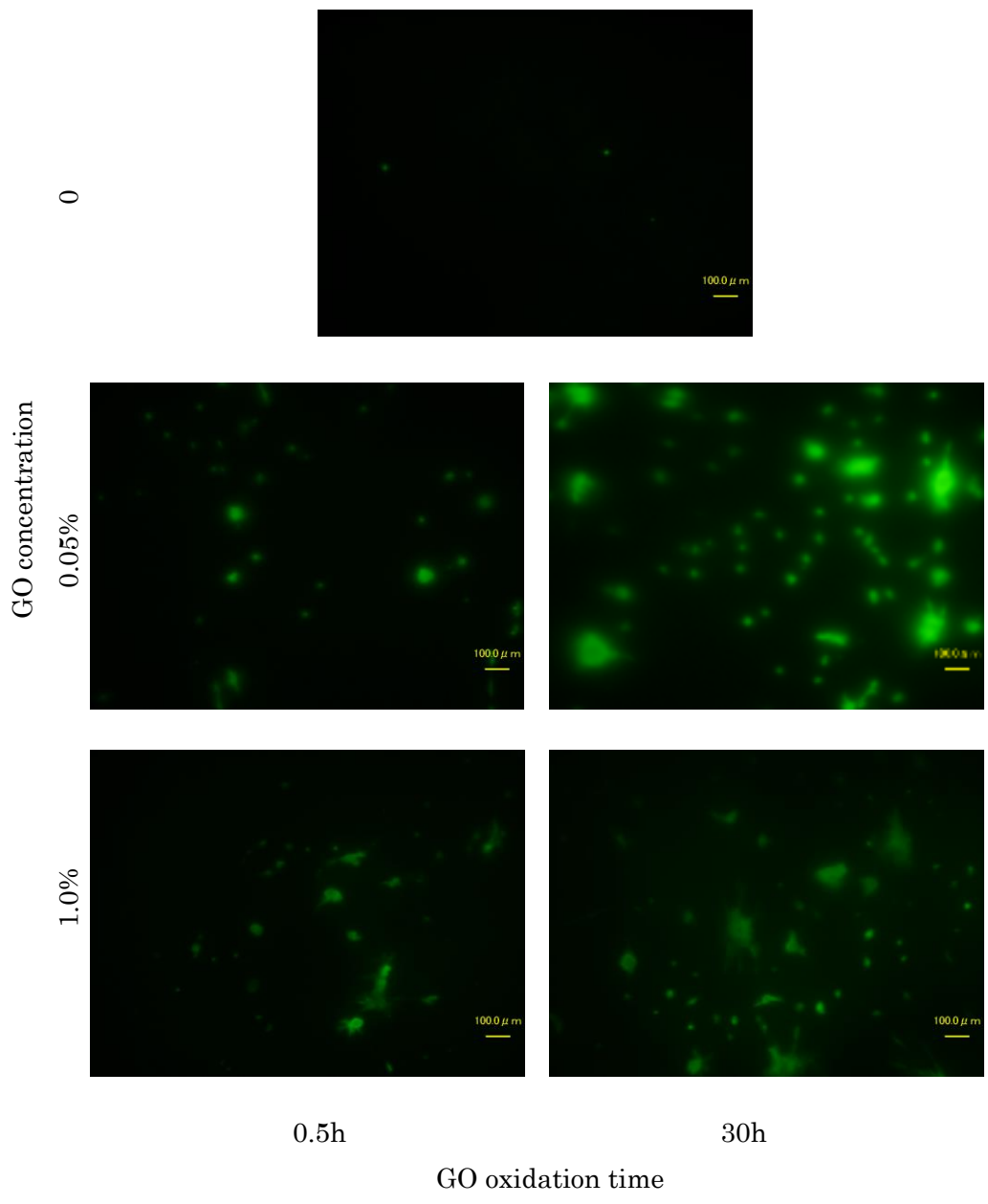


Fig. 3.23 Fluorescence observation

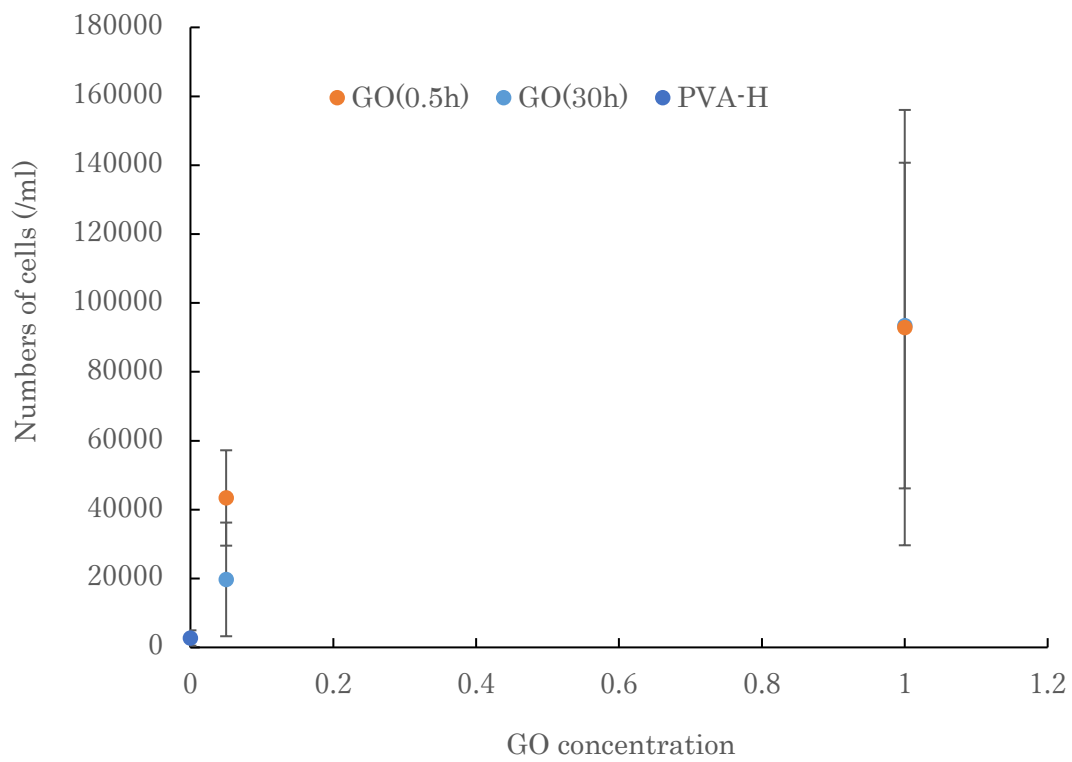


Fig. 3.24 Cell counting after 3 day culture

3.4 Conclusion

Physically crosslinked PVA-GO-H has been successfully prepared by the novel hot pressing method. By analyzing the morphology of hydrogels, no visible porous structure was seen, GO was found to irregularly distribute on the surface of gels like a layer.

WC of hydrogels can be controlled by annealing treatment. By comparing Young's modulus at same WC, GO was found to have a reinforcing effect on the Young's modulus. In addition, 0.5h oxidized GO was found to have better combinations with PVA than 30h oxidized GO due to more hydroxyl groups, resulting in higher Young's modulus. Unexpectedly, however, gels with GO composited showed low tensile strength, which may be due to the aggregation of GO.

By DMA, Tg was found to decrease with the GO concentration increasing. It was inferred that GO molecules were combined with PVA chains through hydrogen bonds and molecular flexibility increased accordingly, leading to the decrease on Tg.

By contact angle measurement and protein absorption test, GO composited gels showed more hydrophobicity and more protein affinity. These facts may affect cell adherence. Therefore, more cells were observed to adhere to GO composited PVA-H than to pure PVA-H at initial cell culture.

In conclusion, GO composited PVA-H showed high Young's modulus and high cell affinity. If GO can distribute more uniformly in the gel

If the problem of non-uniform dispersion of GO in gel was solved, it will become an excellent artificial articular cartilages material with high strength and high biocompatibility.

References

1. Sakaguchi T, Nagano S, Hara M, et al. Facile preparation of transparent poly (vinyl alcohol) hydrogels with uniform microcrystalline structure by hot-pressing without using organic solvents[J]. Polymer journal, 2017, 49(7): 535-542.
2. Qi Y Y, Tai Z X, Sun D F, et al. Fabrication and characterization of poly (vinyl alcohol)/graphene oxide nanofibrous biocomposite scaffolds[J]. Journal of applied polymer science, 2013, 127(3): 1885-1894.
3. Liang J, Huang Y, Zhang L, et al. Molecular - level dispersion of graphene into poly (vinyl alcohol) and effective reinforcement of their nanocomposites[J]. Advanced Functional Materials, 2009, 19(14): 2297-2302.
4. Kawamura F, Hinode K, Miyashita T, et al. Effect of Cooling Conditions of Gelatin Sols on the Formation of Gels[J]. Journal of Home Economics of Japan, 1993, 44(5): 363-368.
5. Ohkura M, Kanaya T, Kaji K. Gelation rates of poly (vinyl alcohol) solution[J]. Polymer, 1992, 33(23): 5044-5048.
6. Shibata M, Nishida K, Koga T. Device for Simultaneous Measurements of Viscosity and Light Transmittance with Example of Application[J]. JOURNAL OF FIBER SCIENCE AND TECHNOLOGY, 2019, 75(5): 58-62.
7. Smith P K, Krohn R I, Hermanson G T, et al. Measurement of protein using bicinchoninic acid[J]. Analytical biochemistry, 1985, 150(1): 76-85.

*Chapter 4 Preparation
and characterization of
monovalent metal salt
composited PVA-H by
hot pressing method*

4.1 Introduction

In chapter 3, GO composited PVA-H were prepared by hot pressing method. However, since the gelation was not in water environment, there was a big problem with the dispersion of GO. Unlike GO, inorganic salt, as small molecule compound, was supposed to have better dispersion in gels. As a result, we tried to prepare salt composited PVA-H by the novel hot pressing method. In this chapter, monovalent metal salt will be used for composite.

In previous studies, monovalent metal salt, especially Li salt, was always used for plasticizer in gels or films [1,2]. Some found that the addition of inorganic salts into aqueous solutions of PVA will change the mechanical properties of cryogels obtained from these solutions, an outcome that can be attributed to a change in the crystallinity of the polymer under the action of salt additives [3]. Furthermore, S.A. Zagorskaya et al. [4] compared the effects on crystallization of adding various kinds of halide salts of alkali metals and found that the size of cation and anion would influence the affinity of oxygen atom of OH group of polymers to affect the crystallization of PVA film. Na salt such as NaCl, was also reported to be used in PVA gels [5]. It was found that the properties of microcrystallites due to hydrogen bonds between -OH groups and PVA depended strongly on NaCl concentration and swelling ratio and breaking stress increased at low NaCl concentration. Almost all of these films or gels were prepared in water environment. It was known to all that each monovalent cation was able to be surrounded by six water molecules [6]. Monovalent cations can affect the crystallization of gels predictably by the competition of water molecules with polymer.

In this study, however, the theories above may not apply to hot pressing method because gels were obtained with a quite high PVA concentration (50 wt%). We would use various of monovalent metal salt as composites, to prepare PVA hydrogels by hot pressing method. The properties of each gel would be evaluated to analyze the effect of salt. In addition, for the application for artificial cartilage material, biocompatibility was evaluated by cell protein absorption test and cell culture.

4.2 Materials and methods

4.2.1 Preparation of pure PVA-H

In chapter 3, I used PVA of high degree of polymerization (DP) to get better combination of graphene oxide (GO). In this chapter, inorganic salt was used as composited material and PVA of normal DP (1700) was used. According to previous study [7], the optimum concentration of PVA was reported as 50%, and the optimal conditions for preparation were found to be 95 °C and 30 min with a pressure increase from 2 MPa to 20 MPa. We imitated these conditions to prepare PVA-H. The procedure was shown below:

1. 25g of PVA powder (DP: 1700, DS: 99.0%) was mixed with 25g of distilled water in a polyethylene bottle and mixed well.
2. After 10 min swelling, the mixture was well dispersed in a metal frame mold sandwiched by two silicon sheets
3. The mold was then placed in hot pressing machine at 95 °C temperature and 2-20MPa pressure for a total 30 min (2 MPa for 5 min, 10 MPa for 10 min, and 20 MPa for 15 min)
4. After heating and pressing, hydrogels enclosed by silicon sheets were taken out and were allowed to gelate in zipper bags for two days
5. The obtained hydrogels were exposed to air and kept at room temperature for 3 days
6. Then the hydrogels were further dried under vacuum for 3 days to remove water remaining in the gels
7. The obtained dried gels were immersed in distilled water for 3 days to rehydrate.

The gels obtained in step 6 were call “dried gels” while the gels obtained in step 7 were called “hydrated gels”.

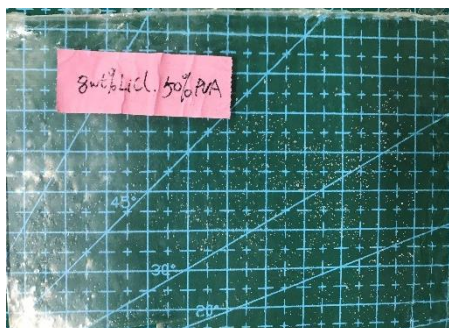
4.2.2 Preparation of salt composited PVA-H

In this chapter, six kinds of monovalent metal salt (LiCl, LiBr, NaCl, NaBr, KCl, KBr) were composited to PVA hydrogels. I used the same conditions for preparation mentioned above. In addition, after hydrating, the salt in hydrogels may elute in solvent over time, which was not beneficial for biocompatible materials. Taking this into consideration, a desalting treatment was carried out to remove the salt inside the gels. The procedure was shown below:

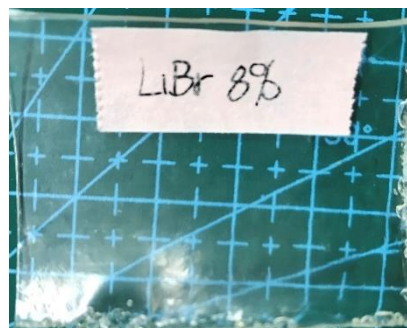
1. Different concentrations of salt solutions were prepared with different kinds of salts
2. 25g of PVA powder (DP: 1700, DS: 99.0%) was added into 25g of obtained salt solution in a polyethylene bottle and mixed well
3. After 10 min swelling, the mixture was well dispersed in a metal frame mold sandwiched by two silicon sheets
4. The mold was then placed in hot pressing machine at 95 °C temperature and 2-20 MPa pressure for a total 30 min (2 MPa for 5 min, 10 MPa for 10 min, and 20 MPa for 15 min)
5. After heating and pressing, hydrogels enclosed by silicon sheets were taken out and were put into zipper bags for gelation for two days
6. The obtained hydrogels were exposed to air and kept at room temperature for 3 days
7. Then the hydrogels were further dried under vacuum for 3 days to remove water remaining in the gels
8. The obtained dried gels were immersed in distilled water for 3 days to rehydrate.
9. Then, the hydrogels were stirred in distilled water for a week, during which the distilled water should be changed every day
10. After that, the desalted hydrogels were dried on air and then dried on vacuum to get dried desalted hydrogels for further experiment

Same as above, the gels obtained in step 7 were call “dried gels” while the gels obtained in step 8 were called “hydrated gels”. In addition, the gels obtained in steps 9 and 10 were called “hydrated desalted hydrogels” and “dried desalted hydrogels” respectively.

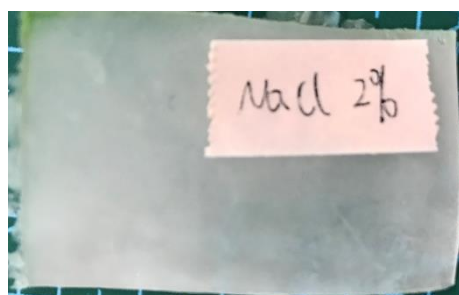
The exterior of obtained dried hydrogel was shown in Fig. 4.1. Samples with Li salt composited were observed to be clean and transparent (a, b) even at high salt concentration (8%). Samples with NaCl and KCl composited, however, were found to be opaque even at a low salt concentration (c, d). For NaBr and KBr composited gels, white turbidity appeared as the salt concentration increasing. In KBr-added gels, white turbidity appeared when KBr concentration was over 5%, and in NaBr-added gels, the concentration was 8%, correspondingly. It needed to be pointed out that water evaporated a lot from such gels when drying on air thus white turbidity was formed on the surface during drying. From the result, both anion and cation can interact with water molecules. They can break hydrogen bonds of water and form $\text{OH}\cdots\text{X}^-$ or $\text{M}^+\cdots\text{OH}$ bonds [4]. If there were a great difference on bond strengths between anions and cations, water molecules would depart, leading to evaporation of water during gelation.



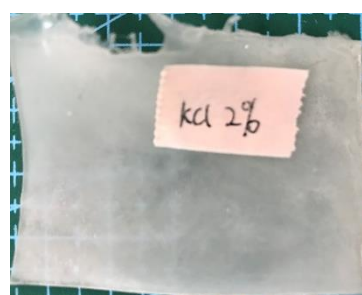
a



b



c



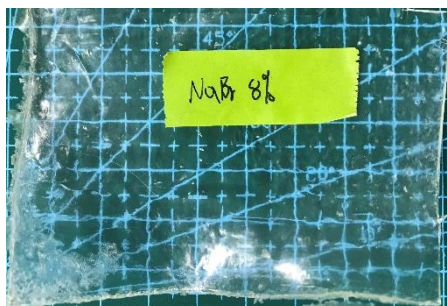
d



e



g



f

Fig. 4.1 Photos of each sample after drying.

4.2.3 Determination of PVA content by mass measurement

Since there were no mass changes of PVA before and after heating and compressing, the mass change in samples can be regarded as the result of evaporation or acquisition of water. Therefore, PVA concentrations of obtained hydrogels can be calculated by measuring the mass of the samples before and after preparation. PVA concentration of dried hydrogels (ω_p) can be calculated by the following formula:

$$\omega_p = \frac{0.5 \times W_{\text{total}}}{W_{\text{dry}}} \times 100\%$$

where W_{total} is total weight used for preparation, and W_{dry} is the weight of dried hydrogel.

Equally, there were no mass changes of salt before hydrating. Water concentration of dried hydrogels (ω_w) can be calculated by the following formula:

$$\omega_w = 1 - \frac{(0.5 + \omega_{\text{salt}}) \times W_{\text{total}}}{W_{\text{dry}}} \times 100\%$$

where ω_{salt} is salt concentration used for preparation, W_{total} is total weight used for preparation, and W_{dry} is the weight of dried hydrogel.

4.2.4 FTIR spectra

IR spectra of each dried hydrogel were recorded in the range 4000-400 cm^{-1} . The values of A_{1640}/A_{1088} and A_{1144}/A_{1088} can be regarded as relative water content (WC) [8] and relative degree of crystallization (DC) [9], respectively. This study was not for quantitative analysis of WC or DC. Therefore, values of A_{1640}/A_{1088} and A_{1144}/A_{1088} of each hydrogel were used as WC and DC of samples respectively, to evaluate the effect of the addition of salt. In addition, we also measured WC and DC of desalted hydrogels to get further understanding of the effect of salt.

4.2.5 Swelling ratio of hydrated hydrogels

In order to distinguish the water concentration mentioned in the first two bars, we used swelling ratio to evaluate the water content of hydrated hydrogels. Swelling ratio (SR) of samples was calculated by the following formula:

$$SR = (W_{\text{wet}} - W_{\text{dry}})/W_{\text{dry}}$$

where W_{wet} is the weight of samples after swelling equilibrium and W_{dry} is the weight of dried samples. Each hydrogel was tested for three times.

4.2.6 EDS analysis

Energy Dispersive X-ray Spectroscopy (EDS) analysis was carried out using TM3030plus to observe the dispersion of salt in the gels. The cross sections of each gel were also observed to analysis the vertical distribution of salt. In addition, dried gels before and after desalting were both observed to evaluate the effect of desalination.

4.2.7 Tensile test

The tensile mechanical properties of the hydrogels were determined by tensile test underwater. The samples were cut to JIS dumbbell 7 type specimens. An initial load of 0.01 N was applied to eliminate the effect of deflection of the gels. The test was performed at the speed of 5 mm/min and was repeated 5 times to ensure reproducibility. In addition, both hydrated gels and desalted hydrated gels were tested to evaluate the effect of desalination.

4.2.8 DSC

Thermograms were obtained on Exstar6000. Each sample was cut into a small circular piece with a mass within 10 mg. Differential scanning calorimetry (DSC) measurement was carried out from 25-300 °C at a heating rate of 10 °C/min. In addition, both hydrated gels and desalted gels were tested.

4.2.9 DMA

Dynamic mechanical analysis (DMA) of dried gels was carried out by using Rheosol-G5000. Samples were cut to 5 mm × 30 mm rectangles. Considering that the addition of salt may lower the glass transition temperature of hydrogels, dynamic viscoelasticity of gels on temperature dispersion was measured from -20 – 100 °C utilizing liquid nitrogen. Heating rate was set up to 3 °C/min and frequency was 1 Hz.

4.2.10 Protein absorption test

Desalted hydrated hydrogels were used for protein absorption test. As mentioned in chapter 3, protein concentrations were determined by a bicinchoninic acid (BCA) assay [10], using an albumin BSA standard curve according to the manufacturer's instructions (Thermo Fisher Scientific). The absorbance of BCA solutions was measured at 562 nm using a microplate reader. Three identical samples were tested one time for average and each sample were tested three times.

4.2.11 Cell culture

Biocompatibility of gels was evaluated by cell culture. First the gels were immersed in 70% ethanol for 2 days to sterilize and then immersed in Dulbecco's modified eagle medium (DMEM) for 1 day to rehydrate. After that Osteoblast cells MC3T3 were seeded on gels to evaluate cell attachment and proliferation. The rehydrated gels were placed in the well of a 24-well multiplate. Then, 1 mL of a suspension of osteoblast (2×10^4 cells per mL) in DMEM containing 10% fetal bovine serum (FBS) was added to the well. The cells were then cultured at 37 °C in 5% CO₂ for 3 days. After culturing, the cells were fluorescently stained by Calcein-AM (Dojindo, Kumamoto, Japan), and the fluorescence of cells attached to the gels was observed with a fluorescence microscope (Biozero, Keyence, Osaka, Japan).

4.3 Results and discussion

4.3.1 Determination of PVA content by mass measurement

Calculated PVA concentration and water concentration of dried hydrogels were shown in Table 4.1. It was found that although the initial PVA concentration was 50 wt% when heating and compression, with the addition of salt, PVA concentrations of dried samples gradually decreased.

The changes of water concentration and ratio of PVA to water with addition of salt were shown in Fig. 4.2 and Fig. 4.3, respectively. For Li salt composited hydrogels, a certain improvement but no obvious pattern on water concentration were observed. Besides, the ratio of PVA to water significantly decreased, indicating that the gels became soft with Li salt composited.

For Na and K salt composited hydrogels, as mentioned before, water evaporated a lot when dried on air, resulting in a significant decline on water concentration. The ratio of PVA to water also increased as a result. It was inferred that Na^+ and K^+ ions were not only hard to combine with PVA molecules, but also impede the combination of PVA and water molecules. As a result, water molecules failed to form microcrystals with PVA and evaporated continuously.

Table 4.1 PVA concentration, water concentration and mass ratio of PVA to water

additives	concentration of salt		dried hydrogels		
	wt%	mol/kg	PVA concentration (%)	water concentration (%)	PVA/H ₂ O (wt%)
pure PVA	0	0	91.90	8.10	11.34
LiCl	0.42	0.10	89.11	10.14	8.79

LiCl	1.70	0.40	87.01	10.04	8.66
LiCl	2.00	0.47	87.04	9.47	9.19
LiCl	3.39	0.80	82.99	11.39	7.29
LiCl	5.00	1.18	78.99	13.11	6.02
LiCl	8.00	1.89	68.26	20.82	3.28
LiBr	0.87	0.10	88.23	10.24	8.62
LiBr	2.00	0.23	87.70	8.80	9.97
LiBr	3.47	0.40	85.20	8.88	9.60
LiBr	5.00	0.58	82.31	9.46	8.70
LiBr	8.00	0.92	76.80	10.91	7.04
LiBr	10.42	1.20	74.07	10.49	7.06
NaBr	1.03	0.10	89.00	9.17	9.70
NaBr	2.00	0.19	87.70	8.79	9.97
NaBr	4.12	0.40	84.32	8.74	9.65
NaBr	5.00	0.49	83.21	8.47	9.82
NaBr	8.00	0.78	78.36	9.10	8.61
NaBr	10.29	1.00	76.46	7.80	9.80
KBr	1.19	0.10	87.95	9.96	8.83
KBr	2.00	0.17	88.30	8.17	10.81
KBr	5.00	0.42	85.32	6.15	13.88
KBr	5.95	0.50	82.81	7.34	11.28

KBr	8.00	0.67	81.35	5.63	14.45
KBr	9.52	0.80	79.54	5.32	14.96

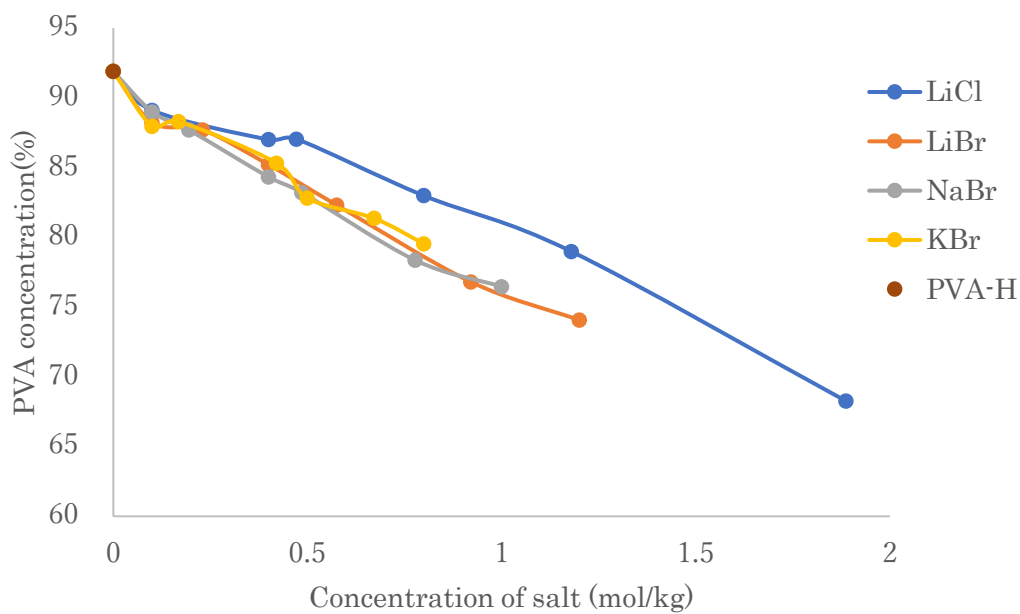


Fig. 4.2 PVA concentration of each sample

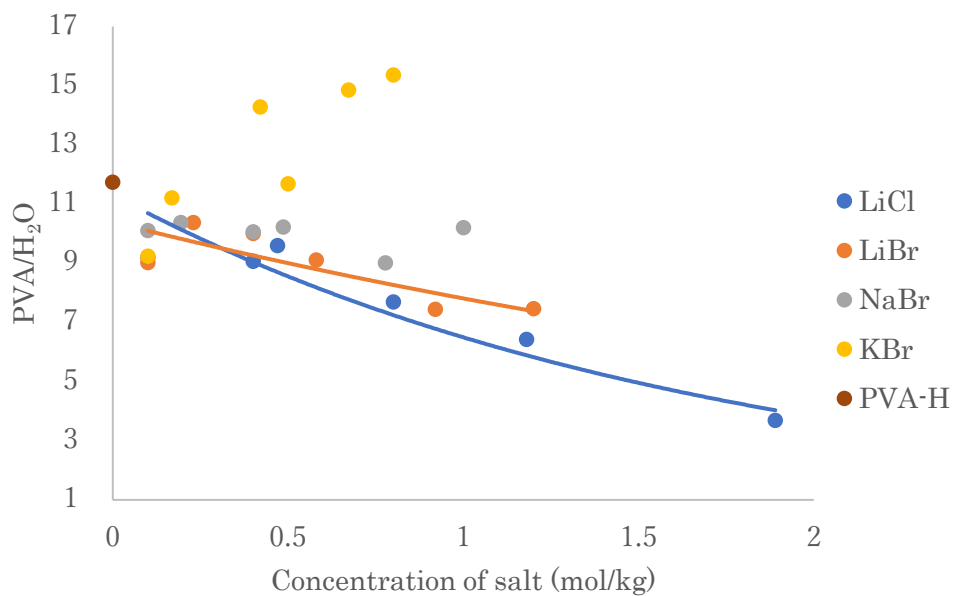


Fig. 4.3 Ratio of PVA to H₂O of each sample

4.3.2 FTIR

Fig. 4.4 showed the absorption bands of pure PVA and LiCl, for example, at the range $1800 - 930 \text{ cm}^{-1}$. No obvious peaks appeared, indicating salt was successfully composited to PVA hydrogel.

The relative degree of crystallization (A_{1144}/A_{1088} , DC) and relative water content (A_{1640}/A_{1088} , WC) of gels before and after desalted were shown in Table.4.2. From the result, Li salt composited gels showed a decrease on DC and an increase on WC. To explain this, we must start with the gelation process in hot pressing method.

Without adding salt, PVA combined well with water molecules by hydrogen bonds. Some parts of polymer began to crystallize in a certain condition (in this study, heat and compress), and some water molecules formed microcrystals with PVA molecules. During drying, some of the water that didn't form microcrystals would evaporate. On the one hand, when Li salt was added, since Li^+ ions were not able to form network structure with PVA molecules, instead, the addition of Li^+ impeded the combination of PVA and water molecules, the opportunity for PVA intermolecular to forming microcrystals became lower, causing a decrease on the size of microcrystal. On the other hand, a large number of water molecules were locked in PVA amorphous due to the presence of Li salt, resulting in an increase in volume of network structure. Therefore, DC considerably decreased, and WC increased simultaneously. The decrement in WC changes of LiCl and LiBr may be due to the size of cation of Cl^- and Br^- . Cl^- ions can retain more water molecules than Br^- ions because of the higher bond strength of $\text{OH}\cdots\text{X}$ bonds. Since the white turbidities on Na and K salt composited gels may influence the result of IR, we just took transparent part for measurement. From the results of NaBr and KBr, DC was found to have an increase trend with the salt concentration arose, and DC of KBr-added gels was higher than that of NaBr-added gels. This might because Na^+ and K^+ ions had weak bond strength with water molecules compared to Li^+ , they were not able to retain water molecules in amorphous like Li^+ . As a result, the volume of network structure decreased because of evaporation of water during gelation. Finally, DC increased.

Considering that the crystallization of PVA-H may damage by drying again

after hydrating, we also measured DC and WC of pure PVA-H after an identical desalting treatment. The result showed a decrement on DC of pure PVA-H, indicating some crystallization might destroy by drying again. Although there was no obvious pattern observed in the changes of DC and WC from the result, all salt-added samples showed a trend that DC and WC became closer to that of pure PVA-H. This indicated the interactions between salt and PVA and the effect of desalination was confirmed at same time.

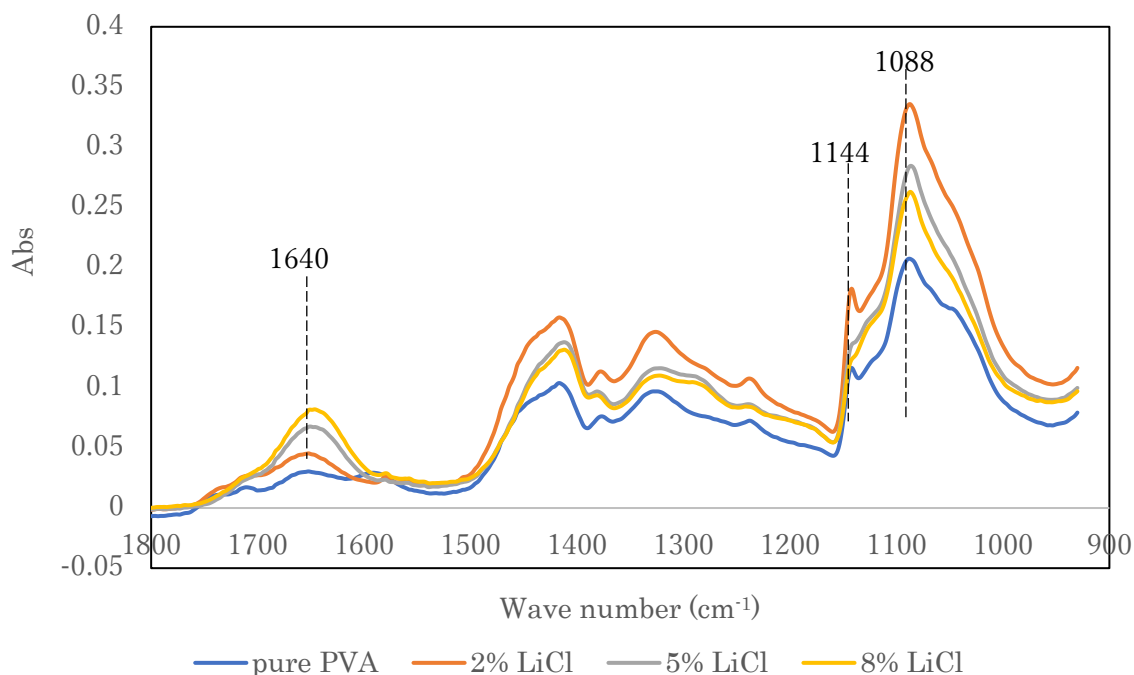


Fig. 4.4 FTIR spectrum of each LiCl –added sample

Table.4.2 DC and WC before and after desalted

Additives	concentration of salt		before desalted		after desalted	
	wt%	mol/kg	A_{1144}/A_{1088} (DC)	A_{1640}/A_{1088} (WC)	A_{1144}/A_{1088} (DC)	A_{1640}/A_{1088} (WC)
pure PVA	0	0	0.519	0.063	0.491	0.066
LiCl	0.42	0.10	0.527	0.067	0.497	0.073
LiCl	1.70	0.40	0.519	0.067	0.524	0.070
LiCl	2.00	0.47	0.508	0.112	0.513	0.060

LiCl	3.39	0.80	0.487	0.082	0.512	0.075
LiCl	5.00	1.18	0.442	0.193	0.511	0.069
LiCl	8.00	1.89	0.407	0.352	0.508	0.059
LiBr	0.87	0.10	0.499	0.069	0.513	0.073
LiBr	2.00	0.23	0.474	0.066	0.510	0.068
LiBr	3.47	0.40	0.498	0.061	0.516	0.062
LiBr	5.00	0.58	0.480	0.074	0.512	0.071
LiBr	8.00	0.92	0.452	0.116	0.517	0.070
LiBr	10.42	1.20	0.431	0.141	0.519	0.069
NaBr	1.03	0.10	0.506	0.047	0.527	0.059
NaBr	2.00	0.19	0.509	0.051	0.529	0.070
NaBr	4.12	0.40	0.527	0.058	0.531	0.068
NaBr	5.00	0.49	0.523	0.056	0.521	0.132
NaBr	8.00	0.78	0.567	0.081	0.557	0.062
NaBr	10.29	1.00	0.563	0.141	0.545	0.062
KBr	1.19	0.10	0.509	0.050	0.509	0.054
KBr	2.00	0.17	0.527	0.048	0.529	0.129
KBr	5.00	0.42	0.516	0.052	0.512	0.062
KBr	5.95	0.50	0.574	0.061	0.538	0.074
KBr	8.00	0.67	0.574	0.042	0.533	0.073
KBr	9.52	0.80	0.628	0.051	0.520	0.058

4.3.3 Swelling ratio of hydrated hydrogels

Obtained swelling ratios SRs of hydrogels of each salt composited were shown in Fig. 4.5. It was found that SR of all salt composited hydrogels exhibited a significant decrease with the increase of salt concentration. A part of the reason for the decrease of SR was that the water content in the samples were originally higher than pure PVA. By comparing WC of LiBr composited

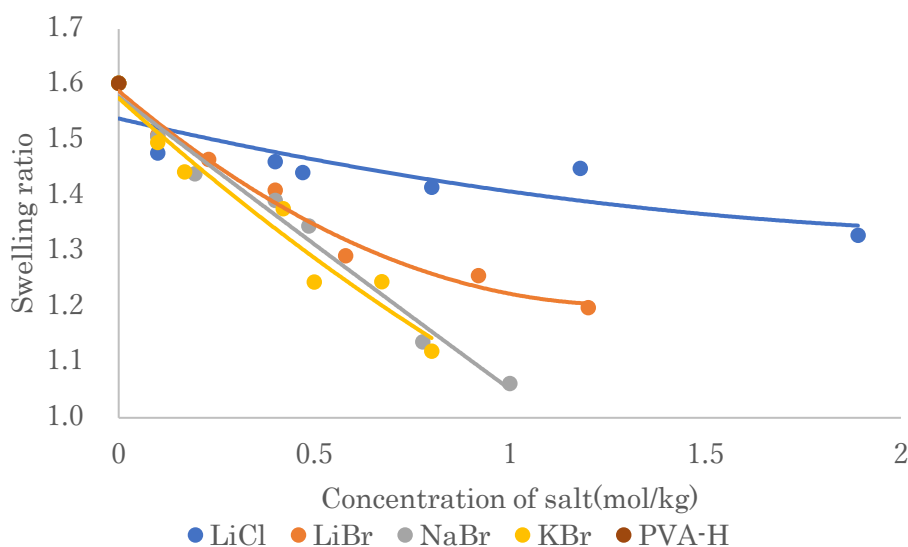


Fig. 4.5 SR at various salt concentrations

samples and pure PVA in Table 4.2, however, it was found that although WC of LiBr composited hydrogels kept a certain value around 10% despite of LiBr concentration, SR of LiBr composited hydrogels decreased obviously according to Fig. 4.5. It can be inferred that the addition of salt prevented water molecules from entering the network structure of gels when swelling.

4.3.4 EDS analysis

Fig. 4.6 showed SEM images of the surface (a) and cross section (b) of 8% LiCl-added hydrogel, for example, without desalting. Some impurity appeared thus an element distribution analysis by EDS was carried out to investigate the composition of it. The result was shown in Fig.4.7 and 4.8, which clearly reflected the distribution of elements on the yellow line. Counts per second (CPS) can be regarded as the relative concentration of the element. From the result, it was found that the impurity was mainly composed of C

atoms, indicating that PVA that incompletely reacted aggregated in the gels. The result of elements distribution in cross section was shown in Fig. Although there were some aggregations of PVA observed, Li and Cl were found to uniformly distribute on the yellow line. Concluded from the results above, salt distributed uniformly whether on the surface or in cross section of the gel.

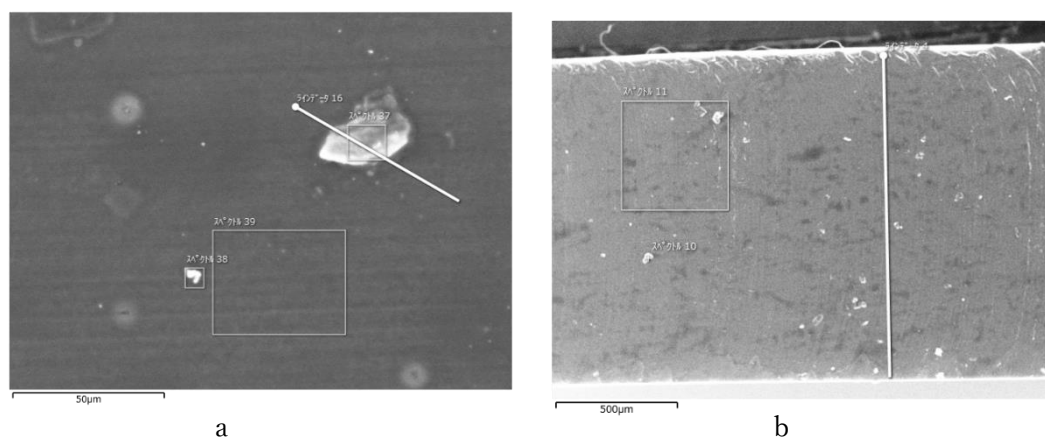


Fig. 4.6 SEM images of LiCl-added hydrogel
a: surface; b: cross section

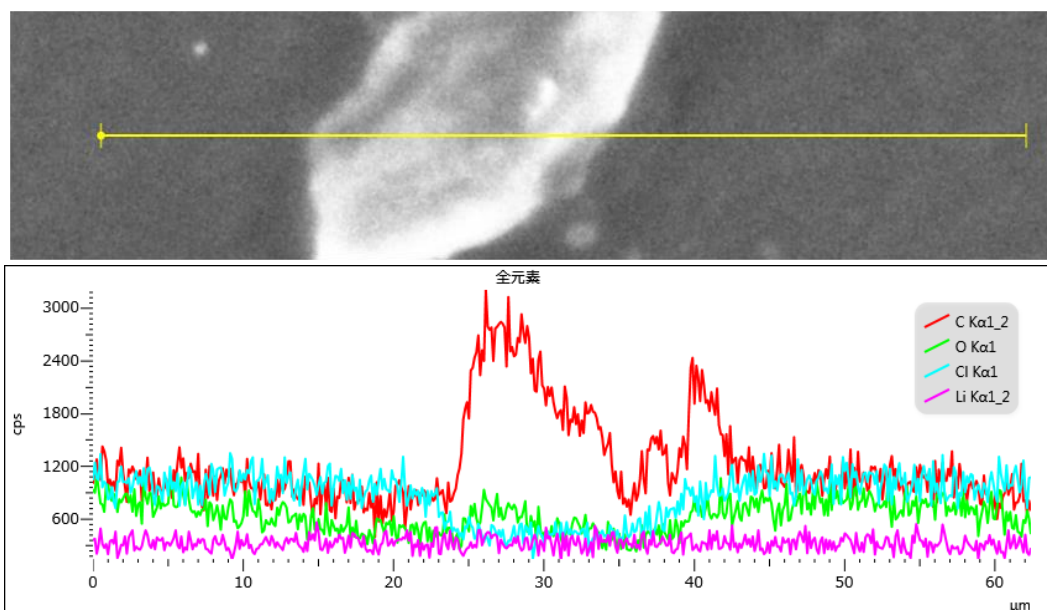


Fig. 4.7 Element distribution analysis of the surface of gel

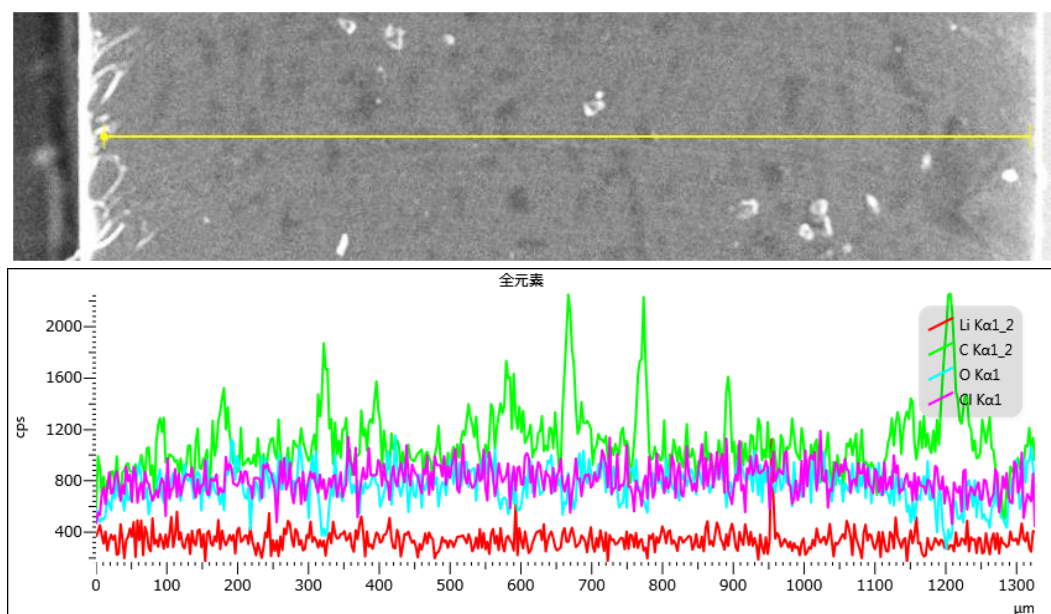


Fig. 4.8 Element distribution analysis of the cross section of gel

The results of element concentration of each gel before and after desalting were shown in Table 4.3. The corresponding energy in the X-ray spectrum of Li was too small and hard to distinguish by EDS. Therefore, Cl or Br concentrations were seen as relative salt concentration for Li salt composited hydrogels. From the result, although there were certain amounts of salt found in the gels before desalting, through the desalting treatment, salts were confirmed to be almost removed. The concern about the influence on biocompatibility by adding salt was solved.

Table 4.3 Element concentration before and after desalted

Samples	Element	Atomic % (before desalted)	Atomic % (after desalted)
8% LiCl	Cl	2.87	0.01
8% LiBr	Br	2.21	0.01
8% NaBr	Br	2.43	0.01
	Na	2.69	0
8% KBr	Br	2.89	0.01
	K	3.43	0.01

4.3.5 Tensile test

For convenient analysis, all of the salt concentrations were converted into mol/kg. Young's modulus at various salt concentrations were shown in Fig. 4.9. With the increase of salt concentration, LiCl-added gels showed a clear decrease on Young's Modulus while LiBr-added gels showed a not obvious decline on Young's Modulus. NaBr and KBr composited gels showed irregular changes on Young's Modulus and even rose at high salt concentration. In order to clarify these actions, we introduced SR and PVA concentration of hydrated gels ($\omega_{P,h}$). $\omega_{P,h}$ can be calculated in the similar way mentioned in 4.3.1. The formular was shown as follow:

$$\omega_{P,h} = \frac{\omega_P \times W_{\text{dry}}}{W_{\text{hydrated}}} \times 100\%$$

where ω_P was PVA concentration obtained in 4.3.1, W_{dry} was weight of dried sample and W_{hydrated} was weight of hydrated sample.

The result was shown in Table 4.4. The lower the SR, the lower the expansion ratio, and water content in the network structure was also supposed to be lower. However, with the decrease of SR, Li salt composited gels even showed a decrement on Young's Modulus. Young's modulus seemed to be related to $\omega_{P,h}$. Since monovalent salts cannot form crosslinks, the high PVA concentration suggested more intermolecular combination of PVA itself, leading to a stronger network structure. The addition of Li salt, on the one hand, prevented PVA from combining with water molecules, on the other hand, it would weaken the intermolecular forces on the side chains, resulting in an improvement of flexibility. The irregular changes on Young's Modulus of Na and K salt composited gels may be due to the large amount of evaporation of water during preparation, which led to uniformed distribution.

Maximum stress and breaking extension of each sample at various salt concentrations were shown in Fig. 4.10 and Fig. 4.11. It was found that both maximum stress and breaking extension declined with the addition of salt. Although NaBr and KBr composited gels showed an increase on Young's Modulus, the dramatical decline on Maximum stress and breaking extension suggested an increase on brittleness, which was unfavorable for artificial cartilage materials. Although the addition of Li salt had a significant decrease in Young's Modulus and maximum stress, the decrease in the tensile strength was not so obvious, suggesting the possibility of the application on plasticizer.

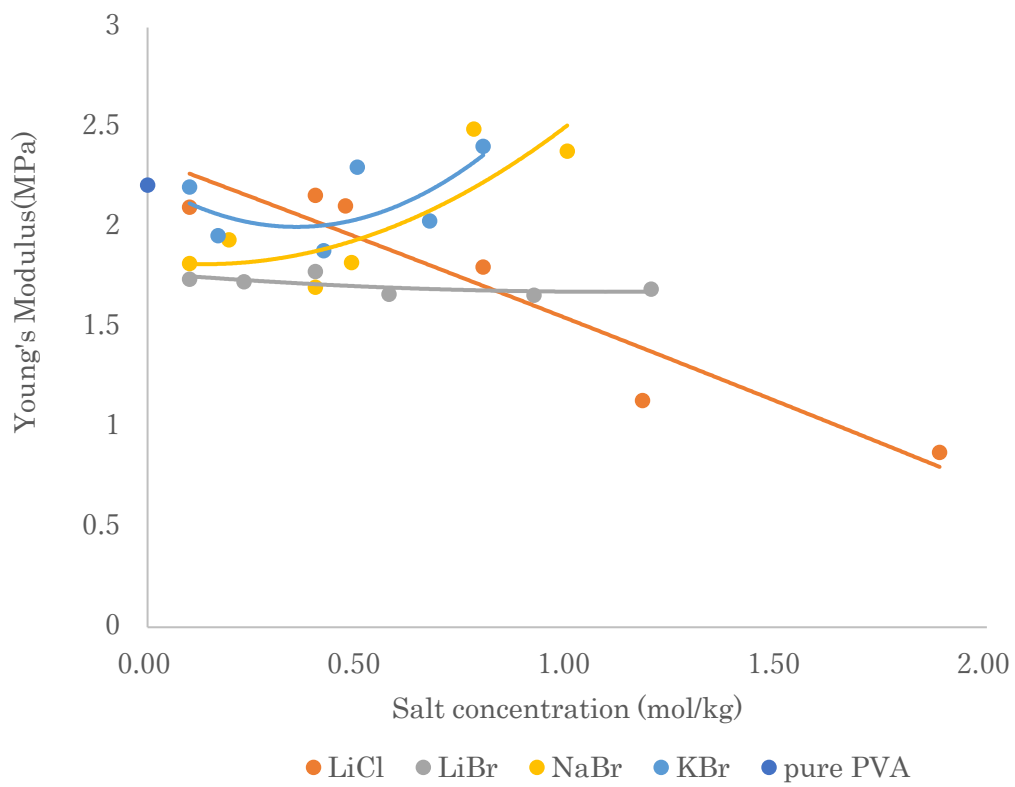


Fig. 4.9 Young's Modulus of each hydrated hydrogel

Table 4.4 Young's Modulus of each hydrated hydrogel

Additives	concentration of salt(mol/kg)	$\omega_{p,h}$ / %	SR	Young's Modulus/MPa
pure PVA	0	35.31	1.60	2.21
LiCl	0.10	35.98	1.48	2.10
LiCl	0.40	35.35	1.46	2.16
LiCl	0.47	37.99	1.29	2.11
LiCl	0.80	34.36	1.42	1.80
LiCl	1.18	32.25	1.45	1.13
LiCl	1.89	29.32	1.33	0.87
LiBr	0.10	35.16	1.51	1.74
LiBr	0.23	35.58	1.46	1.73
LiBr	0.40	35.35	1.41	1.78
LiBr	0.58	35.92	1.29	1.67
LiBr	0.92	34.05	1.26	1.66
LiBr	1.20	33.70	1.20	1.69
NaBr	0.10	35.51	1.51	1.82
NaBr	0.19	35.95	1.44	1.94
NaBr	0.40	35.26	1.39	1.70

NaBr	0.49	35.48	1.35	1.82
NaBr	0.78	36.68	1.14	2.49
NaBr	1.00	37.09	1.06	2.38
KBr	0.10	40.06	1.20	2.20
KBr	0.17	36.15	1.44	1.96
KBr	0.42	35.90	1.38	1.88
KBr	0.50	36.90	1.24	2.30
KBr	0.67	36.24	1.24	2.03
KBr	0.80	37.52	1.12	2.41

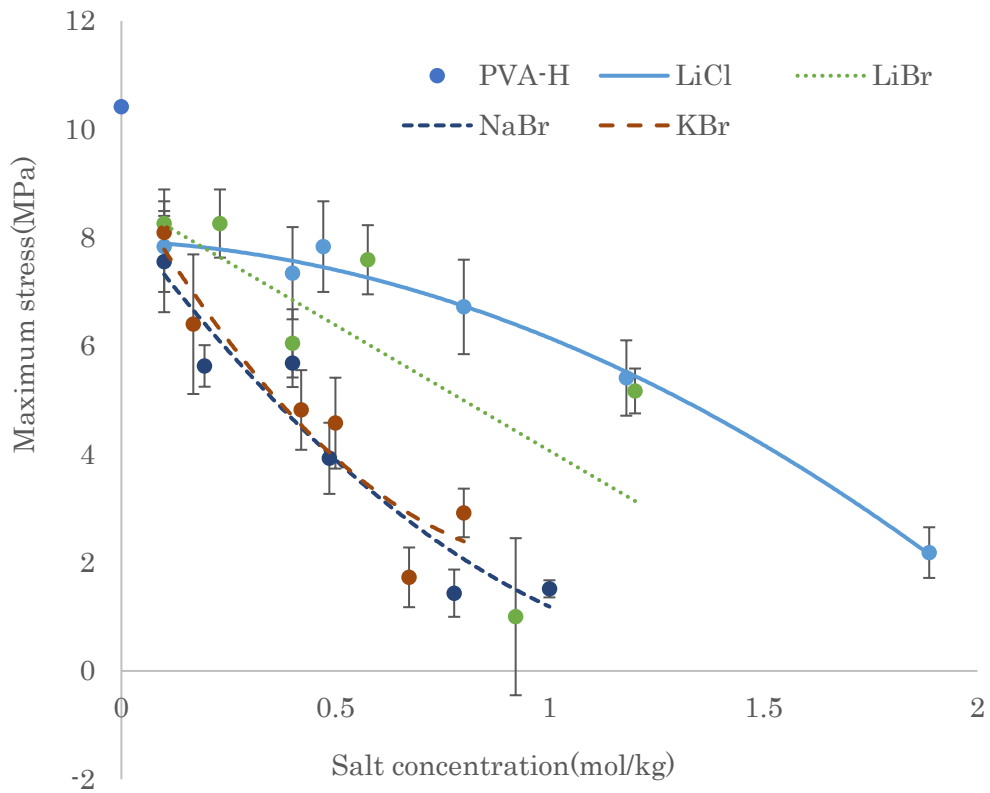


Fig. 4.10 Maximum stress of each hydrated

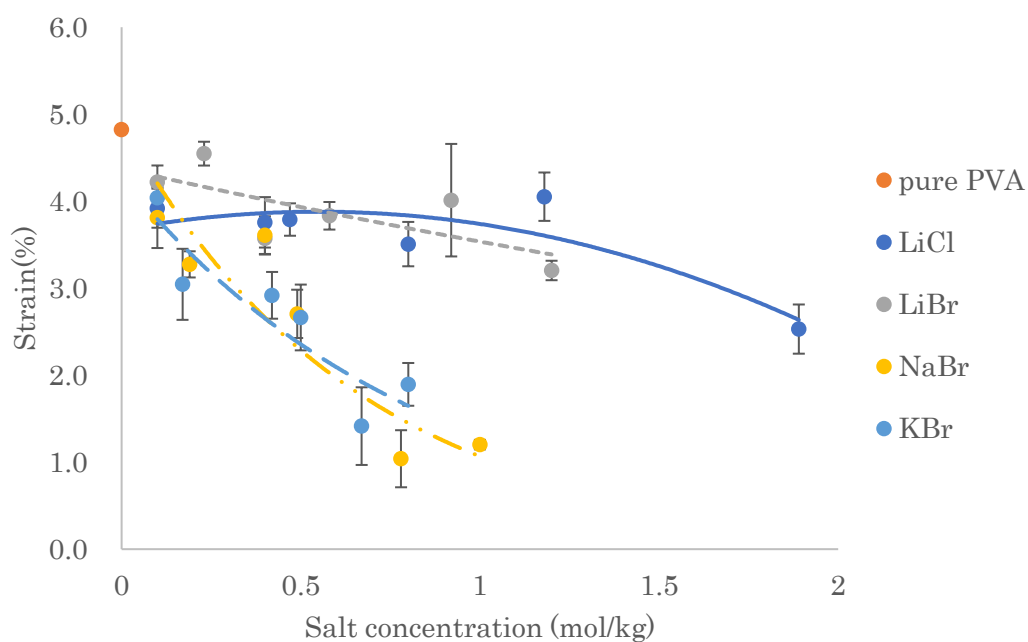


Fig. 4.11 Strain(%) at break of each hydrated hydrogel

Table 4.5 Young's modulus and breaking extension before and after desalted

samples	salt concentration(mol/kg)	before desalted				after desalted			
		Young's modulus(MPa)	mean \pm S.E	strain(%)	mean \pm S.E	Young's modulus(MPa)	mean \pm S.E	strain(%)	mean \pm S.E
pure PVA	0	2.21	0.08	4.82	0.12	1.95	0.06	4.12	0.32
LiCl	0.1	2.08	0.02	3.92	0.22	2.00	0.05	3.64	0.30
LiCl	0.4	2.20	0.05	3.76	0.29	2.13	0.02	3.57	0.07
LiCl	0.47	2.21	0.06	3.79	0.19	1.98	0.03	3.72	0.14
LiCl	0.8	2.07	0.03	3.51	0.26	1.93	0.12	2.40	0.63
LiCl	1.18	1.13	0.07	4.05	0.28	1.22	0.03	2.64	0.26

LiCl	1.89	0.87	0.04	2.53	0.28	0.89	0.03	2.43	0.57
LiBr	0.1	1.74	0.04	4.22	0.19	2.19	0.07	3.18	0.16
LiBr	0.23	1.73	0.05	4.55	0.14	1.75	0.07	4.31	0.22
LiBr	0.4	1.78	0.04	3.57	0.18	2.15	0.03	3.98	0.35
LiBr	0.58	1.67	0.07	3.83	0.16	2.03	0.09	3.91	0.76
LiBr	0.92	1.66	0.12	4.01	0.65	1.33	0.04	3.01	0.48
LiBr	1.2	1.69	0.04	3.20	0.11	1.62	0.02	2.91	0.33
NaBr	0.1	1.82	0.02	3.81	0.35	1.83	0.02	4.03	0.11
NaBr	0.19	1.94	0.07	3.27	0.15	1.90	0.03	3.84	0.18
NaBr	0.4	1.70	0.04	3.61	0.22	2.06	0.09	2.81	0.50
NaBr	0.49	1.83	0.07	2.70	0.28	2.26	0.07	3.50	0.30
NaBr	0.78	2.49	0.08	1.04	0.33	2.36	0.06	1.64	0.41
NaBr	1	2.38	0.05	1.20	0.05	2.09	0.04	1.06	0.13
KBr	0.1	2.20	0.04	4.04	0.22	1.77	0.04	3.67	0.32
KBr	0.17	1.96	0.07	3.04	0.41	1.97	0.04	3.85	0.16
KBr	0.42	1.88	0.07	2.92	0.27	1.92	0.08	3.04	0.38
KBr	0.5	2.30	0.05	2.66	0.38	2.23	0.08	3.23	0.18
KBr	0.67	2.03	0.10	1.41	0.45	2.06	0.07	0.25	0.04
KBr	0.8	2.41	0.09	1.89	0.25	2.46	0.12	1.69	0.35

By comparing the Young's Modulus and breaking extensions of each sample before and after desalted (Table 4.5), however, the changes of these two

statistics seemed to have no obvious regular pattern by desalting treatment. Pure PVA hydrogel also showed decrease on Young's Modulus and extensions after desalted. This may be due to long time stirring and some intermolecular bonds broke. Irregular changes in other samples may be due to the fact that after the salt originally in the network structure removed, the defect in gels would recombine by intermolecular bond in water environment. As a result, it was difficult to decide how tensile strength of gels changed after desalted.

4.3.6 DSC

DSC thermograms of LiBr-added samples for various LiBr concentration was shown in Fig. 4.12. Pure PVA hydrogel showed a sharp exothermic peak around 240°C and with the salt concentration increasing, width of the exothermic peak was observed to be widened, indicating that crystallization became disordered by adding salt [11].

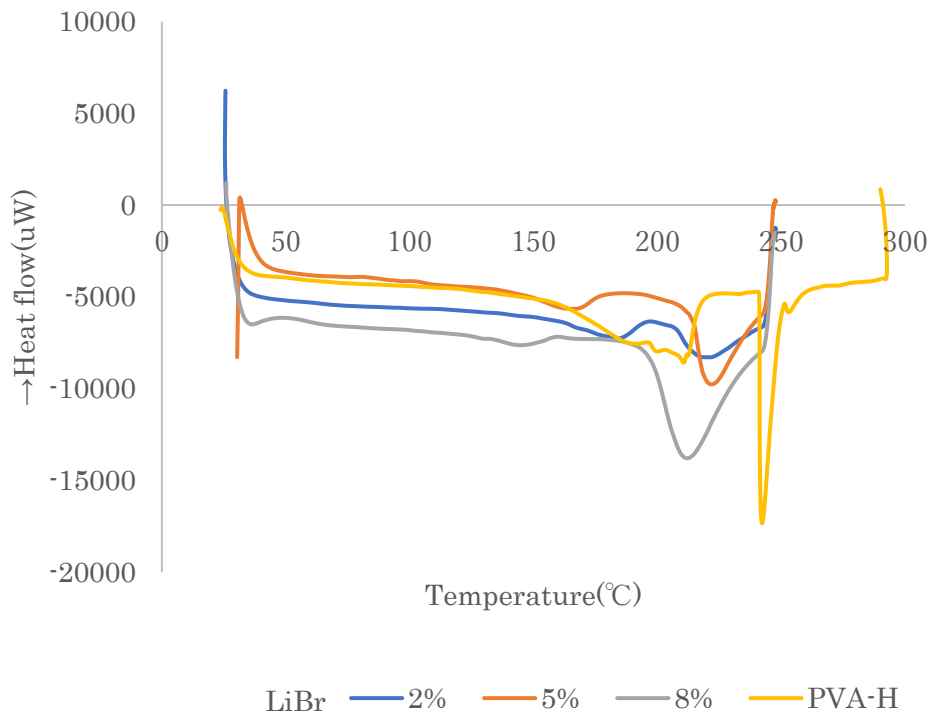


Fig. 4.12 DSC thermograms of LiBr-added gels of each LiBr concentration

In addition, melting points of each sample with various salt concentration

was shown in Fig. 4.13. It was clearly observed that melting points were decreased with the increasing of salt concentration. Before and after the addition of salt, it was considered that no new functional groups were introduced, and there were almost no changes in molecular weight or polarity. Therefore, the decrease on melting point was inferred to be attributed to the decrease of rigidity. The addition of salt cracked some of the intermolecular bonds thereby made the gels softer, suggesting the salt can be applied on plasticizer.

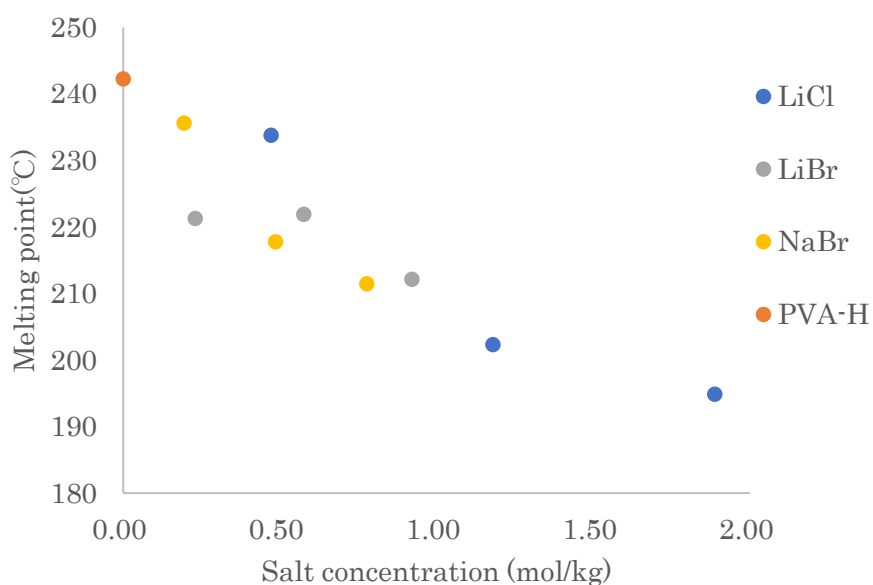


Fig. 4.13 Melting points of each gel of various of salt concentration

4.3.7 DMA

Storage modulus (E'), loss modulus (E'') and loss tangent ($\tan\delta$) on temperature dispersion of LiCl-added samples, for example, of each LiCl concentration were shown in Fig. 4.14, Fig. 4.15, and Fig. 4.16, respectively. With LiCl concentration increasing, the temperature at which E' began to fall became lower, and E' declined more sharply. In addition, as the salt concentration increased, E'' tended to shift to the left and so as the peak of $\tan\delta$. These all indicated that the gels became more flexible by adding salt.

Glass transition temperature (T_g) of each sample for various salt concentration, obtained from the peak of $\tan\delta$, which was shown in Fig. 4.17. It was found all the samples showed apparent decrease on T_g with salt concentration increasing, indicating the flexibility of molecular chain was improved by adding salt.

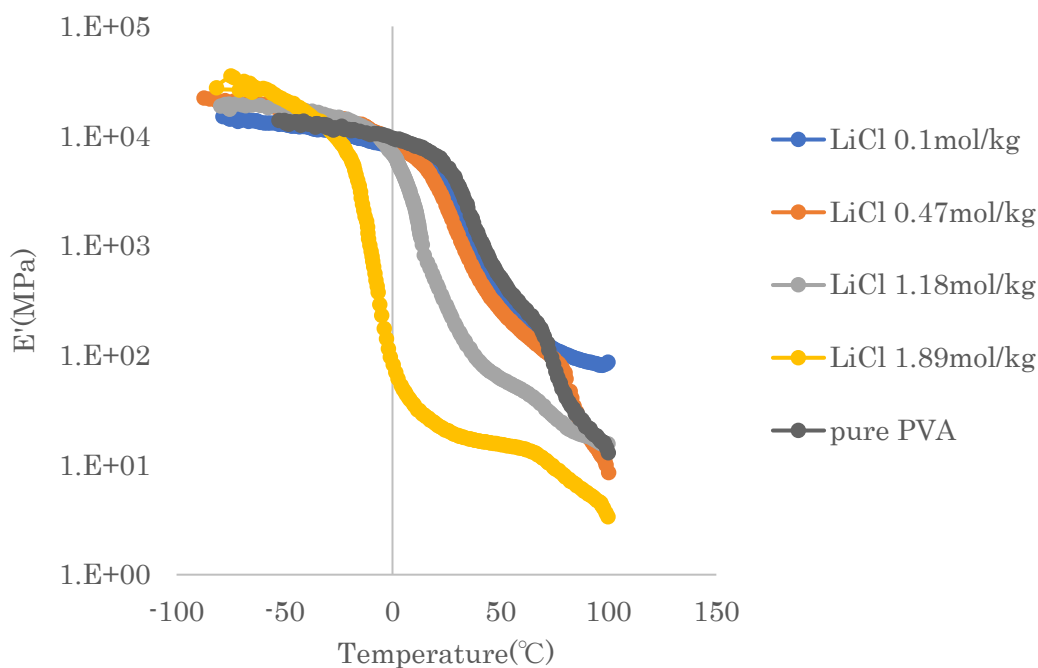


Fig. 4.14 E' of each LiCl-added sample on temperature dispersion

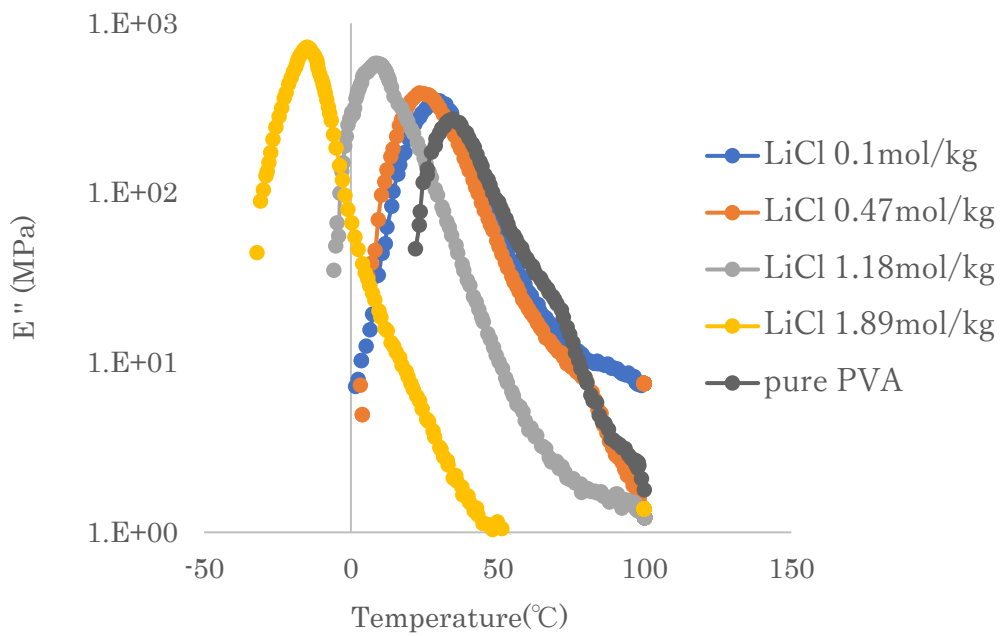


Fig. 4.15 E'' of each LiCl-added sample on temperature dispersion

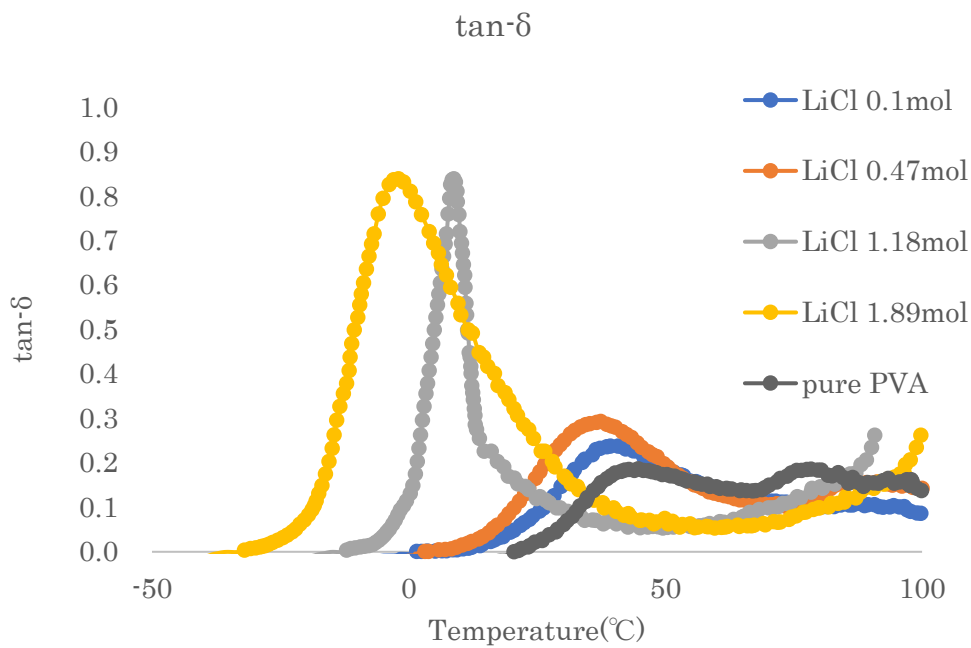


Fig. 4.16 $\tan-\delta$ of each LiCl-added sample on temperature dispersion

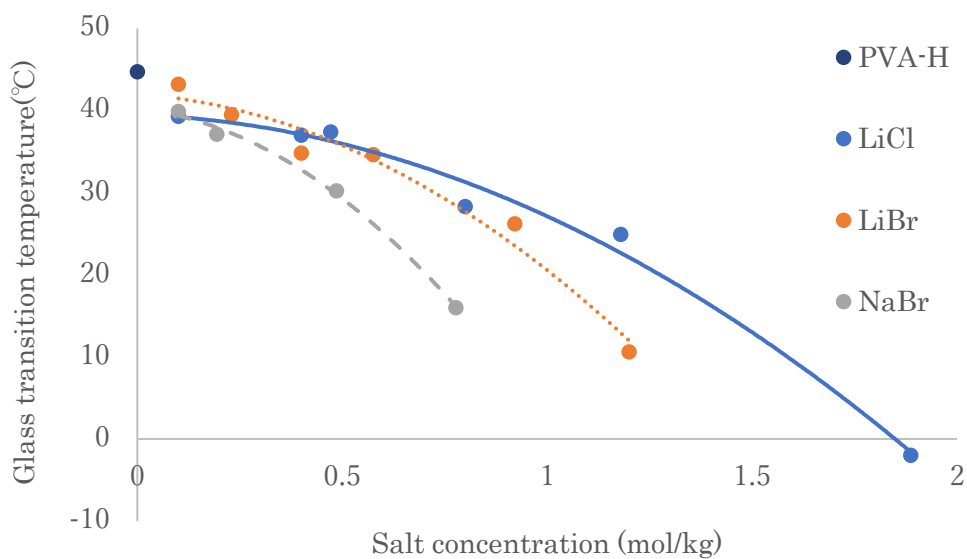


Fig. 4.17 T_g of each gel of various salt concentration

4.3.8 Protein absorption test

The result of protein absorption of each desalted hydrated sample was shown in Fig. 4.18. It was found the gels absorbed more protein with the

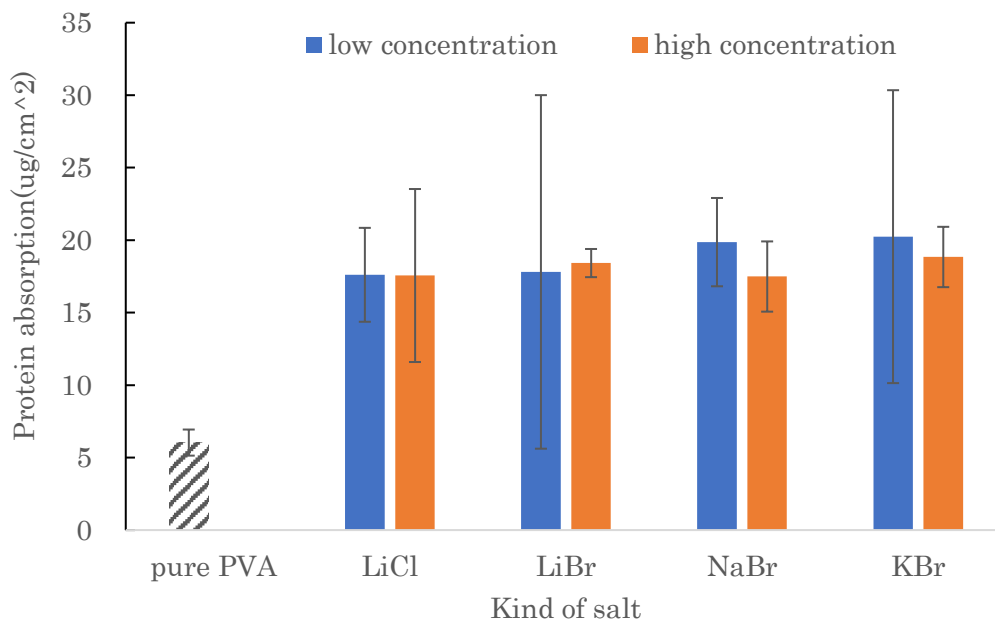


Fig. 4.18 Protein absorption of each sample at two concentrations (mol/kg) as follows: LiCl: 0.1, 1.89; LiBr: 0.1, 0.92; NaBr: 0.1, 0.78; KBr: 0.1, 0.8.

addition of salt regardless of the kind of salt. In addition, concentration of salt seemed to have no effect on protein adhesion. It was speculated that some defects existed after the salt removed, making it easier for proteins to enter such the network structure. However, some of these defects can be repaired in a water environment. Therefore, the results of different salt concentration were almost the same.

4.3.9 Cell culture

Fluorescence observations of each sample after 3-day culture were shown in Fig. 4.19. It was observed that many more cells adhered to salt composited PVA-H than to PVA-H after 3 days of inoculation. Not so much adhered, cells were more likely to aggregate on gels. In addition, some hollows were observed in cell aggregation, where cells seemed difficult to adhere. These can be explained as follow: Surface of gels became rough by adding salt and some convex parts occurred. These parts were hard for cells to adhere, causing some hollow observed in fluorescence observations. On the other hand, defects left in the network structure allowed more proteins to absorb, and cells were thereby easy to adhere to such areas, resulting in the cell aggregation observed in fluorescence observations. It was proved from all the results that cell affinity of PVA-H was improved by adding and removing salt.

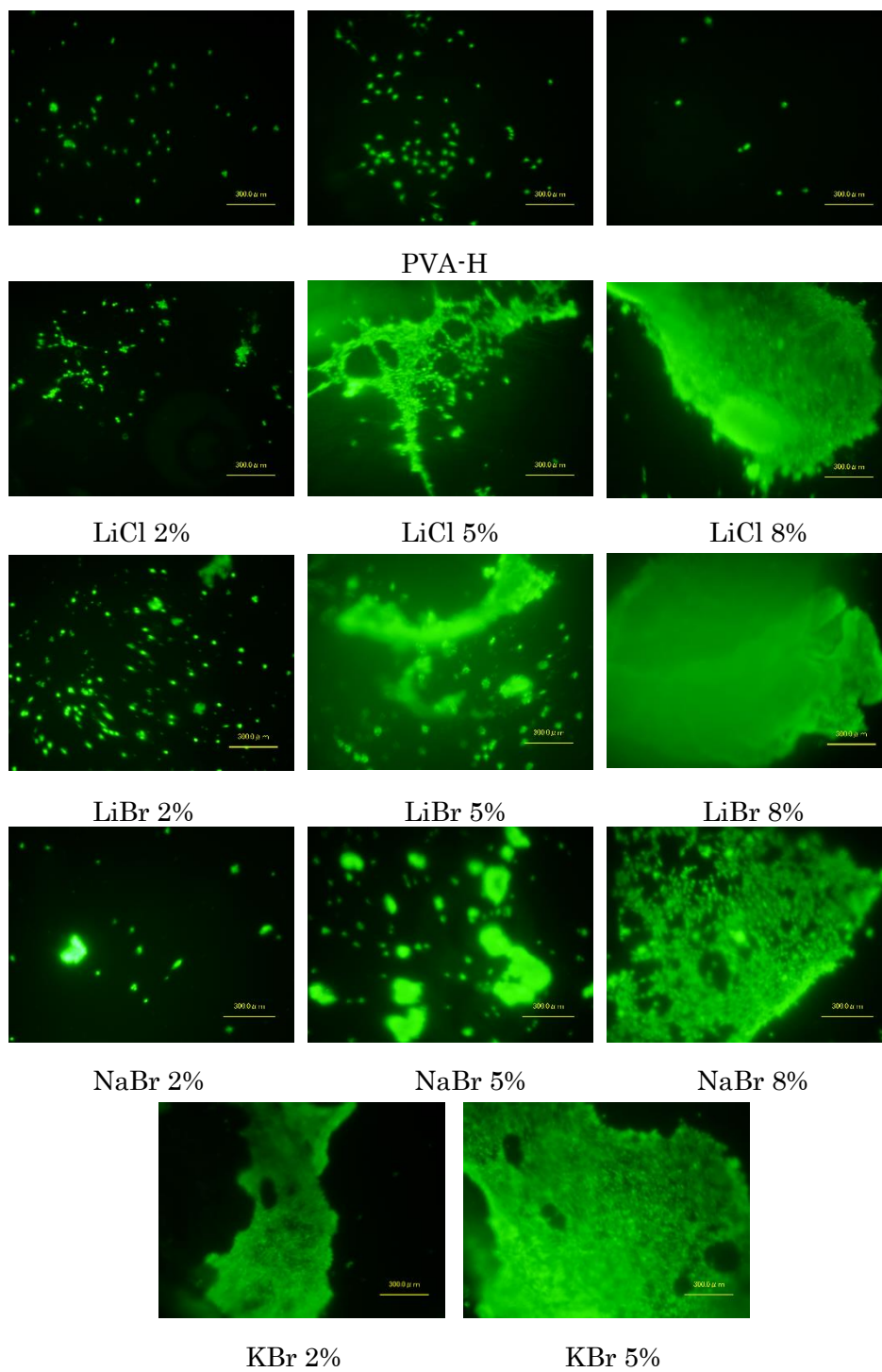


Fig. 4.19 Fluorescence observations of each sample after 3-day culture

4.4 Conclusion

Four kinds of monovalent metal salt (LiCl, LiBr, NaBr, KBr) composited physically crosslinked PVA hydrogels were successfully prepared by the novel hot pressing method. The properties of hydrogels were reformed by adding salt mainly due to the competition between salt ions and PVA molecules for water molecules during gelation. Li salt composited gels were apparent and clean while Na and K salt composited gels presented some white turbidity on the gel surface as salt concentration increasing, which was due to the interaction of water molecules and both anions and cations.

By EDS analysis of gels before and after desalted, it was found that salts uniformly distributed in the gels and almost no salt left after desalting treatment.

Salts were found to affect the properties of gels mainly in two ways. On the one hand, the addition of salt impeded the combination of PVA and water molecules. On the other hand, anions and cations of salt can interact with water molecules by $\text{OH}\cdots\text{X}^-$ or $\text{M}^+\cdots\text{OH}$ bonds in amorphous. These led to the fact that the gels became more flexible by adding salt, confirming the feasibility of application of salt, especially Li salt, in plasticizer.

By protein absorption measurement and cell culture, salt composited gels were found to have no toxicity and more protein affinity after a desalting treatment due to the defects left after desalted. Furthermore, many more cells were observed to adhere to salt composited gels, which was very beneficial for biomaterials.

References

1. Kobayashi, K., Pagot, G., Vezzù, K. et al. Effect of plasticizer on the ion-conductive and dielectric behavior of poly(ethylene carbonate)-based Li electrolytes. *Polym J* 53, 149–155 (2021)
2. Shawna R. S., Roger F., Plasticizer interactions with polymer and salt in propylene carbonate-poly(acrylonitrile) lithium triflate, *Electrochimica Acta*, Volume 42, Issue 3, 1997, Pages 471-474,
3. Tretinnikov, O.N., Zagorskaya, S.A. & Sushko, N.I. An attenuation total reflectance fourier transform spectroscopic study of crystallinity in the bulk and on the surface of aqueous and aqueous salt cryogels of poly(vinyl alcohol). *Polym. Sci. Ser. A* 56, 264–268 (2014)
4. Zagorskaya, S.A., Tretinnikov, O.N. Infrared Spectra and Structure of Solid Polymer Electrolytes Based on Poly(vinyl alcohol) and Lithium Halides. *Polym. Sci. Ser. A* 61, 21–28 (2019).
5. Komiya, S., Otsuka, E., Hirashima, Y., and Suzuki, A., Salt effects on formation of microcrystallites in poly(vinyl alcohol) gels prepared by cast-drying method, *Progress in Natural Science: Materials International*, Volume 21, Issue 5, 2011, Pages 375-379,
6. Lee, H.M., Tarakeshwar, P., Park, J., et al. Insights into the Structures, Energetics, and Vibrations of Monovalent Cation-(Water)₁₋₆ Clusters. *J. Phys. Chem. A* 2004, 108, 15, 2949–2958.
7. Sakaguchi T, Nagano S, Hara M, et al. Facile preparation of transparent poly (vinyl alcohol) hydrogels with uniform microcrystalline structure by hot-pressing without using organic solvents[J]. *Polymer journal*, 2017, 49(7): 535-542.
8. Tretinnikov, O. N., Sushko N. I., and Zagorskaya, S. A. Effect of salt concentration on the structure of Poly (vinyl alcohol) cryogels obtained from aqueous salt solutions. *J. Appl. Spectrosc.* 82, No.1, 40–45 (2015)
9. Tretinnikov, O.N., Zagorskaya, S.A. Determination of the degree of crystallinity of poly(vinyl alcohol) by FTIR spectroscopy. *J. Appl. Spectrosc.* 79, 521–526 (2012)
10. Smith, P. K., Krohn, R. I., Hermanson, G. T., et al, Measurement of protein using bicinchoninic acid, *Analytical Biochemistry*, Volume 150, Issue 1, 1985, Pages 76-85,

11. Park, J.-S., Park, J.-W., Ruckenstein, E., Thermal and dynamic mechanical analysis of PVA/MC blend hydrogels, *Polymer*, Volume 42, Issue 9, 2001, Pages 4271-4280,

*Chapter 5 Preparation
and characterization of
divalent metal salt
composited PVA-H by
hot pressing method*

5.1 Introduction

In the last chapter, monovalent metal salt composited PVA-Hs were prepared by hot pressing method and in this chapter, divalent metal salt would be used for composite.

Divalent salts, such as $\text{Ca}(\text{NO}_3)_2$ [1], MgCl_2 [2,3], $\text{Mg}(\text{NO}_3)_2$ [4], at. were widely used as plasticizer. The effect of divalent salt on crystalline and thermal properties of PVA was mainly due to the strong interaction with PVA molecules and the replacement of hydrogen bonding within PVA modules.

In this chapter, divalent salts were added to PVA hydrogels by the novel hot pressing method. To eliminate the effect of anions, three kinds of chloride salt (MgCl_2 , CaCl_2 , MnCl_2) were used for composite. The properties of each gel would be evaluated to investigate the effect of salt. In addition, for the application for an artificial cartilage material, biocompatibility was evaluated by cell protein absorption test and cell culture.

5.2 Materials and methods

5.2.1 Preparation of pure PVA-H

In chapter 3, PVA hydrogels were successfully prepared by hot press method referred to the previous study [5]. In this chapter, I used the same method to prepare pure PVA hydrogels.

Identically, I obtained “dried gels”, “hydrated gels”, for different experiments.

5.2.2 Preparation of salt composited PVA-H

In this chapter, three kinds of divalent metal salt (CaCl_2 , MgCl_2 , MnCl_2) were composited to PVA hydrogel. The preparation method was the same as chapter 4. In addition, I have also carried out a desalting treatment for better biocompatibility.

Same as above, “dried gels”, “hydrated gels”, “hydrated desalted hydrogels” and “dried desalted hydrogels” were obtained for different experiments.

The photo of obtained dried hydrogel was shown in Fig. 5.1. All the samples showed high transparency. No obvious deficiency was observed in salt composited samples (b, c, d) compared to pure PVA hydrogel (a), indicating salt was successfully composited to PVA hydrogels

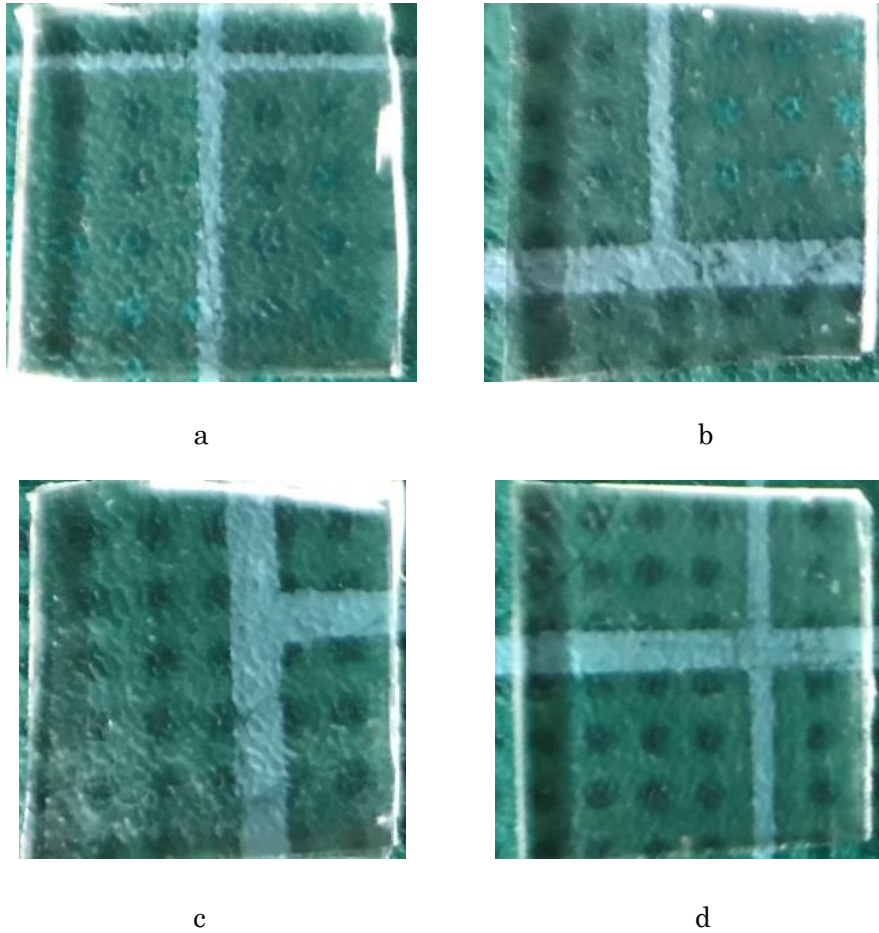


Fig.5.1 Photos of each dried gel a: pure PVA, b:5%MgCl₂ c:5%CaCl₂ gel and d:5% MnCl₂

5.2.3 Determination of PVA content by mass measurement

As mentioned in chapter 3, PVA concentrations of obtained hydrogels can be calculated by measuring the mass of the samples before and after preparation. PVA concentration of dried hydrogels (ω_p) was calculated by the following formula:

$$\omega_p = \frac{0.5 \times W_{\text{total}}}{W_{\text{dry}}} \times 100\%$$

where 0.5 is initial concentration of PVA, W_{total} is total weight used for preparation, and W_{dry} is the weight of dried hydrogel.

Equally, water concentration of dried hydrogels (ω_w) can be calculated by the following formula:

$$\omega_w = 1 - \frac{(0.5 + \omega_{salt}) \times W_{total}}{W_{dry}} \times 100\%$$

where 0.5 is initial concentration of PVA, ω_{salt} is salt concentration used for preparation, W_{total} is total weight used for preparation, and W_{dry} is the weight of dried hydrogel.

5.2.4 FTIR spectra

IR spectra of each dried hydrogel were recorded in the range 4000-400 cm^{-1} . Same as chapter 4, the values of A_{1640}/A_{1088} and A_{1144}/A_{1088} was regarded as relative water content (WC) [6] and relative degree of crystallization (DC) [7], respectively. This study was not for quantitative analysis of WC or DC. Therefore, values of A_{1640}/A_{1088} and A_{1144}/A_{1088} of each hydrogel were used as WC and DC of samples respectively, to evaluate the effect of the addition of salt. In addition, we also measured WC and DC of desalted hydrogels to get further understanding of the effect of salt.

5.2.5 Swelling ratio of hydrated hydrogels

Same as chapter 4, swelling ratio (SR) of each sample was calculated by the following formula:

$$SR = (W_{wet} - W_{dry})/W_{dry}$$

where W_{wet} is the weight of samples after swelling equilibrium and W_{dry} is the weight of dried samples. Each hydrogel was tested for three times.

5.2.6 EDS analysis

Energy Dispersive X-ray Spectroscopy (EDS) analysis was carried out using TM3030plus to observe the dispersion of salt in the gels. The cross sections of each gel were also observed to analysis the vertical distribution of salt. In

addition, dried gels before and after desalting were both observed to evaluate the effect of desalination.

5.2.7 Tensile test

The tensile mechanical properties of the hydrogels were determined by tensile test underwater. The samples were cut to JIS dumbbell 7 type specimens. An initial load of 0.01 N was applied to eliminate the effect of deflection of the gels. The test was performed at the speed of 5 mm/min and was repeated 5 times to ensure reproducibility. In addition, both hydrated gels and desalted hydrated gels were tested to evaluate the effect of desalination.

5.2.8 DSC

Thermograms were obtained on Exstar 6000. Each sample was cut into a small circular piece with a mass within 10 mg. Differential scanning calorimetry (DSC) measurement was carried out from -25-300 °C at a heating rate of 10 °C/min. In addition, both hydrated gels and desalted gels were tested.

5.2.9 DMA

Dynamic mechanical analysis (DMA) of dried gels was carried out by using Rheosol-G5000. Samples were cut to 5 mm × 30 mm rectangles. Considering that the addition of salt may lower the glass transition temperature of hydrogels, dynamic viscoelasticity of gels on temperature dispersion was measured from -20 – 100 °C utilizing liquid nitrogen. Heating rate was set up to 3 °C/min and frequency was 1 Hz.

5.2.10 Protein absorption test

Desalted hydrated hydrogels were used for protein absorption test. As mentioned above, protein concentrations were determined by a bicinchoninic

acid (BCA) assay [8], using an albumin BSA standard curve according to the manufacturer's instructions (Thermo Fisher Scientific). The absorbance of BCA solutions was measured at 562 nm using a microplate reader. Three identical samples were tested one time for average and each sample were tested three times.

5.2.11 Cell culture

Biocompatibility of gels was evaluated by cell culture in the same way mentioned in chapter 4. Osteoblast cells MC3T3 were used for culturing, and a fluorescence observation was performed after 3-day culture to analyze the cell adhesion status.

5.3 Results and discussion

5.3.1 Determination of PVA content by mass measurement

Calculated PVA concentration and water concentration of dried hydrogels were shown in Table 5.1. It was found that PVA concentrations of dried samples gradually decreased with the addition of salt. However, different from monovalent metal salt in chapter 4, hydrogels with CaCl_2 , MgCl_2 , and MnCl_2 composited showed a decrease on water content at 2% salt concentration and then increase obviously. What needs to be pointed out was that although PVA concentrations decreased at 2% salt addition, the ratios of PVA to H_2O were enhanced compared to that of pure PVA. It can be inferred that the addition salt of a certain concentration may replace water molecules to form microcrystals through the combination with PVA molecules. Over the certain concentration of salt, however, the formation of microcrystals would be hindered by excessive salt molecules.

Table 5.1 PVA concentration and water concentration and mass ratio of PVA to water

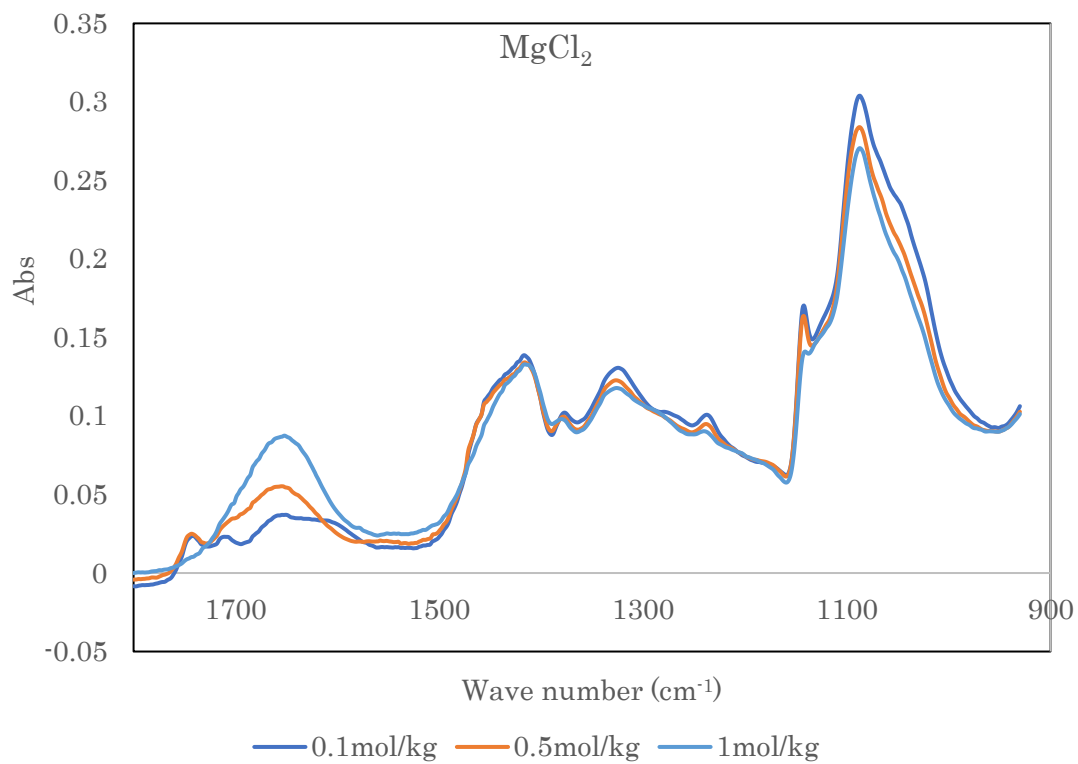
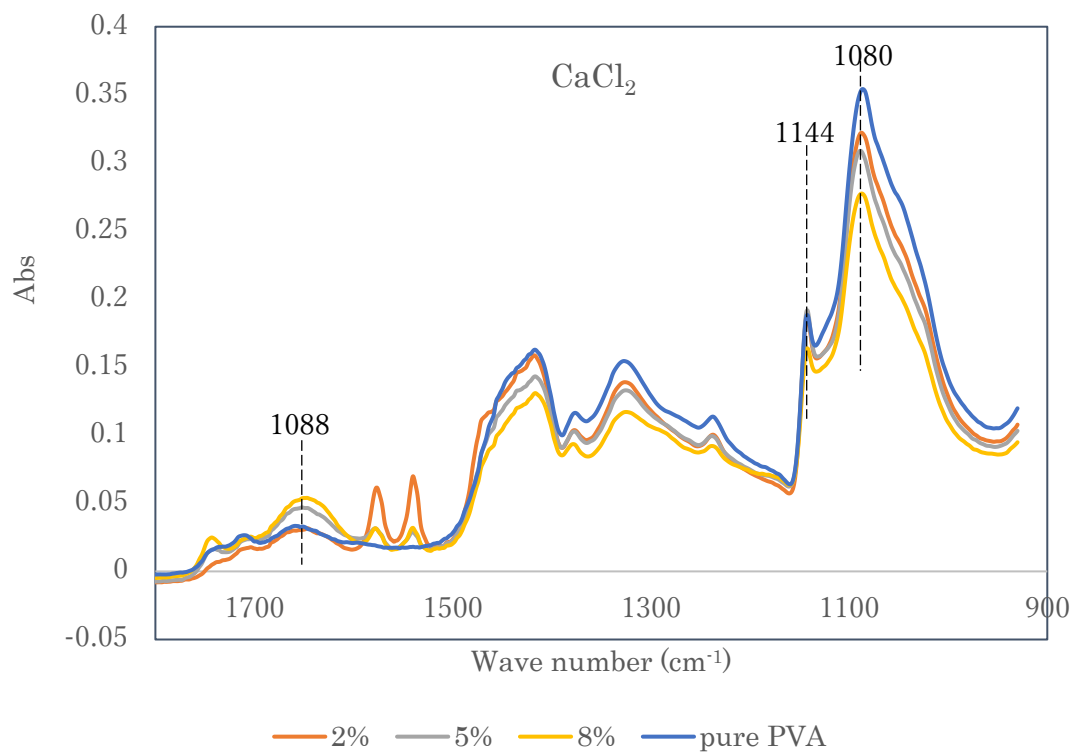
additives	concentration of salt		dried hydrogels		PVA/ H_2O (wt%)
	wt%	mol/kg	PVA concentration / %	water concentration	
pure PVA			91.90	8.10	11.34
MgCl_2	2	0.21	89.88	6.52	13.78
MgCl_2	5	0.53	84.41	7.15	11.80
MgCl_2	8	0.84	79.55	7.72	10.30
MnCl_2	2	0.16	89.16	7.28	12.25

MnCl ₂	5	0.40	81.87	9.94	8.23
MnCl ₂	8	0.64	75.18	12.79	5.88
CaCl ₂	2	0.18	89.21	7.23	12.34
CaCl ₂	5	0.45	81.58	10.27	7.95
CaCl ₂	8	0.72	76.22	11.59	6.58

5.3.2 FTIR

Fig. 5.2. showed the absorption bands of pure PVA-H and CaCl₂, MgCl₂ and MnCl₂ composited PVA-H, at the range 1800 – 930 cm⁻¹. It was of great interest that doublet IR absorbance band at around 1540 and 1575 cm⁻¹ was observed in the CaCl₂-added samples, whereas MgCl₂ and MnCl₂-added samples were insignificant. This doublet absorbance band may be due to O...Ca²⁺ connection. It was reported [9-11] that carboxylate groups can interact with metal cations, especially Ca²⁺, in four different modes as shown in Fig. 5.3. The ionic type of interaction was usually observed in the alkali metal salts of carboxylic acids and the doublet absorption band at 1540 and 1575 cm⁻¹ was attributed to the coexistence of at least two types of carboxylate groups in the three-dimensional calcium-carboxylate complex. The unidentate carboxylate group contributed to the asymmetric vibration at around 1575 cm⁻¹, and the bidentate carboxylate group was corresponded to the asymmetric vibration at around 1540 cm⁻¹. In the case of PVA-H, although there were very few amount of carboxylate groups due to incomplete saponification of PVA, in the three-dimensional network structure of PVA hydrogel, O...Ca²⁺ connection may exist and form the other mesh structure.

The relative degree of crystallization (A_{1144}/A_{1088} , DC) and relative water content (A_{1640}/A_{1088} , WC) of gels before and after desalted were shown in Table.5.2. Different from monovalent metal salt composite in chapter 4, divalent metal salt composited hydrogels showed an increase first and then decrease on DC with salt concentration arose. This can be explained as follow: when a small amount of divalent metal salt was added, the cation may



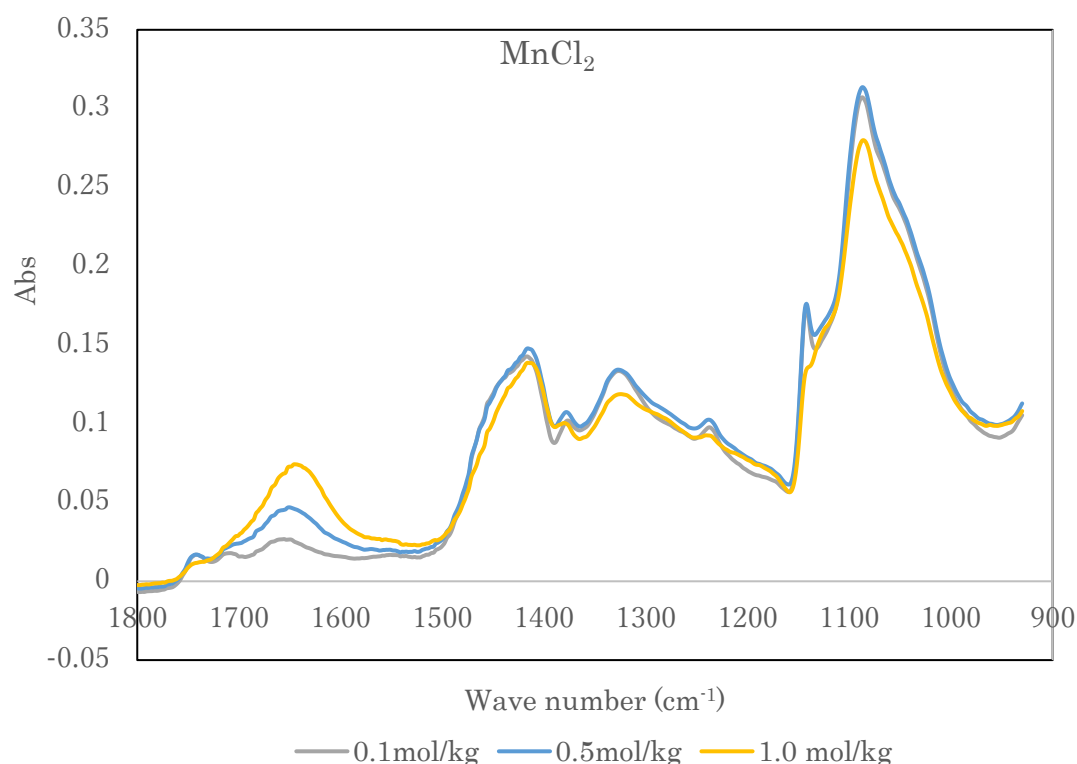


Fig. 5.2 FTIR spectrum of CaCl_2 , MgCl_2 and MnCl_2 composited gels of each salt concentration

connect with oxygen atoms like bridging type and form a more complex network structure. Cation ions became cross-linking points and improved the crystallinity of PVA, causing an initial increasement on DC. Over a certain concentration, the excessive cation ions would reduce crystallinity. Therefore, DC decreased after a certain concentration of salt.

An increase on WC with salt concentration arising was observed. As mentioned above, cations of divalent metal salt were supposed to intergrate with oxygen atoms. As a result, a large number of water molecules were retained due to the presence of salt, resulting in an increase on WC. The different of WC increment between three kinds of salt may be due to bond strength to water molecules.

Same as chapter 4, after desalted, DC and WC of all salt-added samples became closer to that of pure PVA-H, indicating the interactions between salt and PVA. The effect of desalination was also confirmed.

Table. 5.2 Relative DC and WC of each sample before and after desalted

additives	concentration of salt		before desalted		after desalted	
	wt%	mol/kg	A ₁₁₄₄ /A ₁₀₈₈ (DC)	A ₁₆₄₀ /A ₁₀₈₈ (WC)	A ₁₁₄₄ /A ₁₀₈₈ (DC)	A ₁₆₄₀ /A ₁₀₈₈ (WC)
pure PVA	0	0	0.519	0.063	0.491	0.066
CaCl ₂	1.11	0.10	0.549	0.082	0.527	0.083
CaCl ₂	2.00	0.18	0.568	0.068	0.509	0.066
CaCl ₂	5.00	0.45	0.583	0.144	0.544	0.074
CaCl ₂	5.55	0.50	0.542	0.174	0.526	0.078
CaCl ₂	8.00	0.72	0.523	0.208	0.520	0.067
CaCl ₂	11.10	1.00	0.488	0.356	0.539	0.065
MgCl ₂	0.95	0.10	0.516	0.092	0.517	0.075
MgCl ₂	2.00	0.21	0.559	0.104	0.495	0.069
MgCl ₂	4.76	0.50	0.528	0.183	0.522	0.072
MgCl ₂	5.00	0.53	0.555	0.169	0.524	0.078
MgCl ₂	8.00	0.84	0.447	0.334	0.505	0.073
MgCl ₂	9.52	1.00	0.451	0.353	0.509	0.086
MnCl ₂	1.26	0.10	0.542	0.057	0.514	0.077
MnCl ₂	2.00	0.16	0.544	0.068	0.498	0.073
MnCl ₂	5.00	0.40	0.542	0.095	0.510	0.063

MnCl ₂	6.29	0.50	0.526	0.130	0.523	0.095
MnCl ₂	8.00	0.64	0.490	0.157	0.510	0.063
MnCl ₂	12.58	1.00	0.429	0.276	0.513	0.069

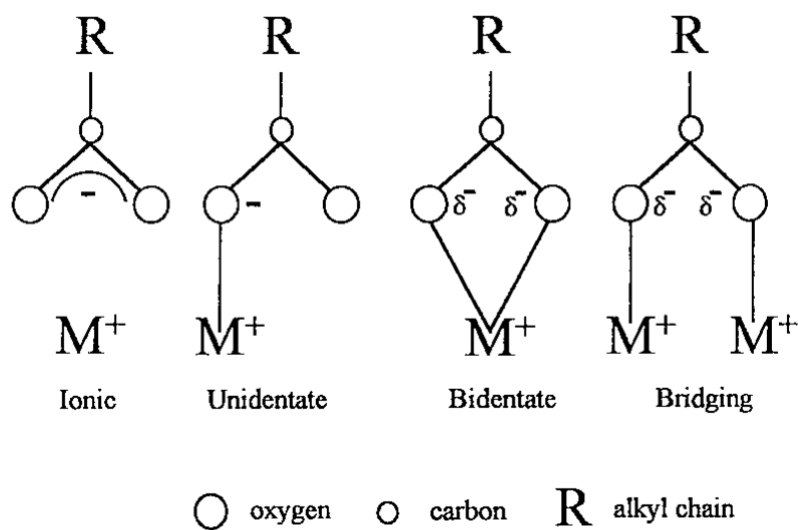


Fig. 5.3 Four different modes of the interaction of O with metal cations

5.3.3 Swelling ratio of hydrated hydrogels

Swelling ratios SRs of hydrogels of each salt composited were shown in Fig. 5.4. It was found that SR of all salt composited hydrogels considerably decreased with the increase of salt concentration. It can be inferred that the addition of salt prevented water molecules from entering the network structure of gels when swelling.

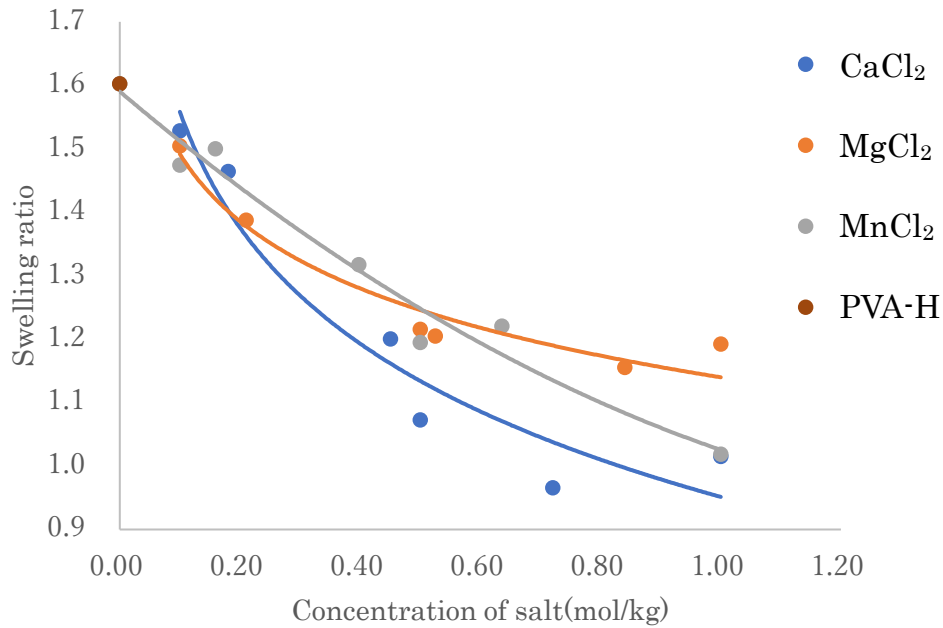


Fig. 5.4 SR of each gel of various salt concentrations

5.3.4 EDS analysis

Fig. 5.5 showed SEM images of the surface (a) and cross section (b) of 8% MgCl₂-added hydrogel, for example, without desalting. Same as monovalent salt composited hydrogels, some impurities were observed. The results of element distribution analysis by EDS were shown in Fig. 5.6 and Fig. 5.7. From the distribution of the elements on the yellow line, it was found that the impurity was mainly composed of C atoms, indicating that PVA that

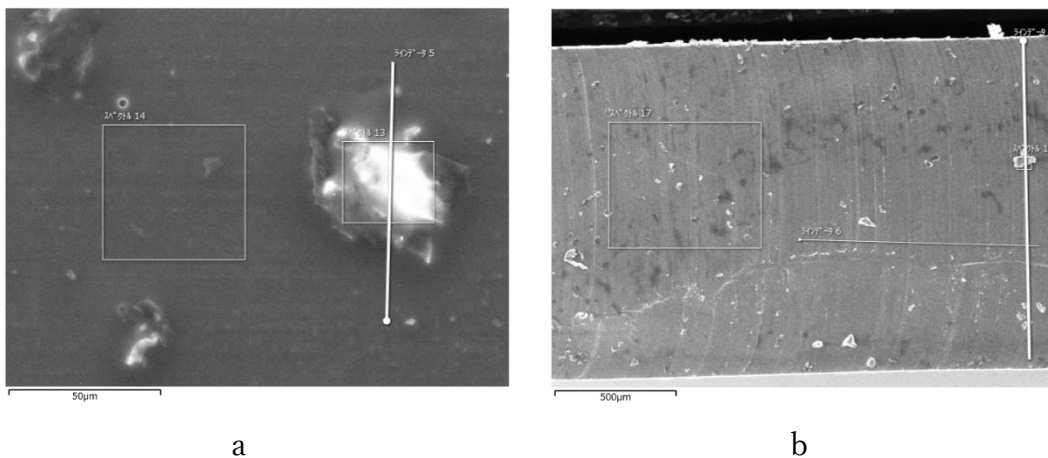


Fig. 5.5 SEM images of MgCl₂-added gel
a: surface; b: cross section

incompletely reacted aggregated in the gels. In addition, it can be inferred from the result of elements distribution in the surface and cross section that Mg and Cl uniformly distribute on the gels. Same as chapter 4, divalent salts were also found to distribute uniformly whether on the surface or in cross section of the gel.

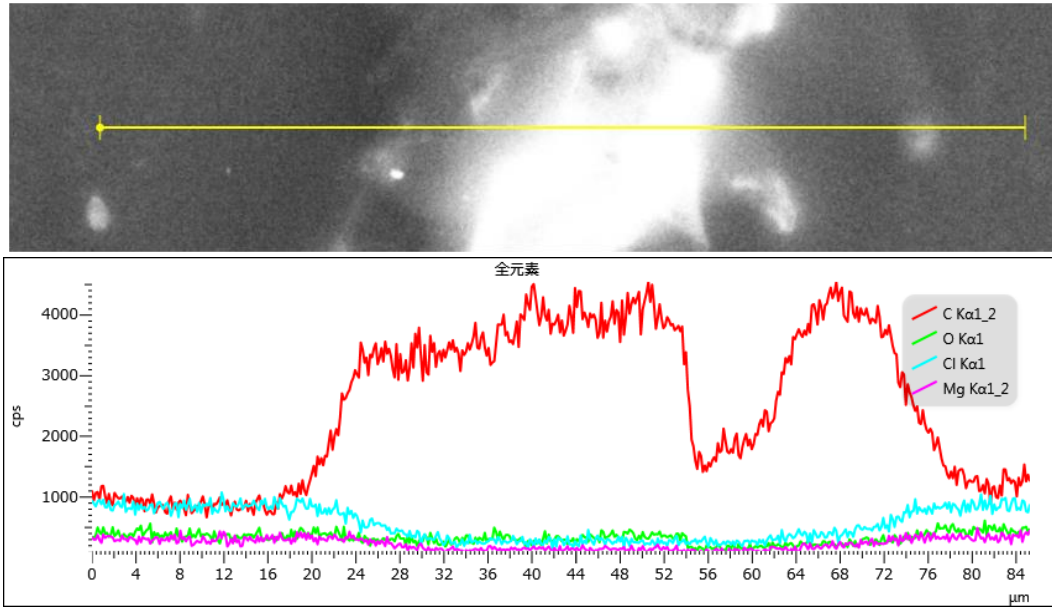


Fig. 5.6 Elements distribution on surface of gel

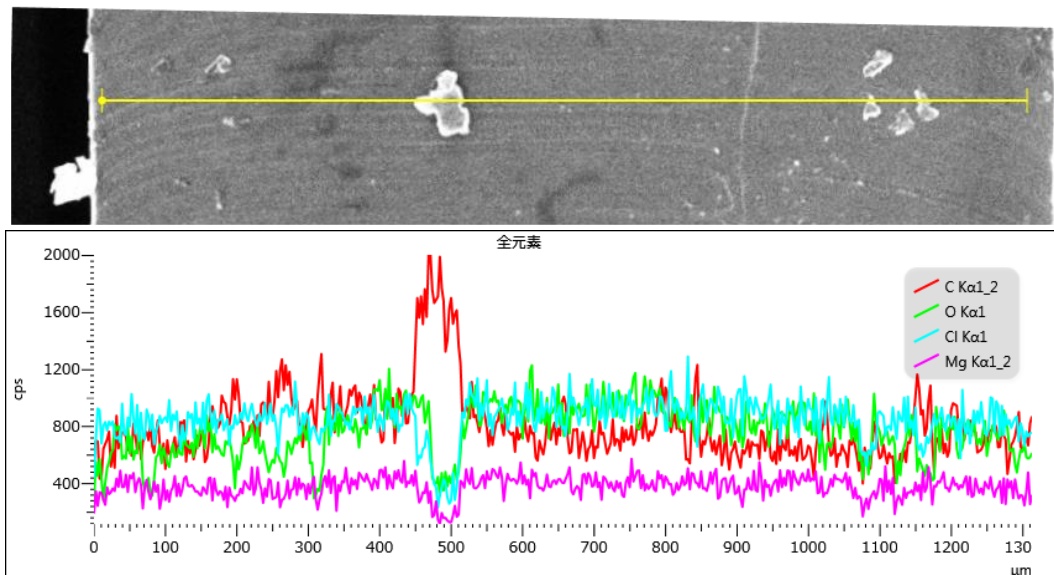


Fig. 5.7 Elements distribution on cross section of gel

The results of element concentration of each gel before and after desalting were shown in Table 5.3. Almost all the salts were found to be eliminated after desalted. The effects of desalting treatment were confirmed.

Table 5.3 Element concentrations before and after desalted

Samples	Element	Atomic % (before desalted)	Atomic % (after desalted)
8% CaCl ₂	Cl	3.2	0
	Ca	1.67	0.01
8% MgCl ₂	Cl	3.21	0.01
	Mg	1.81	0.01
8% MnCl ₂	Cl	2.43	0.01
	Mn	1.34	0

5.3.5 Tensile test

Young's modulus at various salt concentrations were shown in Fig. 5.8. Different from monovalent salt in chapter 4, divalent salt composited gels showed almost constant (MgCl₂, MnCl₂) or a slight increase (CaCl₂) on Young's Modulus and then decreased after a certain salt concentration. This may be due to the bridging structure mentioned in 5.3.2. Unlike monovalent metal ions, divalent metal salt, especially Ca²⁺, can form a tighter network structure by bridging with oxygen atoms. When salt was excessively added, however, the ratio of divalent metal ions and oxygen atoms became out of balance, resulting in a damage to the network structure.

Fig. 5.9 and Fig. 5.10 showed maximum stress and breaking extension of each sample at various salt concentrations, respectively. It was found that although Young's Modulus had a slight increment at salt concentration around 0.5 mol/kg, both maximum stress and breaking

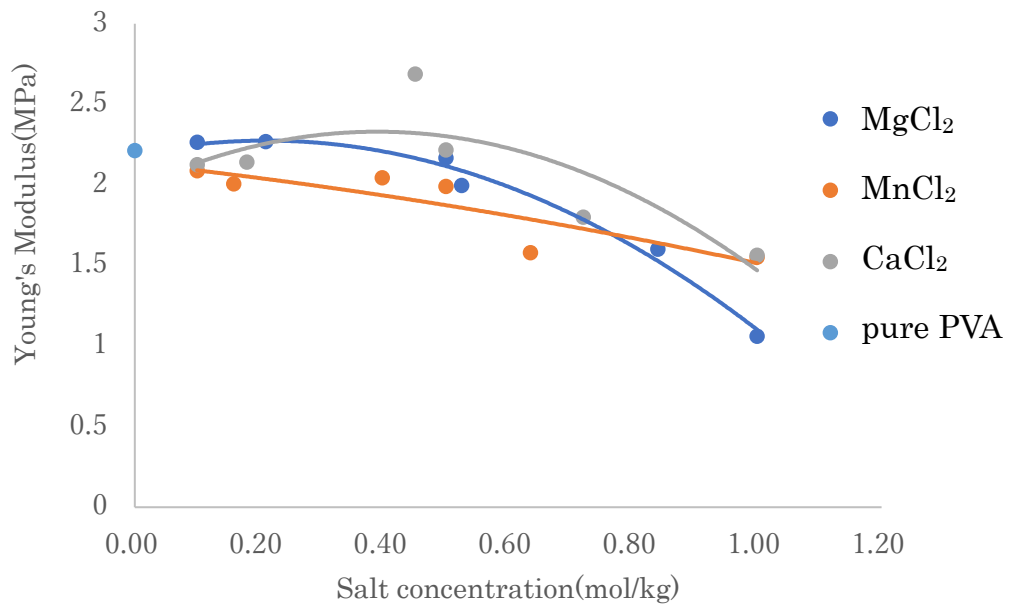


Fig. 5.8 Young's modulus at various salt concentrations

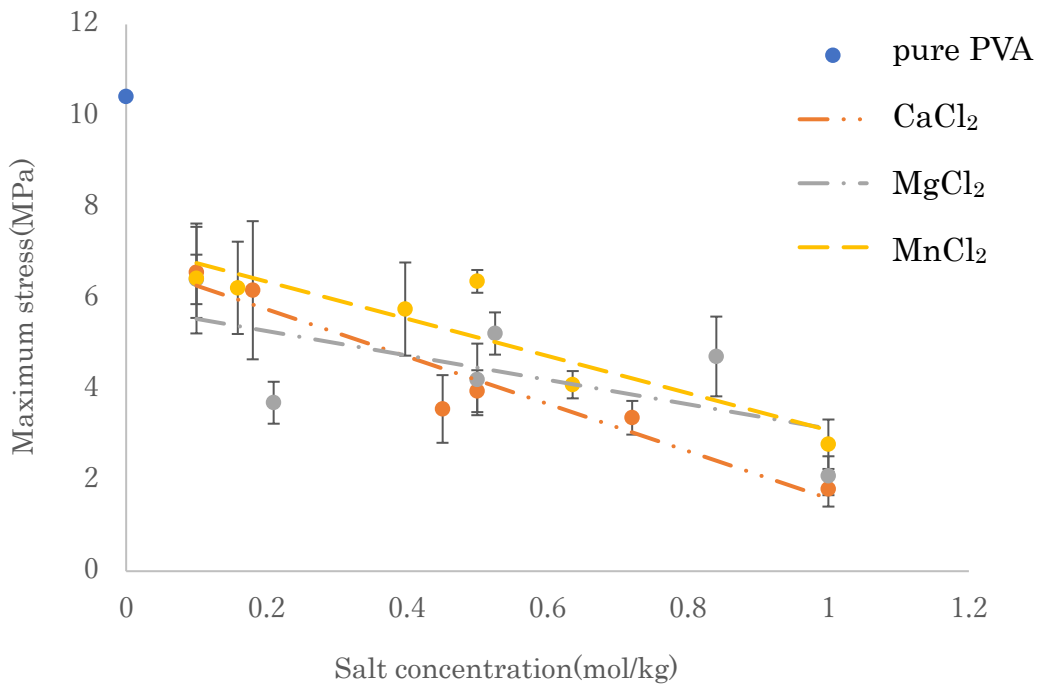


Fig. 5.9 Maximum stress at various salt concentrations

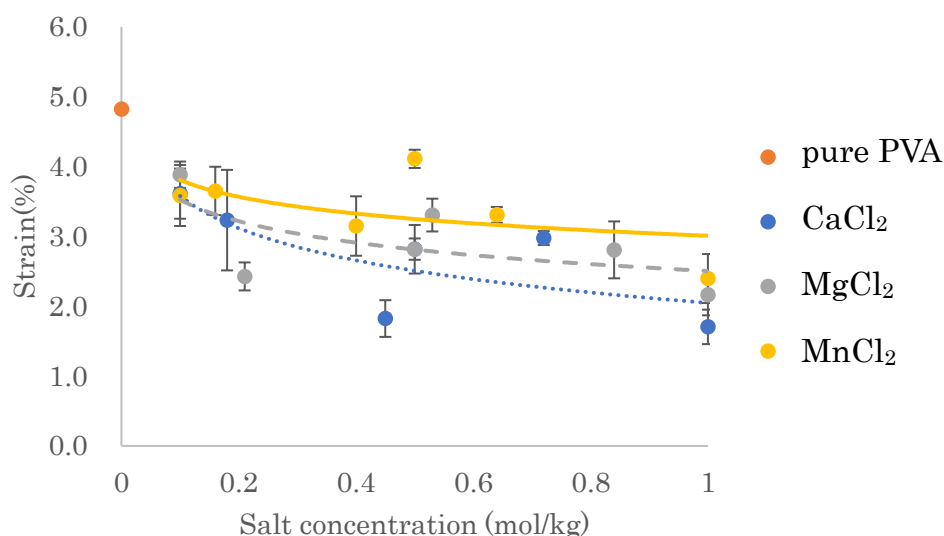


Fig. 5.10 Strain(%) at break of each hydrogel

extension of all samples decreased obviously with the increase of salt concentration. It was inferred that $O \cdots M^{2+}$ combinations were quite easy to break. Although it can provide some resistance in the initial stage of stretching, a very small force led to crack and defect in the gel, resulting in the increase on Young's Modulus and the decrease on maximum stress and breaking extension.

Table 5.4 showed Young's Modulus and breaking extensions of each sample before and after desalted. Similar as monovalent salt in chapter 4, the changes of these two statistics seemed to have no obvious regular pattern by desalting treatment. Pure PVA hydrogel also showed decrease on Young's Modulus and extensions after desalted. It was difficult to conclude how the structure of gels changed after desalted.

Table 5.4 Young's modulus of gels before and after desalted

samples	salt concentration(mol/kg)	before desalted				after desalted			
		Young's modulus(MPa)	mean \pm S.E	strain(%)	mean \pm S.E	Young's modulus(MPa)	mean \pm S.E	strain(%)	mean \pm S.E
pure PVA	0.00	2.21	0.08	4.82	0.12	1.95	0.06	4.12	0.32
CaCl ₂	0.10	2.13	0.03	3.61	0.36	2.13	0.04	3.29	0.57
CaCl ₂	0.18	2.14	0.04	3.23	0.72	2.18	0.02	3.66	0.28
CaCl ₂	0.45	2.69	0.07	1.82	0.26	1.96	0.13	2.68	0.62
CaCl ₂	0.50	2.22	0.07	2.82	0.15	2.01	0.04	2.86	0.30
CaCl ₂	0.72	1.80	0.12	2.98	0.10	1.83	0.08	2.26	0.32
CaCl ₂	1.00	1.56	0.19	1.70	0.25	2.15	0.10	1.22	0.20
MgCl ₂	0.10	2.26	0.04	3.88	0.19	2.32	0.05	3.18	0.45
MgCl ₂	0.21	2.27	0.08	2.43	0.20	2.17	0.05	3.13	0.31
MgCl ₂	0.50	2.17	0.07	2.82	0.35	2.34	0.03	1.21	0.12
MgCl ₂	0.53	2.00	0.11	3.31	0.23	2.31	0.05	1.81	0.31
MgCl ₂	0.84	1.60	0.07	2.81	0.41	1.63	0.05	1.98	0.40
MgCl ₂	1.00	1.06	0.07	2.16	0.29	1.36	0.07	1.84	0.34
MnCl ₂	0.10	2.09	0.11	3.59	0.44	2.19	0.03	3.04	0.24
MnCl ₂	0.16	2.00	0.06	3.65	0.35	1.97	0.06	3.45	0.39

MnCl ₂	0.40	2.05	0.15	3.15	0.43	1.78	0.03	3.67	0.30
MnCl ₂	0.50	1.99	0.05	4.11	0.13	2.10	0.05	3.85	0.20
MnCl ₂	0.64	1.59	0.01	3.31	0.11	1.48	0.04	3.32	0.37
MnCl ₂	1.00	1.55	0.03	2.40	0.35	1.56	0.04	1.63	0.18

5.3.6 DSC

Melting points of each sample with various salt concentration obtained from melting peaks was shown in Fig. 5.11. As monovalent salt in chapter 4, the addition of divalent salt also showed a great influence on decrease of melting point of PVA hydrogels. As mentioned above, divalent metal ions, especially Ca²⁺, can form O...Ca²⁺ structure. However, these combinations were quite easy to crack even blow 100°C, which almost had no effect on melting point. On the other hand, the addition of salt broke the original intermolecular bonds, causing a decrease on melting points.

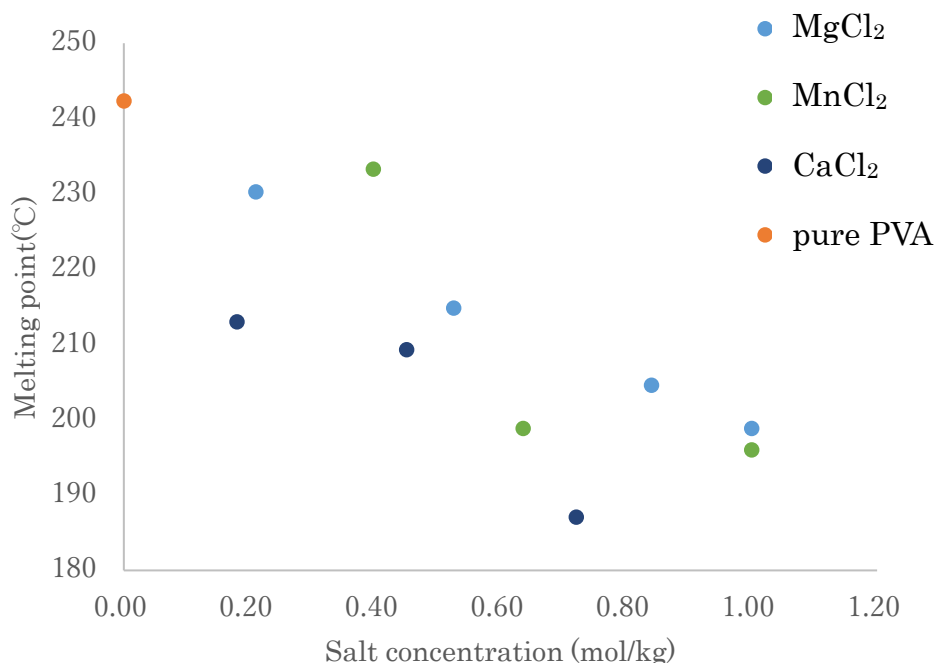


Fig. 5.11 Melting point of each gel of different salt concentration

5.3.7 DMA

Loss tangent ($\tan\delta$) on temperature dispersion of CaCl_2 -added samples, for example, of each CaCl_2 concentration was shown in Fig. 5.12 and glass transition temperature T_g of each sample obtained from the peak of $\tan\delta$ was shown in Fig. 5.13. Different from monovalent salt in chapter 4, divalent composited gels showed a slight increase below a certain salt concentration around 0.5 mol/kg, especially CaCl_2 . This result was similar to Young's Modulus in 5.3.5. Ca^{2+} ions were able to form crosslink by $\text{O}\cdots\text{Ca}^{2+}$ combinations, thereby the movement of molecular chains were hindered, flexibility was reduced, and finally leading to an increase on T_g .

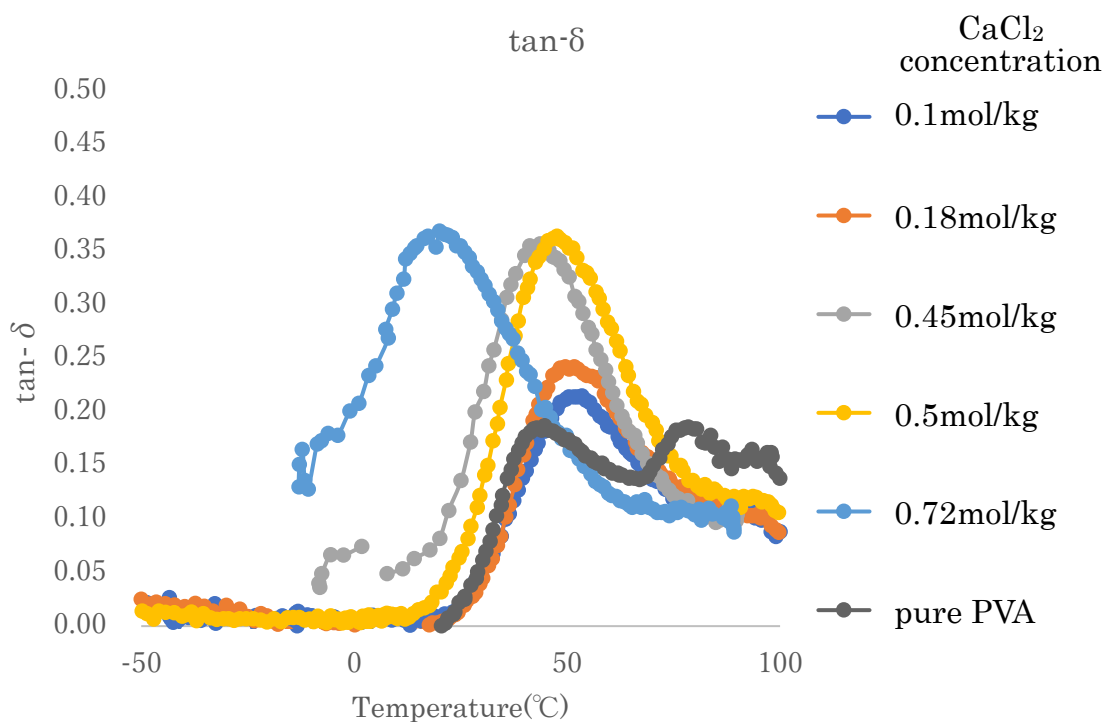


Fig. 5.12 $\tan\delta$ of CaCl_2 -added gels on temperature dispersion of different CaCl_2 concentration

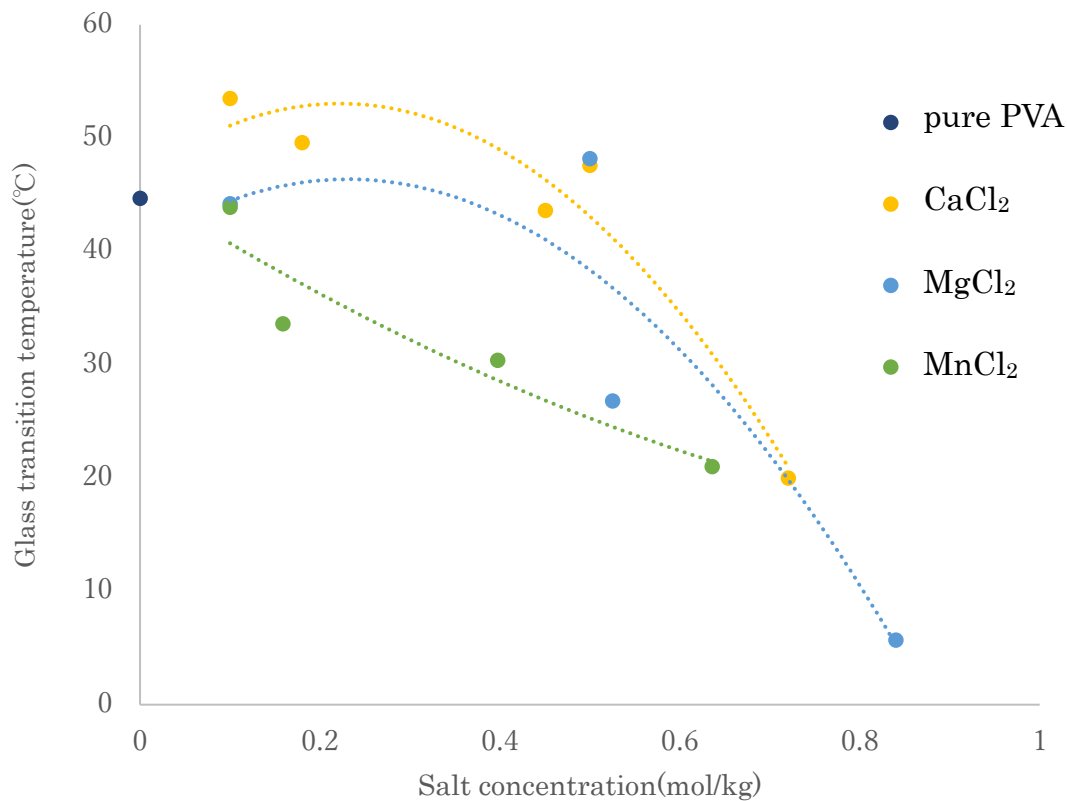


Fig. 5.13 T_g of each sample with different salt concentration

5.3.8 Protein absorption test

The result of protein absorption of each desalted hydrated sample was shown in Fig. 5.14. It was found the gels absorbed more protein with the addition of salt regardless of the kind of salt. Different from monovalent salt in chapter 4, samples of different kinds of salt showed different protein adsorption quantities, where CaCl_2 showed the highest. Considered with previous conclusions, Ca^{2+} ions were easiest to form $\text{O}\cdots\text{M}^{2+}$ combinations in these three kinds of divalent metal. After desalting treatment, CaCl_2 composited gels left more defects than others, thereby more proteins can enter and be retained in network structure.

In addition, protein absorption values slightly increased with salt concentration increasing, suggesting that irreversible defects were left after desalted by adding divalent metal salts.

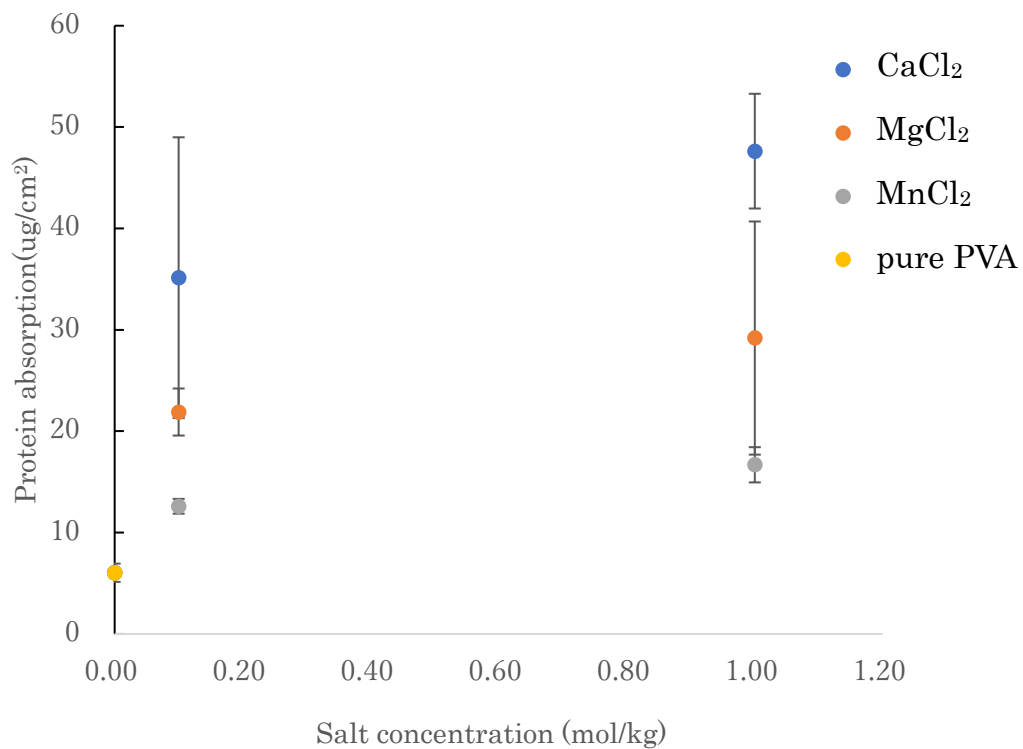


Fig. 5.14 Protein absorption of each sample.

5.3.9 Cell culture

Fluorescence observations of each sample after 3-day culture were shown in Fig. 5.15. It was observed that many more cells adhered to salt composited PVA-H than to pure PVA-H after 3 days of inoculation. Similar to chapter 4, cells were more likely to aggregate on gels. Addition and removing of divalent salt also can improved cell affinity of PVA-H.

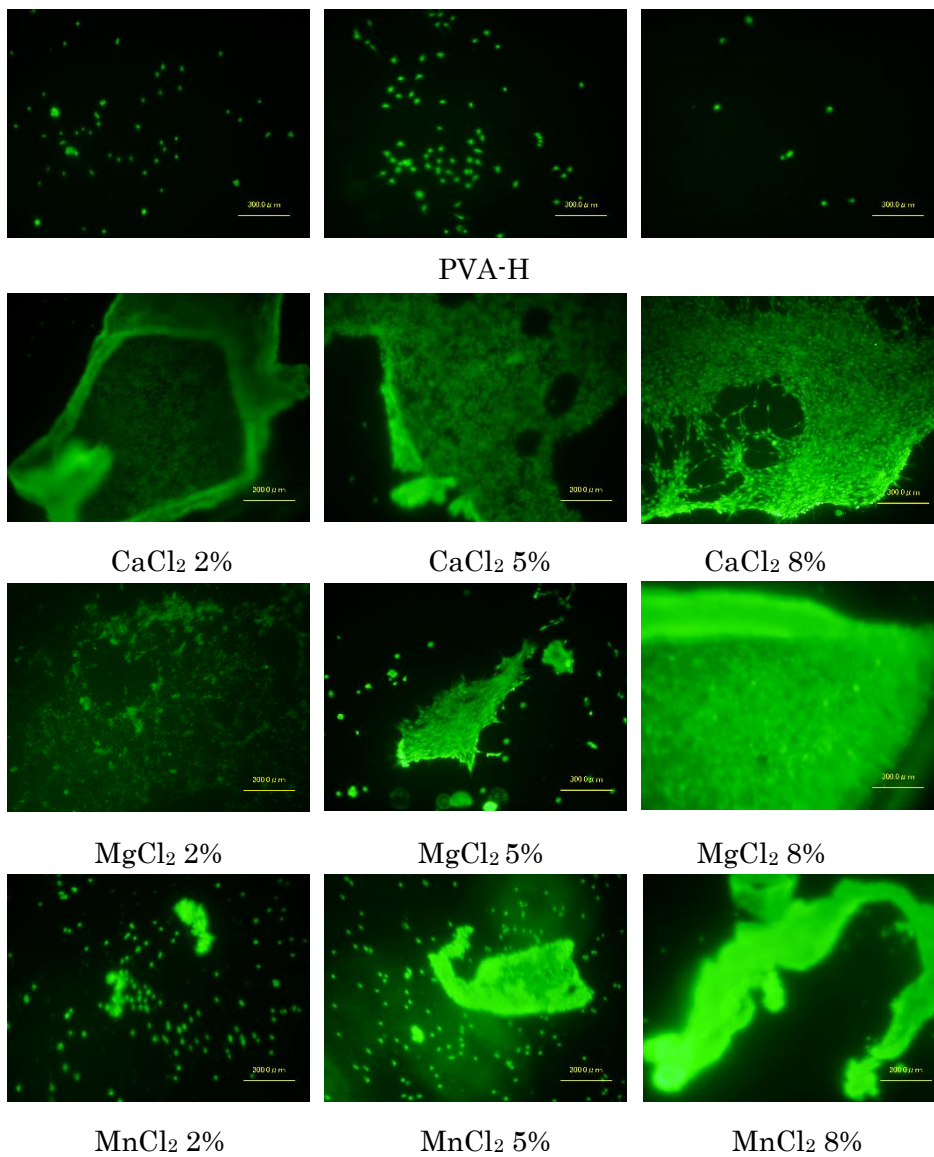


Fig. 5.15 Fluorescence observations after 3 days culturing

5.4 Conclusion

Three kinds of divalent metal salt (CaCl_2 , MgCl_2 , MnCl_2) composited physically crosslinked PVA hydrogels were successfully prepared by the novel hot pressing method and all of the composited gels showed high transparency.

Salts were found to affect the properties of gels mainly in two ways. On the one hand, salt would compete with PVA molecules for water molecules. On the other hand, divalent metal ions, especially Ca^{2+} , can form a bridging structure with oxygen atoms so as to form a network structure in amorphous. Therefore, Young's modulus and T_g increased at low salt concentration. However, these combinations were so weak that mechanical properties still became low due to the decrease on intermolecular connection. These divalent salts can also be applied for plasticizers.

By EDS analysis of gels before and after desalted, it was found that salts uniformly distributed in the gels and almost no salt left after desalting treatment. In addition, by protein absorption measurement, salt composited gels showed better protein affinity, especially CaCl_2 . Furthermore, the results of cell culture showed that salt composited gels presented no toxicity after a desalting treatment due to the defects left after desalted. Moreover, many more cells were observed to adhere to salt composited gels, which was very beneficial for biomaterials.

References

1. Jiang X, Jiang T, Zhang X, et al. The plasticizing effect of calcium nitrate on poly (vinyl alcohol)[J]. *Polymer Engineering & Science*, 2013, 53(6): 1181-1186.
2. Jiang X, Jiang T, Zhang X, et al. Melt processing of poly (vinyl alcohol) through adding magnesium chloride hexahydrate and ethylene glycol as a complex plasticizer[J]. *Polymer Engineering & Science*, 2012, 52(10): 2245-2252.
3. Jiang X, Zhang X, Ye D, et al. Modification of poly (vinyl alcohol) films by the addition of magnesium chloride hexahydrate[J]. *Polymer Engineering & Science*, 2012, 52(7): 1565-1570.
4. Kubo J, Rahman N, Takahashi N, et al. Improvement of Poly (vinyl alcohol) Properties by the Addition of Magnesium Nitrate[J]. *Journal of applied polymer science*, 2009, 112(3): 1647-1652.
5. Sakaguchi T, Nagano S, Hara M, et al. Facile preparation of transparent poly (vinyl alcohol) hydrogels with uniform microcrystalline structure by hot-pressing without using organic solvents[J]. *Polymer journal*, 2017, 49(7): 535-542.
6. Tretinnikov O N, Sushko N I, Zagorskaya S A. Effect of salt concentration on the structure of Poly (vinyl alcohol) cryogels obtained from aqueous salt solutions[J]. *Journal of Applied Spectroscopy*, 2015, 82(1): 40-45.
7. Tretinnikov O N, Zagorskaya S A. Determination of the degree of crystallinity of poly (vinyl alcohol) by FTIR spectroscopy[J]. *Journal of Applied Spectroscopy*, 2012, 79(4): 521-526.
8. Smith P K, Krohn R I, Hermanson G T, et al. Measurement of protein using bicinchoninic acid[J]. *Analytical biochemistry*, 1985, 150(1): 76-85.
9. Nelson J H. A Review of: "Metal Carboxalates. RC Mehrotra and R. Bohra, Academic Press, New York, 1983. VIII+ 396 pp. \$65.00." [J]. 1984..
10. Boel E, Brady L, Brzozowski A M, et al. Calcium binding in. alpha.-amylases: an x-ray diffraction study at 2.1-ANG. resolution of two enzymes from *Aspergillus* [J]. *Biochemistry*, 1990, 29(26): 6244-6249.
11. Lu Y, Miller J D. Carboxyl stretching vibrations of spontaneously adsorbed and LB-transferred calcium carboxylates as determined by FTIR internal reflection spectroscopy[J]. *Journal of colloid and interface science*, 2002, 256(1): 41-52.

*Chapter 6 General
conclusion*

In chapter 2, a normal low temperature crystallization (LTC) method was used to prepare GO composited PVA-H. GO was interacted with PVA molecules by hydrogen bonds, wherein hydrogen atoms of hydroxyl and carboxyl groups of GO interact with oxygen atoms of hydroxyl groups in PVA while hydrogen atoms of hydroxyl groups in PVA interact with oxygen atoms of hydroxyl, carboxyl, epoxy, and carbonyl groups in GO. This fact led to an increase on Young's modulus by adding GO. By hydrophilicity evaluation, PVA-GO-H was found to exhibit hydrophobicity compared with PVA-H. In addition, by cell culture, cell attachment of gels was improved obviously with the addition of GO due to the rough structure in the surface of gels. GO composited PVA-H was expected to be an excellent artificial articular cartilage material with high strength and high biocompatible.

However, LTC method must use DMSO as a cryoprotectant, which was considered to be harmful for our bodies. Therefore, a novel hot pressing method was proposed, by which no organic solvent was used and PVA concentration can be achieved at 50 wt%. By this method, GO composited PVA-Hs were successfully prepared and GO was found to irregularly distribute on the surface of gels like a layer according to SEM images. However, by TEM observation, GO distributed uniformly in the gel. Although Young's modulus increased at low GO concentration, breaking strength of gels decreased significantly due to the uniform distribution of GO, which was not beneficial for artificial cartilage material. By contact angle measurement and protein absorption test, GO composited gels showed more hydrophobicity and more protein affinity. Moreover, more cells were observed to adhere to GO composited PVA-H than to pure PVA-H at initial cell culture, indicating that GO can reform the properties of the gel surface thereby improved the cell attachment of PVA-H.

Taking into account the special conditions of hot pressing method that the gelation was conducted not in water environment, inorganic salts of small molecule were use as composite materials for better dispersion in gels. The mechanical and thermal properties of each gel were measured to investigate the effect of salt on gels. To conclude, the addition of salt impeded the combination of PVA and water molecules and the anions (X) and cations (M) of salt can interact with water molecules by $\text{OH}\cdots\text{X}$ or $\text{M}\cdots\text{OH}$ bonds in amorphous, thus affected the crystallinity of gels. In addition, divalent metal

ions, especially Ca^{2+} , can form a bridging structure with oxygen atoms to form a network structure in amorphous. Therefore, Young's modulus and T_g increased at low salt concentration. Salt of each gel can be completely removed by a desalted treatment. The desalted hydrogels were found to have no toxicity show higher protein and cell affinity than to PVA-H, which was beneficial for artificial cartilage materials.

For cartilage materials, high mechanical strength and good biocompatibility were required. Low concentration CaCl_2 composited PVA-H prepared by hot pressing method seemed to be an excellent cartilage material. In addition, friction performance is also a very important property for cartilage material. For future work, we will evaluate the friction coefficient and wear of hydrogels. Moreover, the effect of desalting is still being investigated.

Acknowledgement

I would like to express my gratitude to all those who have helped me during the writing of this theses. I gratefully acknowledge the help of my supervisor Professor Matsumura Kazuaki. I do appreciate his patience, encouragement, and professional instructions during my thesis writing. Also, I would like to thank those in Matsumura lab who kindly helped me a lot during my PhD career.

Last but not the least, my gratitude also extends to my family who have been assisting, supporting and caring for me all of my life.

Achievements

Papers:

1. Zhao Y, Terai W, Hoshijima Y, Gotoh K, Matsuura K and Matsumura K. Development and characterization of a poly (vinyl alcohol)/graphene oxide composite hydrogel as an artificial cartilage material[J]. Applied Sciences, 2018, 8(11): 2272.
2. Zhao Y, Matsumura K. Effect of salts on the hydrogel formation of poly (vinyl alcohol) by hot-pressing method. In preparation

Conferences:

1. Modification of PVA composite hydrogel as artificial joint cartilage material by hot pressing method. 67th Symposium on Macromolecules (SPSJ), 12 -14 September, 2018.
2. Modification of PVA hydrogel as artificial joint cartilage material. 68th Symposium on Macromolecules (SPSJ), 25 -27 September, 2019.
3. Preparation and characterization of salt composite PVA-H made by low temperature crystallization method and a novel hot pressing method. 11th World Biomaterials Congress, 11 -15 December, 2020